



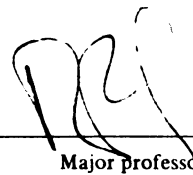
This is to certify that the
thesis entitled
A Model of Average Adult Male Human Skeletal and Leg
Muscle Geometry and Hamstring Length for
Automotive Seat Designers

presented by

Robert L. Boughner

has been accepted towards fulfillment
of the requirements for

Master's degree in Mechanics



Major Professor

Date April 23, 1991

LIBRARY
Michigan State
University

PLACE IN RETURN BOX to remove this checkout from your record.
TO AVOID FINES return on or before date due.

DATE DUE	DATE DUE	DATE DUE
AUG 8 1994	AUG 29 2000	
SEP 5 1994	JUL 25 2003	
SEP 2 1995		
OCT 12 2001		
AUG 17 2002		

MSU is An Affirmative Action/Equal Opportunity Institution

c:\circ\dtdedua.pm3-p.1

A MODEL OF AVERAGE ADULT MALE HUMAN SKELETAL AND LEG MUSCLE
GEOMETRY AND HAMSTRING LENGTH FOR AUTOMOTIVE SEAT DESIGNERS

By

Robert Lee Boughner

A THESIS

Submitted to
Michigan State University
in partial fulfillment of the requirements
for the degree of

MASTER OF SCIENCE

Department of Metallurgy, Mechanics, and Material Science

1991

ABSTRACT

A MODEL OF AVERAGE ADULT MALE HUMAN SKELETAL AND LEG MUSCLE GEOMETRY AND HAMSTRING LENGTH FOR AUTOMOTIVE SEAT DESIGNERS

by

Robert Lee Boughner

The need for comfortable, safe, and efficient use of interior space in the modern automobile is creating a need for anatomically and physiologically correct representations of the human body.

This thesis describes the development of a detailed geometric computer model representing the average adult male. A skeletal model capable of assuming any human posture functions as a framework to which models of other tissues are referenced. An investigation into how muscles might best be modeled leads to the use of ellipsoids to represent entire muscle groups. A non-invasive method of measuring hamstring length in vivo using sophisticated optical tracking equipment is described. The hypothesis that a limiting hamstring muscle length determines permissible combinations of knee and hip angles is investigated experimentally.

It is concluded that the methods selected for skeletal and muscle modeling produce body contours useful in seat design. It is also shown that a limiting hamstring muscle length causes an interdependence of knee and hip angles in certain postures.

Dedicated to my ever supportive Mother and Father.

ACKNOWLEDGEMENTS

The author wishes to extend heartfelt thanks to the following very special people:

My new wife, Susan, for her love, support, and energetic help during the preparation of this thesis.

Dr. Robert Soutas-Little and Dr. George Mase for their kindness and valuable advice.

Johnson Controls, Inc., for generously funding this research.

Dr. Robert Hubbard, my advisor and friend, for his trust, support, and humor.

TABLE OF CONTENTS

	Page
LIST OF TABLES.....	vii
LIST OF FIGURES.....	viii
1. BACKGROUND AND OBJECTIVES.....	1
2. SKELETAL MODEL.....	7
2.1. Introduction.....	7
2.2. Methods.....	7
2.2.1. Computer System and Software.....	7
2.2.2. Skull.....	7
2.2.3. Pelvis.....	8
2.2.4. Spine.....	8
2.2.5. Rib Cage.....	8
2.2.5.a. The 1st Graphical Model.....	8
2.2.5.b. A 2nd Graphical Attempt.....	10
2.2.5.c. 1st Computer Generated Model.....	13
2.2.5.d. 2nd Computer Generated Model.....	16
2.2.5.e. 3rd Computer Generated Model.....	22
2.2.5.f. The Problem of Rib Motion.....	24
2.2.6. Long Bones.....	26
2.2.7. Hands and Feet.....	27
2.2.8. Positioning the Skeletal Model.....	27
2.2.8.a. Lumbar Spine Positioning Program.....	27
2.2.8.b. Limb Positioning Program.....	35
2.3 Results and Discussion.....	36
3. MUSCLE MODELING.....	43
3.1 Introduction.....	43
3.2 Methods of Muscle Modeling.....	43
3.2.1. The Major Muscle Groups.....	43
3.2.2. Alternate Depictions of Musculature.....	48
3.3 Results and discussion.....	52
4. MUSCLE LENGTH CONSTRAINT OF SKELETAL MOTION.....	56
4.1 Introduction.....	56
4.2 Experimental Methods	57
4.2.1. Biomechanics Evaluatiuon Laboratory.....	57
4.2.2. Data Gathering and Analysis.....	59
4.2.2.a. Description of Exercises.....	60
4.2.2.b. Calculation of Muscle Lengths....	64
4.2.2.c. Calculation of Limb Angles.....	68
4.2.2.d. Link Length Variations.....	70

4.3 Experimental Results.....	77
4.3.1. Experimental Results in Graphical Form..	82
4.3.2. Error Estimation.....	96
4.3.3. Model Predictions Evaluated.....	101
4.3.4. Discussion.....	102
5. CONCLUSION.....	108
APPENDICES	
A. Spinal Joint Center Coordinates.....	110
B. Lumbar Spinal Motion Program.....	115
C. Limb Positioning Program.....	120
D. Linkage Equations.....	132
E. The Exercise Program.....	133
F. Error Estimates.....	147
BIBLIOGRAPHY.....	150

LIST OF TABLES

	page
Table 1. Muscles Which Extend the Thigh.....	44
Table 2. Muscles Which Flex the Thigh.....	45
Table 3. Muscles Which Flex the Shank.....	45
Table 4. Muscles Which Erect the Spine.....	46
Table 5. Muscles Which Flex the Spine.....	47
Table 6. Subject Data.....	60
Table 7. Nominal Link Lengths and Pelvic Constants.....	77
Table 8. Link Length Ratios by Subject.....	82

LIST OF FIGURES

	page
Figure 1: The 2-D Drawing Template.....	2
Figure 2: The 3-D H-Point Machine.....	2
Figure 3: An Earlier 2-D Model.....	5
Figure 4: The 3-D Model Skull.....	9
Figure 5: The 3-D Model Pelvis.....	9
Figure 6: The First Graphically Depicted Rib Cage....	11
Figure 7: An UMTRI Drawing.....	12
Figure 8: The First Geometric Rib Cage.....	14
Figure 9: The Basic X-section Shape of the Rib Cage..	15
Figure 10: The Rib in Polar Coordinates.....	17
Figure 11-14: Orthographic Projections of Ribs 1-4....	18-21
Figure 15: Computer Rib Cage Model #2.....	23
Figure 16: Computer Rib Cage Model #3.....	23
Figure 17: The Final Rib Cage Model.....	25
Figure 18-23: Engineering Drawings of the Long Bones..	28-33
Figure 24: The Model Skeletal Hand and Foot.....	34
Figure 25-26: The Assembled Skeletal Model.....	37, 38
Figure 27: An Alternate Skeletal Posture.....	39
Figure 28: Poor Lumbar Curvature in a Seat Design....	41
Figure 29: Depiction of Spinal Motion in the Model....	42

Figure 30:	Muscle Groups as Straight Lines.....	49
Figure 31:	Alternative Muscle Modeling Techniques.....	51
Figure 32:	Views of the Model Leg with Muscles.....	53
Figure 33:	A Poor Muscle Modeling Result.....	55
Figure 34:	Hip Angle & Knee Angle Defined.....	58
Figure 35:	Creation of a Standing File.....	62
Figure 36:	The Experimental Exercises.....	63
Figure 37-38:	Computer Representations of Subject Targeting Geometry.....	66, 67
Figure 39:	Vector Definitions.....	69
Figure 40:	The Pelvis & Thigh as a Four Bar Linkage...	71
Figure 41:	Link Hip Angle And Laboratory Hip Angle....	72
Figure 42:	The Model Does the Laboratory Exercises....	75
Figure 43:	Hamstring Length Related to Joint Angles...	76
Figure 44-47:	Variations in Skeletal Link Lengths.....	78-81
Figure 48-59:	Unprocessed Experimental Data.....	83-94
Figure 60-63:	Experimental Lengths versus Model Predictions.....	97-100
Figure 64-67:	Experimental Joint Angles Compared to Theory.....	102-105
Figure 68:	The Linkage.....	128
Figure 69:	Error Estimation.....	142

1. BACKGROUND AND OBJECTIVES

The need for comfortable, safe, and efficient use of interior space in the modern automobile is placing demands on the scientific disciplines of anthropometry, ergonomics, and biomechanics to provide better methods of human accommodation in vehicles. Advances in the application of computer technology to the design of automobiles provide new potential for improved comfort and safety in tomorrow's car; however, new representations of the human body are needed if designers and engineers are to create optimal products.

For two decades, human accommodation in the automobile interior has relied primarily upon two tools [1,2]:

1. "Oscar", the 2-dimensional drafting template shown in Figure 1, and
2. the H-point machine, a 3-dimensional seat testing device depicted in Figure 2.

These SAE (Society of Automotive Engineers) tools were originally intended only as a means to assure consistent positioning of the occupant in the vehicle; however, the SAE 2-D template is now often used improperly to represent human geometry during seat design.

The SAE 3-D H-point machine is used to evaluate prototype and production seats to measure the location of

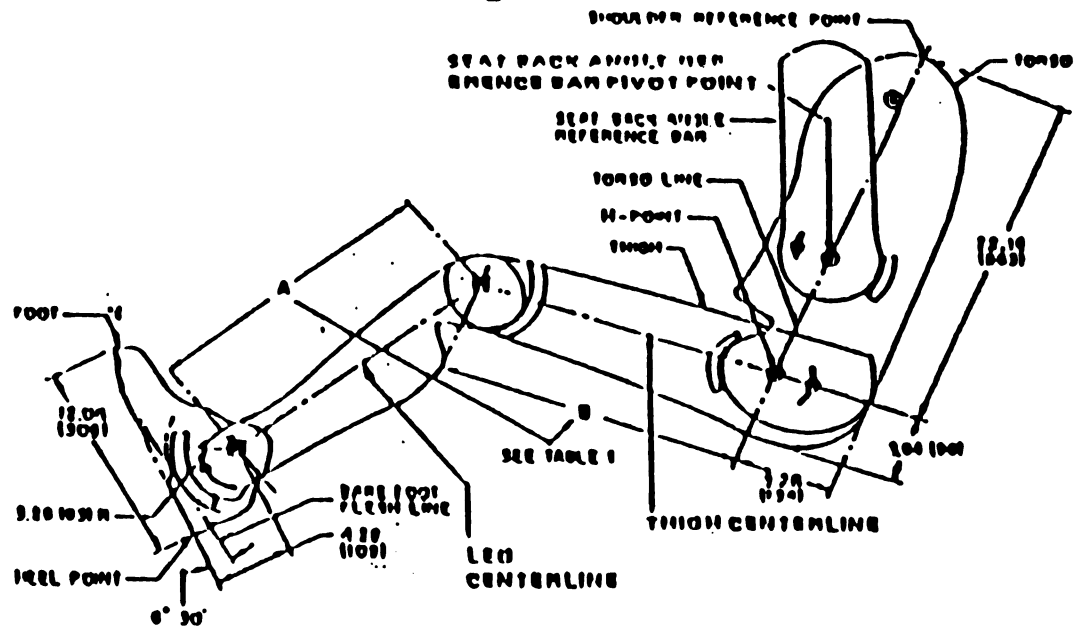


FIGURE 1: THE 2-D DRAFTING TEMPLATE

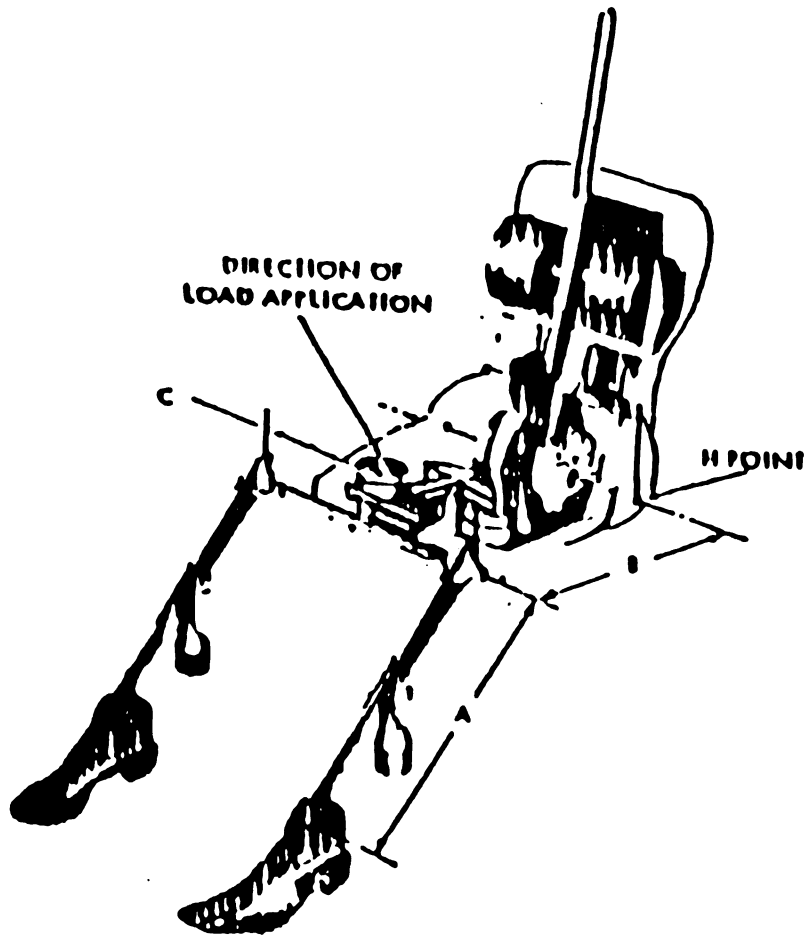


FIGURE 2: THE 3-D H-POINT MACHINE

the H-point (the theoretical location of the center of rotation of the hip joint) and seatback angle for comparison with design values. This design approach is self-consistent in that the seat properly accommodates the tools from which it was designed - it does not necessarily follow that such a seat will adequately or comfortably support a human being.

The 3-D H-point machine can only be used to evaluate existing hardware. If a prototype seat fails to meet specifications, it must be redesigned and another constructed and tested. This often results in an expensive cycle of design and redesign.

These SAE accommodation tools and associated design practices assure that new automobile seat designs conform to earlier standards, rather than to current knowledge of ergonomics and biomechanics. These accommodation tools and design practices will remain in use until the industry adopts a new approach to seat development. For this to happen, a new set of design tools compatible with current knowledge and methods will be required.

It is imperative that future seat designs be based upon what is anatomically and physiologically correct for the occupant. If a truly foresighted design procedure is to become reality, design tools capable of adequately representing people in the seated environment must be developed.

Models which represent significant features of the human body will do much to facilitate the incorporation of

biomechanics into the automotive design process. Such models, capable of accurately representing the geometry, permissible ranges of joint motion, and changes in position of the human body will become powerful new design tools.

For seating, important body regions are the spinal column with its complex motion capabilities, torso, and head. Haas [3] has developed a two dimensional, side view computer model which represents the average adult male's torso geometry and spinal motion (Figure 3).

In this thesis, the torso model is further developed with additions of a three dimensional rib cage, shoulder complex, and limbs. The addition of muscles is explored with attention to simple muscle shapes which result in a realistic body configuration. The role played by muscle (hamstring) length in restriction of possible body positions is also addressed.

The specific objectives of this work have been to:

1. Construct a computer model of the average male adult human skeleton;
2. Investigate how the body's muscle masses might best be represented in such a model, with emphasis placed on the musculature of the legs;
3. Investigate the role played by muscle lengths in the limitation of relative motion between various adjacent skeletal components, with emphasis placed on the muscles of the posterior thigh.

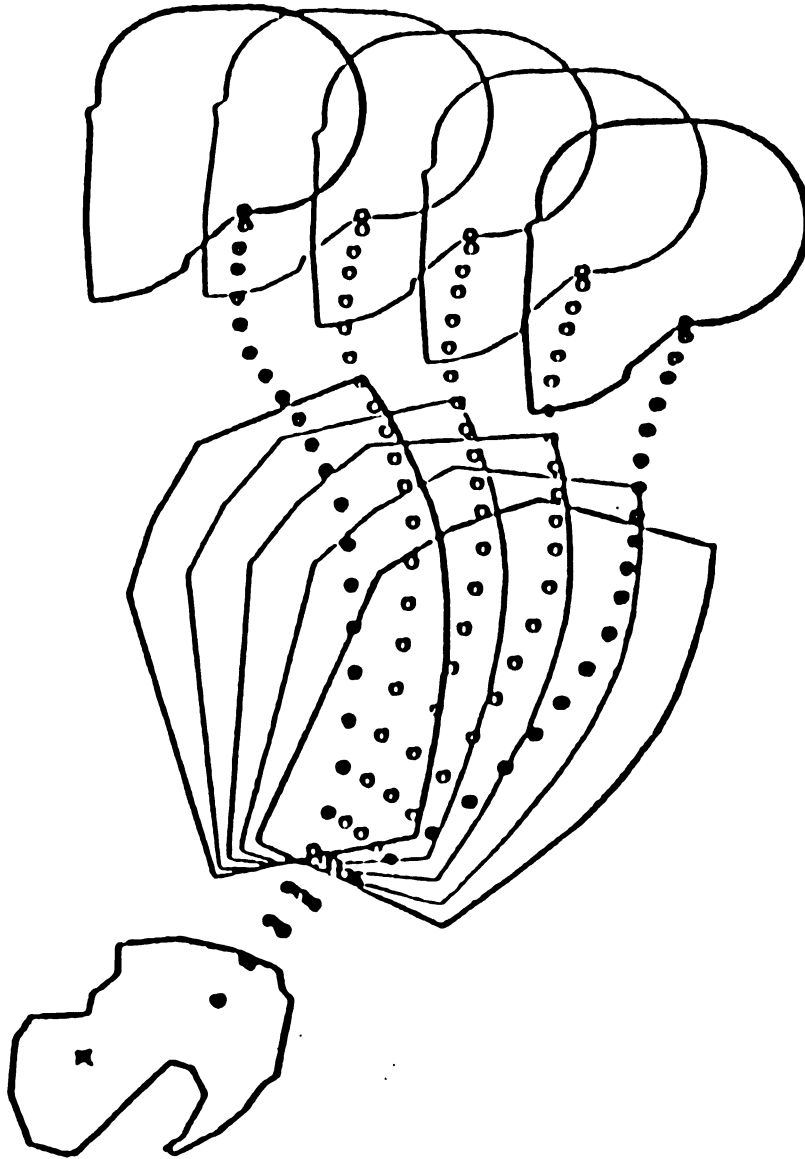


FIGURE 3: AN EARLIER 2-D MODEL

The body of this thesis is organized into three separate sections, one devoted to each of the primary objectives stated above. Each section includes a description of methods used along with presentation and discussion of results.

2. THE SKELETAL MODEL

2.1. Introduction

The external contours of the human body are created primarily by the skin being stretched over underlying structures. The supporting tissues most important to contour creation are the skeleton, muscle masses, and superficial fat pads. The modeling approach used in this study was based on the following assumption: if the skeletal structures could be portrayed in an anatomically correct fashion, then major muscle masses and fat deposits could be simulated and positioned relative to the skeleton. Then, through the use of a surface generating feature of the CAD software, body contours could be represented.

2.2. Methods

2.2.1. Computer System and Software

The computer system used to develop this model of the average size adult human male skeleton was the SUN SYSTEM 3/60 utilizing the SDRC IDEAS 3.8 and 4.0 GEOMOD [4] solid modeling packages. These software packages permit graphical representations of solid objects to be generated and manipulated by the operator.

2.2.2. 3-D Skull

The 3-D skull used in this model is that created by Haas [3] from three-dimensional locations of various landmarks representing the skull of the 50th percentile male. This skull, which is based on work done by Hubbard

and McLeod [5] as a step in their development of what is now the Hybrid III crash dummy head, is illustrated in Figure 4.

2.2.3. 3-D Pelvis

The pelvis for the model was created by Haas [3] using data contained in a report by Reynolds, et al [6]. These data for pelvic geometry have been recognized as the best available information for the development of future crash test dummies [7]. A wireframe depiction of this pelvis can be seen in Figure 5.

2.2.4. The Spine

The spine was represented by Haas [3] as a series of small spheres located at the centers of the intervertebral joints (Figure 3). The spatial coordinates of the joint centers are listed in Appendix A.

2.2.5. 3-Dimensional Rib Cage

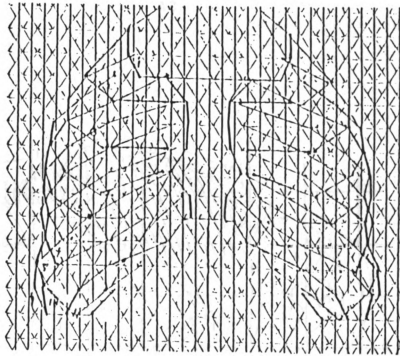
2.2.5.a. The First Attempt at a Graphical Model of the Rib Cage

No known previous attempts had been made to adequately model the human rib cage geometry; thus, no data describing its geometric details were available. The approach taken during this work was to first develop a detailed 3-dimensional rib cage and shoulder geometry which appeared accurate when compared to anatomical references and specimens. This geometry was then modified as required to bring it into compliance with known anthropometric dimensions.

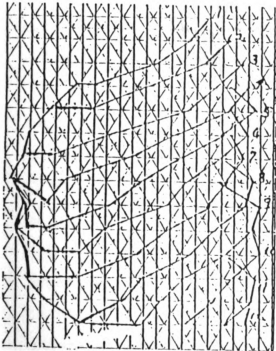
In the first attempt to geometrically represent the rib cage, photographs of horizontal sections of human cadavers [8] were used to generate 3-D coordinates for the ribs and costal cartilages. The three principal directions were specified as x = anterior; y = left lateral; and z = craniad. The origin of each section was placed approximately at the center of vertebral joint rotation, as depicted by Panjabi and White [9]. The X and Y coordinates at each vertebral level obtained for the ribs, costal cartilages, and sternum were plotted against a straight vertical axis to obtain the orthographic projection and other views of the rib cage shown in Figure 6. It was thought that the "kinks" in the ribs were due to the lack of spinal curvature in the plot, and the drawings were repeated, this time using the spinal curvature depicted in the drawings from UMTRI [7] (Figure 7). Unfortunately, this second series of plots were less desirable than the first, being even more grossly distorted. It was concluded that apparently, in spite of elaborate processing of the cadaver [8], it had been fixed in a posture with an unnaturally flat spinal position, and was therefore inappropriate for the study at hand.

2.2.5.b. A Second Attempt at a Graphical Rib Cage Depiction

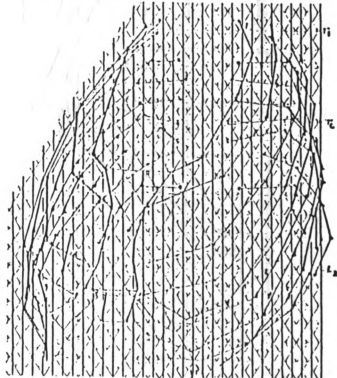
After examination of several skeletal rib cages in the Gross Anatomy Laboratory at Michigan State University and anatomy texts [10,11,12], it was concluded that the rib cage might be modeled by using two basic assumptions:



FRONT VIEW



SIDE VIEW



OBLIQUE VIEW

FIGURE 6: THE FIRST GRAPHICALLY DEPICTED RIB CAGE

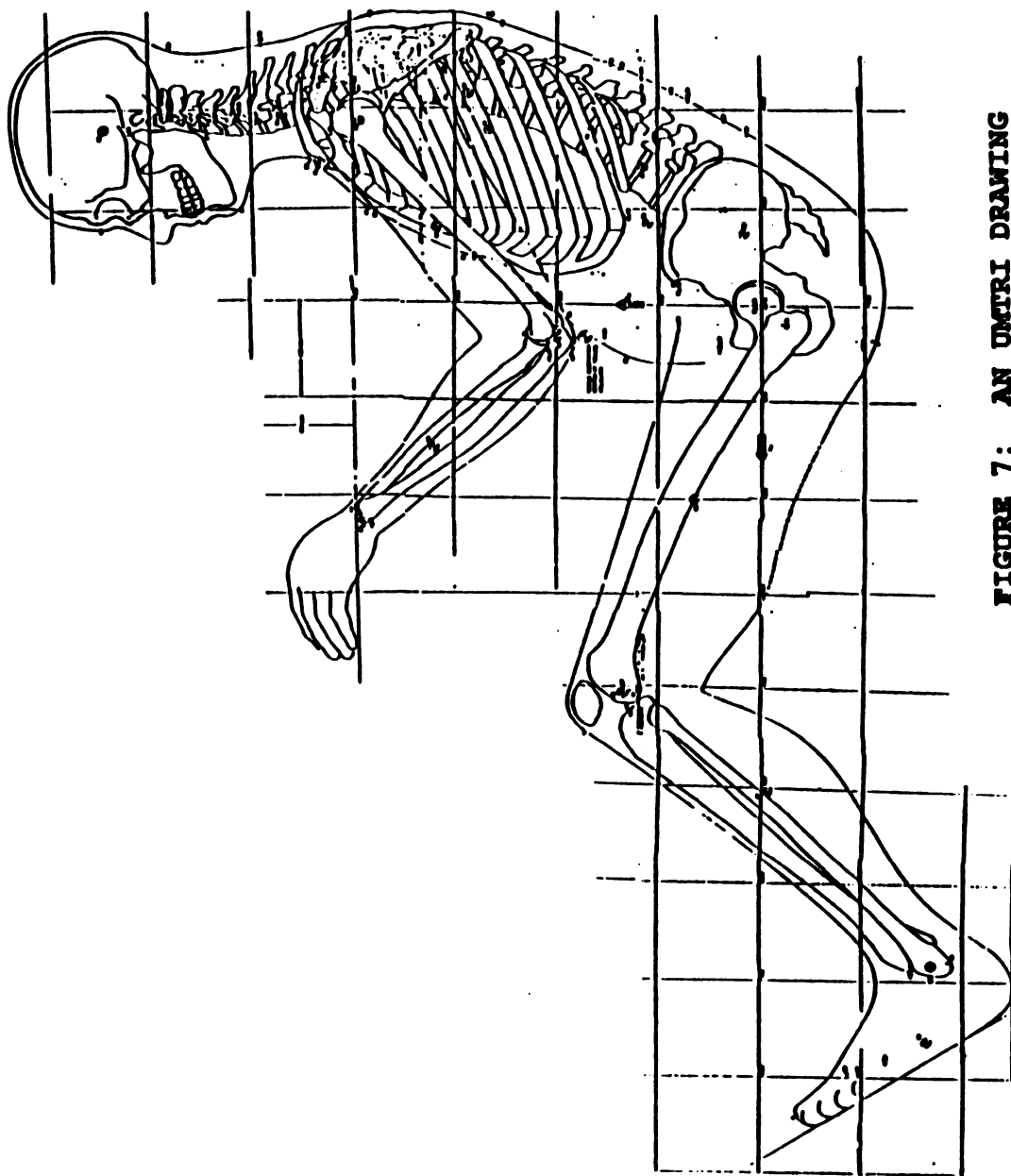


FIGURE 7: AN OMTRI DRAWING

1. When viewed from above, the shape of the human rib cage can be approximated by a six-sided polygon, with each rib having the same basic proportions but altering in scale;
2. When viewed from the side, the ribs appear as straight lines, with each rib descending anteriorly and downward at a constant slope. (Ribs 1 thru 8 descend at an angle of approximately 25 degrees, while Ribs 9 thru 12 descend at successively steeper angles).

Using these two conclusions and the rules of orthographic projection, the highly simplified and symmetric drawings shown in Figure 8 were produced. It was conjectured that by using this approach (with more numerous points) a reasonable model could be produced.

2.2.5.c. The First Computer Generated Rib Cage Model

The best data points available for the rib cage of the 50th percentile male were those located on the thoracic spinal column and sternum contained in the UMTRI study [7] (Figure 7). This study used a coordinate system with the origin located halfway between the centers of the hip joints, with the three principal directions specified as x = anterior, y = left lateral, and z = upward. It was decided to use a basic cross-sectional shape of the rib cage to generate the Y coordinates. The basic shape was assumed to be that shown in Figure 9. By relating the vertebral-sternal distance at the level of each rib in the UMTRI drawings to 25 points on the basic rib shape using the polar

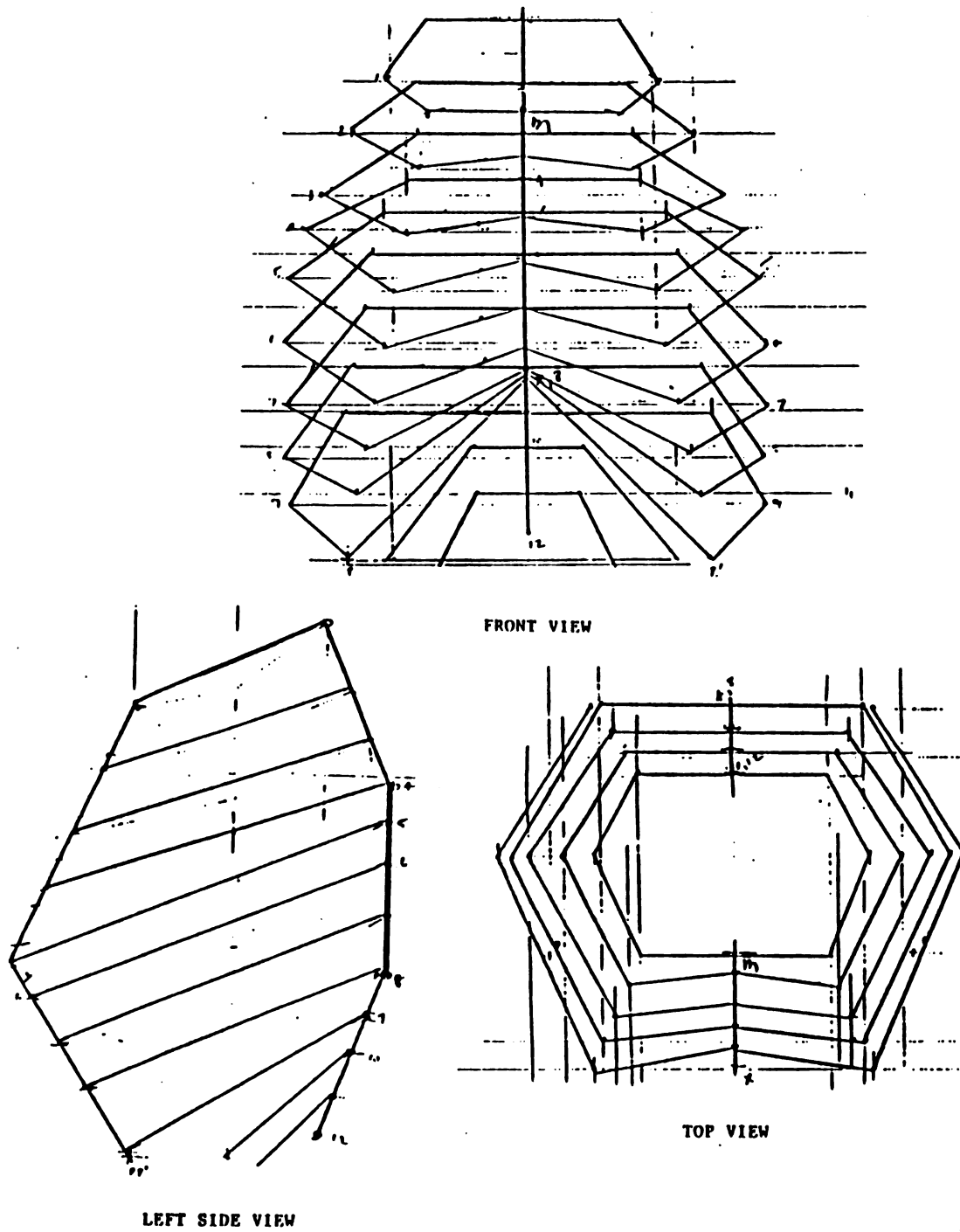


FIGURE 8: THE FIRST GEOMETRIC RIB CAGE

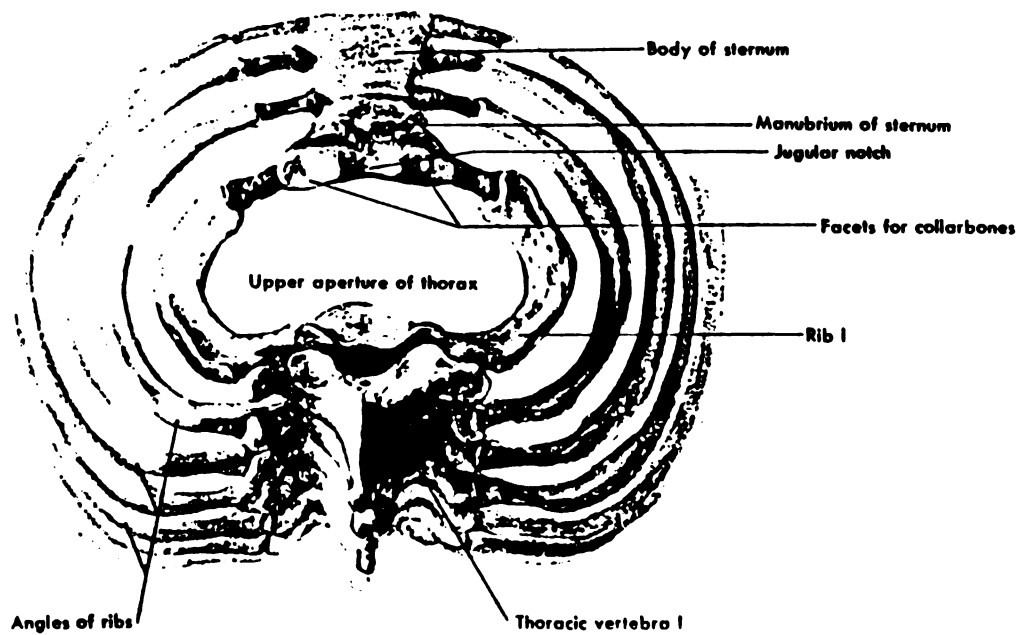


FIGURE 9: THE BASIC X-SECTION SHAPE OF THE RIB CAGE

coordinate system (with the origin at the center of the vertebral bodies) shown in Figure 10, it was possible to create a 3-D depiction of each rib. A straight line connecting the centers of T1 and T12 was used to define the vertical axis.

In this model, it was assumed that all the ribs descended at a slope of $dz/dx = -25$ degrees, with no slope in the y direction. Because this model depicted the ribs as vertical-sided, concentric structures, it was deemed unsuitable for representing the first four ribs, which in actuality have non-vertical sides.

2.2.5.d. The Second Computer Generated Rib Cage Model

To more accurately represent the sloping sides of ribs one through four, trigonometric and orthogonal projections were used to graphically determine the coordinates for these ribs. The known geometry in the Side and Auxillary Views (Figures 11-14) was used to create the Top View, from which the missing Y coordinate could be measured. Ribs 5 through 12 were depicted as in the first computerized model.

Although the best attempt yet, this model had several flaws, the worst of which was the lack of proper slope in the floating ribs (ribs 10,11,12). This defect was due to the fact that these floating ribs are very short, and most of their travel occurs in the Y direction when viewed from above. Since all the slope in the model was dependent upon changes in the X coordinate, these ribs appeared as

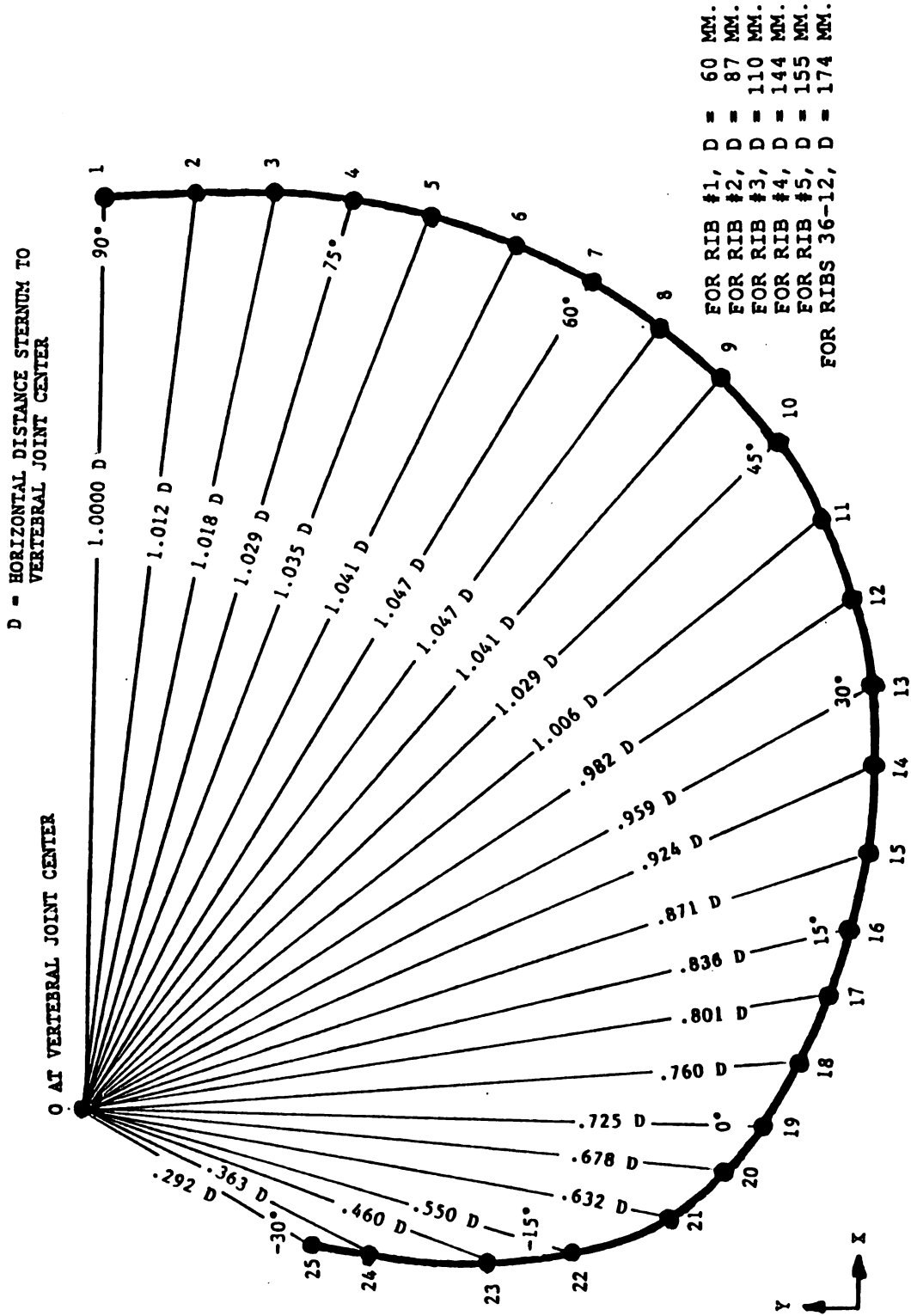


FIGURE 10: THE RIB IN POLAR COORDINATES

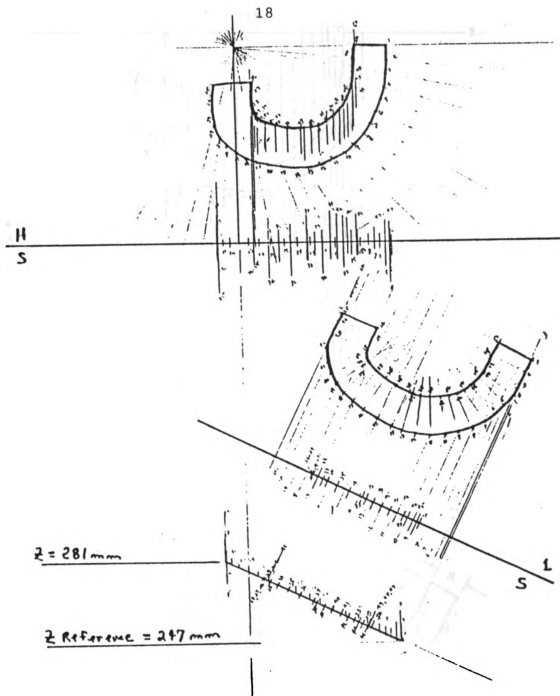


FIGURE 11: ORTHOGRAPHIC PROJECTION OF RIB ONE

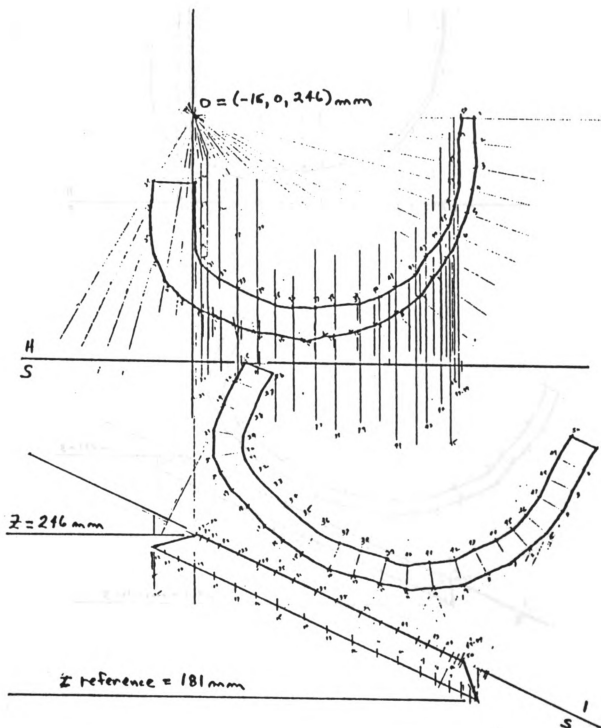


FIGURE 13: ORTHOGRAPHIC PROJECTION OF RIB THREE

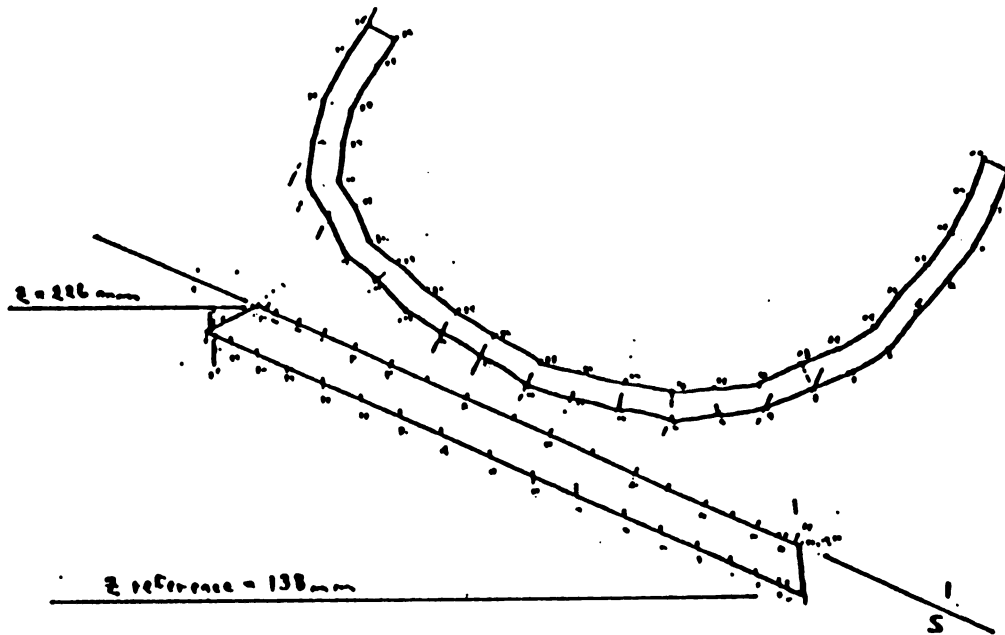
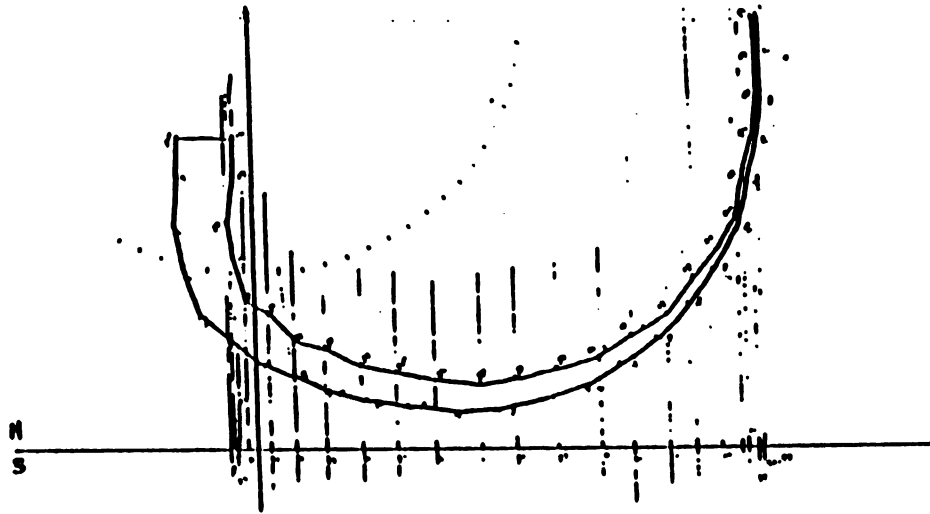


FIGURE 14: ORTHOGRAPHIC PROJECTION OF RIB FOUR

horizontal "stubs" (Figure 15), and not at all like the actual ribs which angle downward.

2.2.5.e. The Third Computer Generated Rib Cage Model

Upon determination of the shortcomings in the second model, corrective changes were incorporated into the third, as follows:

1. The ribs were assumed to articulate with the vertebral column at the level of the disk spaces, instead of at the midpoint of the vertebral bodies as had been the case in the previous models;
2. A variable slope, dz/dy , was included for that portion of rib travel which is dependent primarily upon changes in the Y coordinate (points 23-25 in Figure 10); this slope varies with each rib, progressing from 0 degrees at the fourth rib to -40 degrees at the twelfth rib;
3. The slope dz/dx , included for that portion of rib travel depending primarily upon change in the X coordinate (points 1-22 in Figure 10), varies from -25 degrees at the 5th rib to -32 degrees for the 12th rib. (This had been a constant -25 degrees in the previous models).

This model rib cage, shown in Figure 16, needed only the following minor corrections before it was incorporated into the full-body model:

1. Smoothing of the transition between the dz/dy and dz/dx slopes;
2. Inclusion of the costal cartilages;

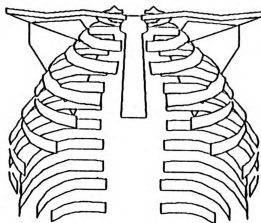
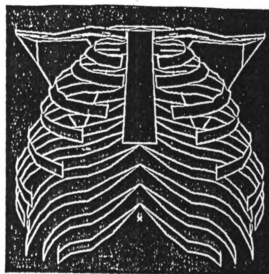


FIGURE 15: COMPUTER RIB CAGE MODEL #2



**COMPUTER MODEL #3
OBLIQUE VIEW**



**COMPUTER MODEL #3
FRONT VIEW**

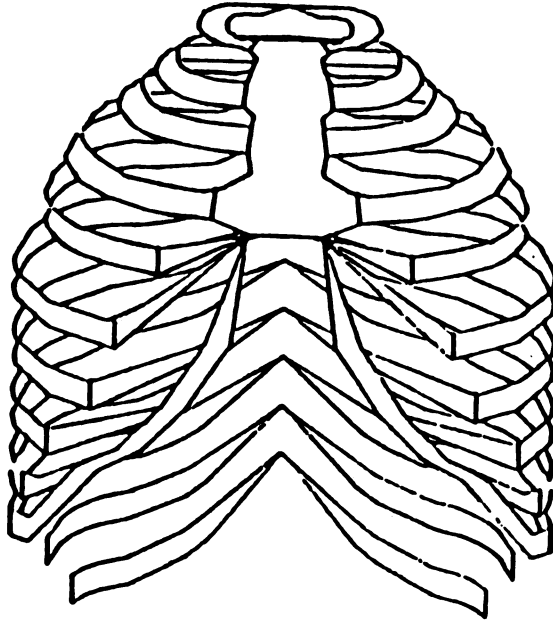
FIGURE 16: COMPUTER RIB CAGE MODEL #3

3. Scaling in all three directions to force the model to comply with known rib cage dimensions; and
4. More anatomically accurate depictions of the sternum, clavicles, and scapulae. (The improved representations of these structures were developed using the methods described in Section 2.2.6. Figure 17 shows the final configuration of the rib cage model.

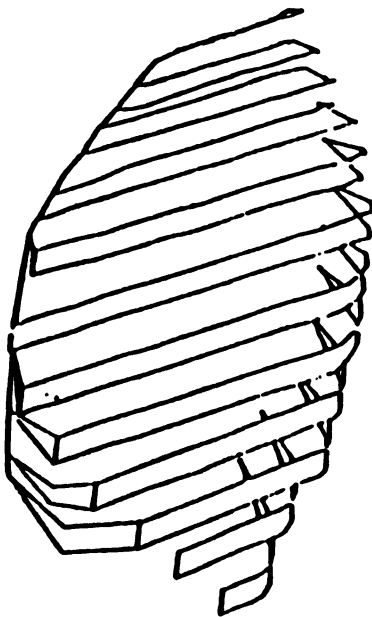
2.2.5.f. The Problems of Depicting Rib Motion

A literature search [13,14,15,16,17] has shown that the problems of incorporating respiratory movements into the rib cage model are varied and complex. They include:

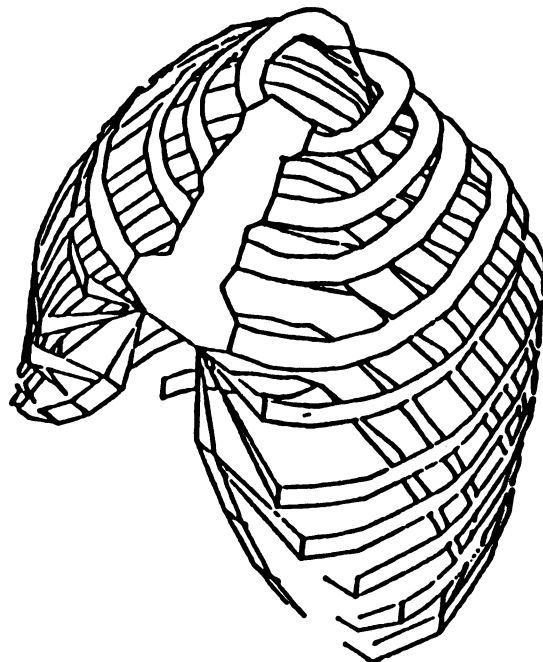
1. Upper ribs move as "pump handles" (fixed at the posterior end, with relatively large motions at the anterior end), while the lower ribs move primarily as "bucket handles" (both ends stationary with the bulk of motion occurring in the center portion via rotation about an imaginary axis between the rib ends). The middle ribs move by a mixture of these two motions.
2. The upper ribs are relatively less mobile than the lower ones due to the stabilizing influences of the clavicles and sternum.
3. The amount of flexion in the thoracic spine is open to debate [3].
4. Children, women, and men all expand the rib cage differently during normal respiratory motions. Men tend to be abdominal breathers, while women usually expand their upper rib cage to a greater degree.



FRONT VIEW



SIDE VIEW



OBLIQUE VIEW

FIGURE 17: THE FINAL RIB CAGE MODEL

5. The relative contributions to thoracic movement of spinal flexibility and respiratory motion are of greatly differing magnitudes - the larger motions of breathing will overshadow any rib motion due to spinal motion.

Because thoracic motions are not well quantified and are small compared to other body movements (Haas [3] represented changes in position of the rib cage relative to the pelvis using lumbar motions only), it was decided to model the thoracic spine as a rigid structure, and to ignore respiratory motions in this model.

2.2.6. The Limb Bones

The long bones of the arms and legs were modeled in the following manner:

1. Study of cadavers in the Gross Anatomy Laboratory at Michigan State University, anatomical preparations, anatomy texts [10,11,12], and live human subjects was undertaken to determine the overall configuration of the bones, with emphasis on the location of structures critical to muscle attachment;
2. Decisions were made as to how the bones could best be represented with simple geometric shapes (cylinders, spheres, etc.) while maintaining critical anatomic relationships and proportions;
3. Engineering drawings, using the simple shapes determined above, were prepared for each bone. A characteristic length (usually overall bone length) known from the UMTRI drawings [7] was used as a reference, against

which all other dimensions of interest were scaled.

These engineering drawings are shown in Figures 18-23.

2.2.7. Hands and Feet

The skeletal hands and feet were modeled using cylinders and cones to represent the bones. Basic proportions were determined through study of skeletal preparations and live subjects. The overall dimensions were set to represent a glove size of eight, and a shoe size of nine (Figure 24).

2.2.8. Positioning the Skeletal Model

For a computerized human model to be truly useful, it must be capable of assuming any posture attainable by the person it represents. Computer programs written in the IDEAL language [4] enable the operator to place this model skeleton in any desired position, using as inputs:

1. TLC (Total Lumbar Curvature),
2. Coordinates for the heels and hands, and
3. Splay angles for the arms and legs.

Once the torso and limbs have been positioned, information vital to designers of automobile interiors, such as hamstring lengths, magnitudes of the knee joint angles, distance between the elbows, and distance between the knees in the selected posture can be provided as output. Further discussion of these computer programs follows.

2.2.8.a. Lumbar Spinal Motion in the Skeletal Model

Using the basic conclusion of Haas [3] (that it is acceptable to evenly distribute total lumbar curvature

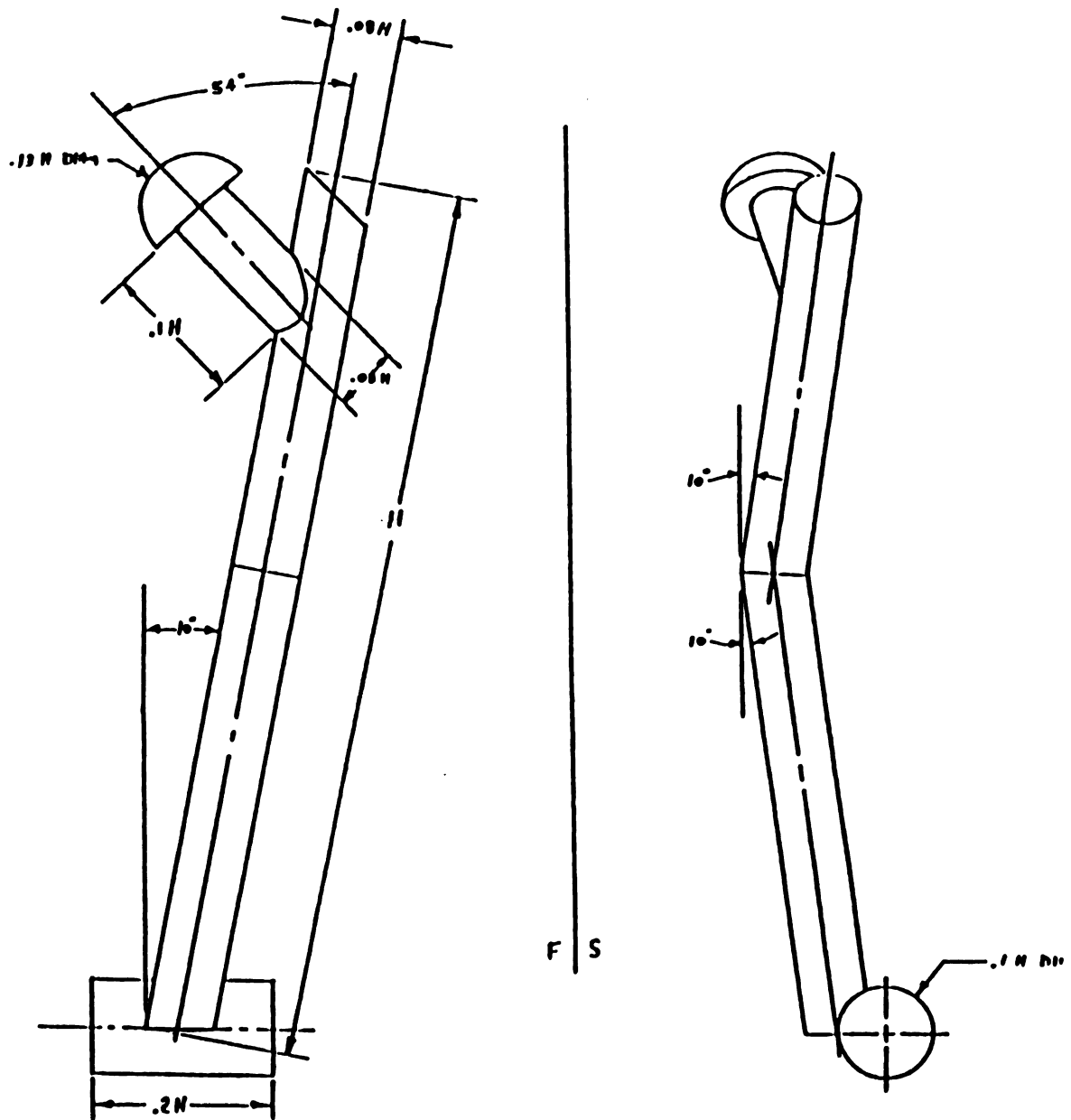
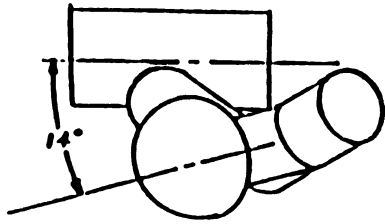


FIGURE 18: ENGINEERING DRAWING OF THE FEMUR

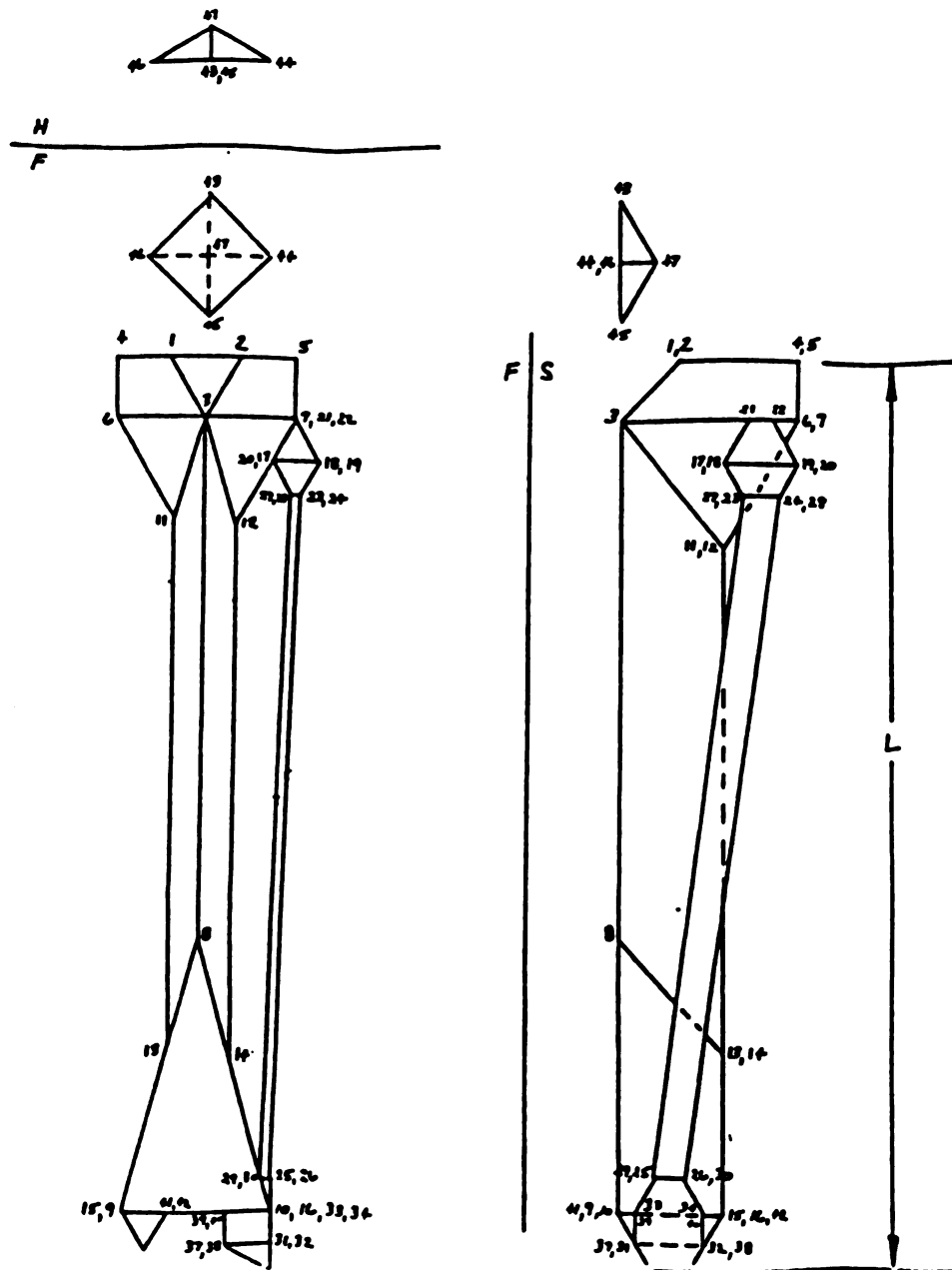


FIGURE 19: ENGINEERING DRAWING OF THE LOWER LEG

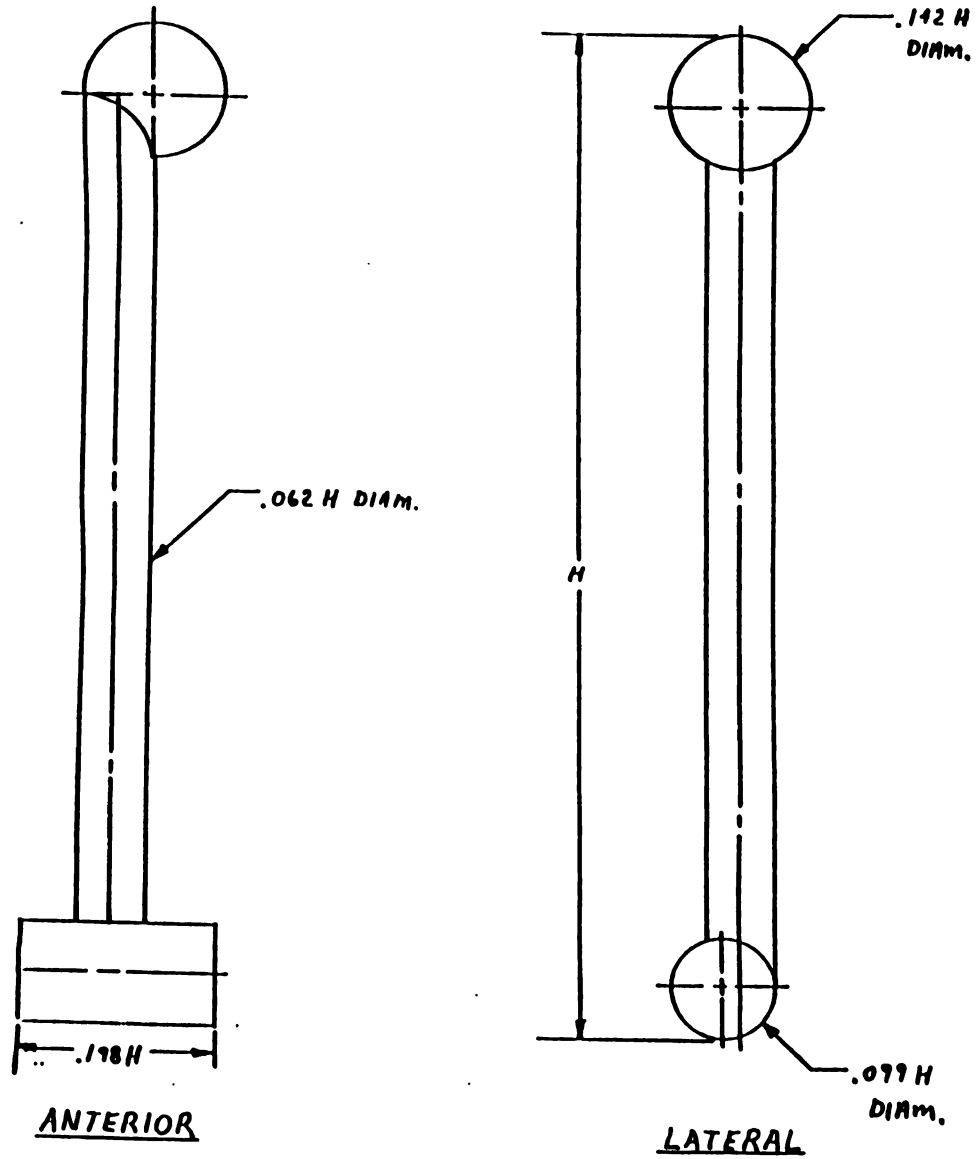
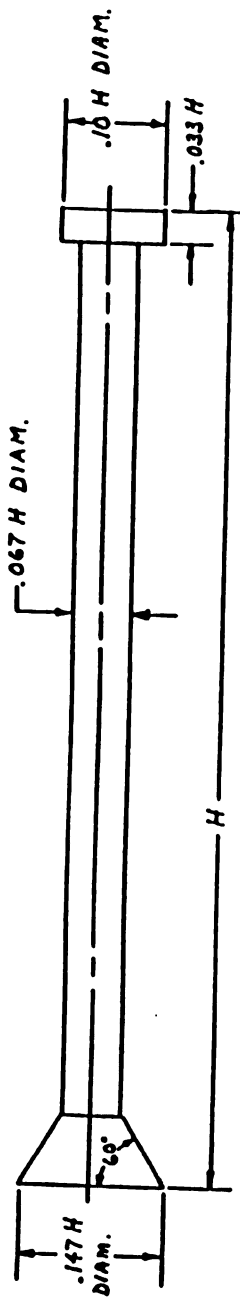


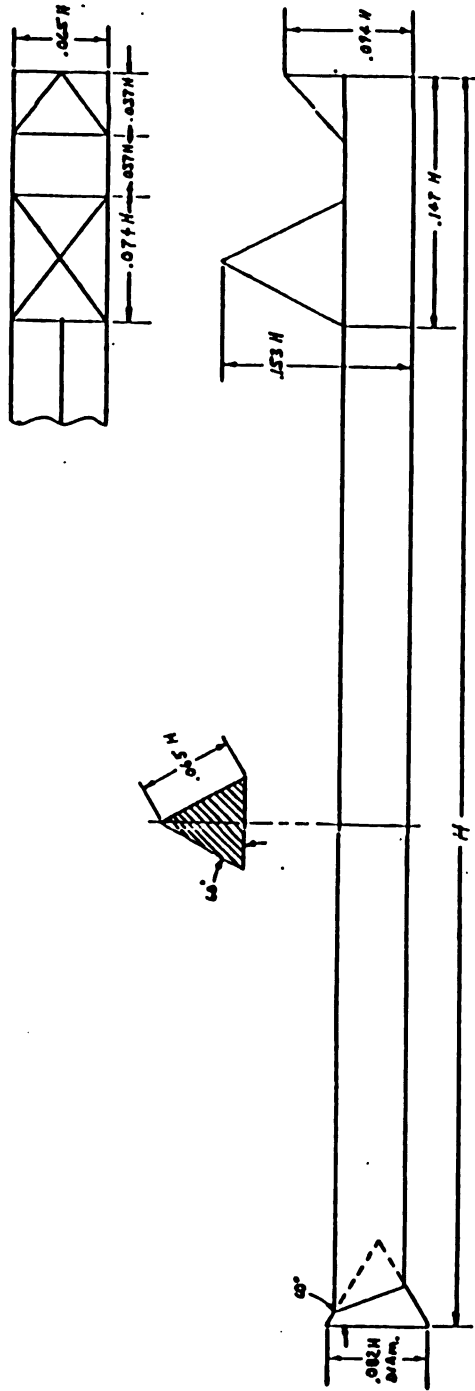
FIGURE 20: ENGINEERING DRAWING OF THE HUMERUS



RADIUS

NOTE: $H = 10.0" (254\text{mm})$

FIGURE 21: ENGINEERING DRAWING OF THE RADIUS



ULNA

NOTE: $H = 11.25$ " (286 mm) FOR 50% MALE

FIGURE 22: ENGINEERING DRAWING OF THE ULNA

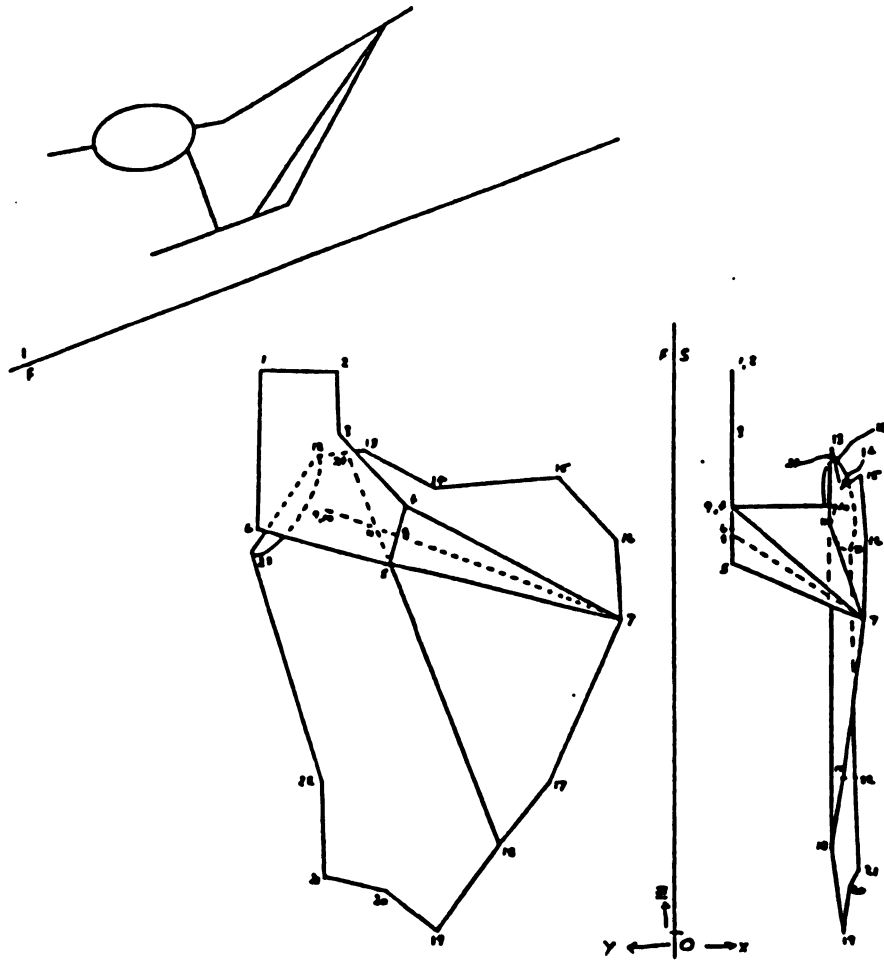
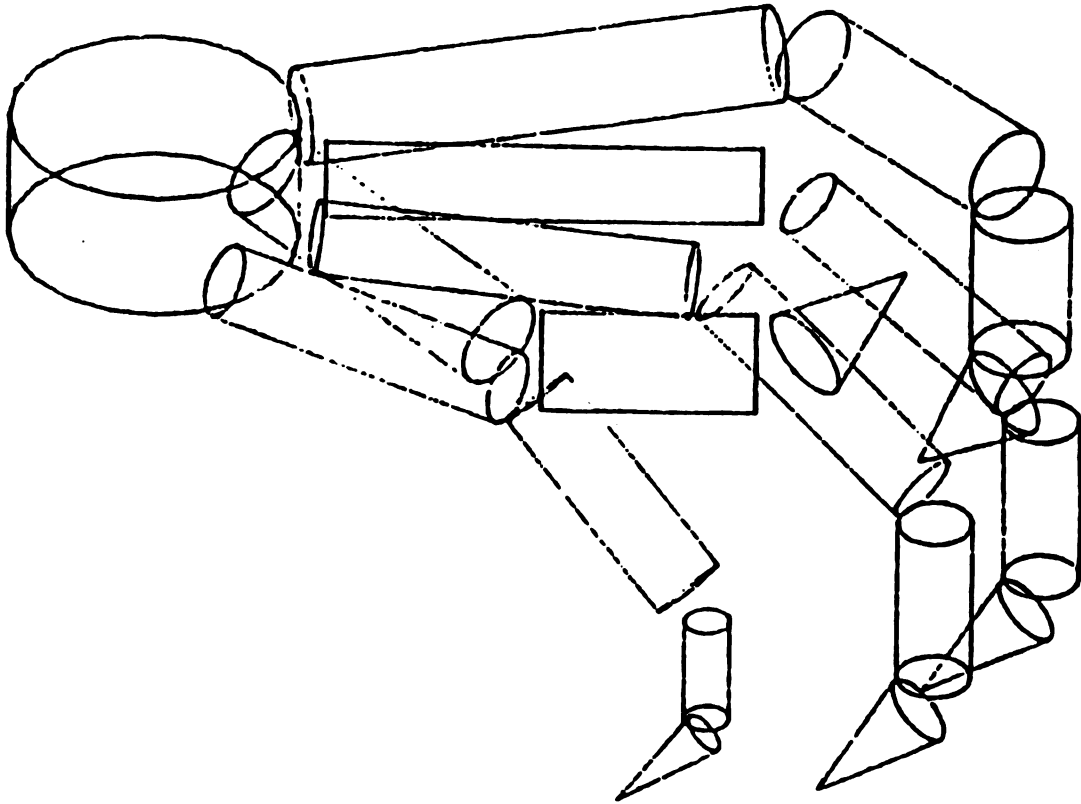
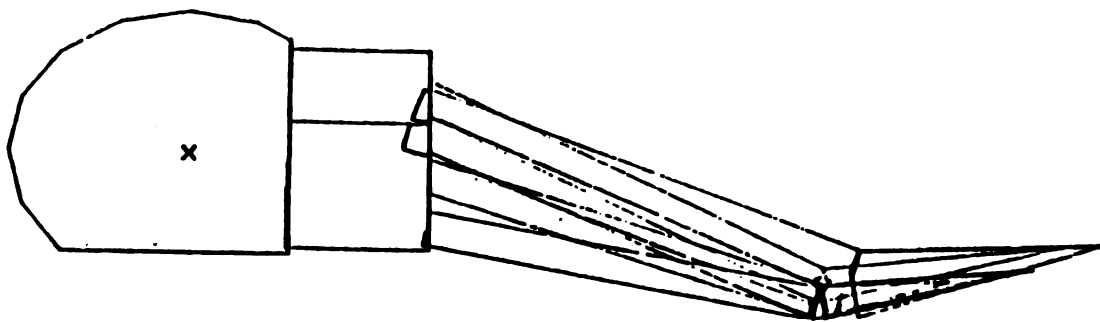


FIGURE 23: ENGINEERING DRAWING OF THE SCAPULA



Oblique View of Skeletal Hand



Side View of Skeletal Foot

FIGURE 24: THE MODEL SKELETAL HAND AND FOOT

between the joints of the lumbar spine) in conjunction with the assumption of a rigid thoracic spine from section 2.2.5.f., a computer program was written to facilitate positioning the model spinal column. This program uses the desired amount of total lumbar curvature (TLC) as input. Spinal flexion (bending forward) is negative TLC, spinal extension (bending rearward) is positive TLC. The program first rotates all model components above the T12-L1 interspace about the T12-L1 joint center by one sixth the desired TLC. During the next iteration, these components plus the sphere representing the T12-L1 joint center are rotated about the L1-L2 joint center. The process continues for a total of six iterations. Appendix B contains the entire text of this program, written in the I-DEAS language [4].

2.2.8.b. The Limb Positioning Program

The basic algorithm of the program, repeated four times to position all four limbs, is as follows:

1. Variables required for the mathematical manipulations are named and initialized;
2. The Law of Cosines is used to determine the 3-D coordinates of the knee joint or elbow in question;
3. The distal ends of the long bones are translated to their chosen locations, and then rotated into their final position;
4. The appropriate foot or hand is translated to its new position;

5. Distances and angles of interest are calculated.

Appendix C contains the complete text of the Limb Positioning Program, written in the I-DEAS language [4].

2.3. Results and Discussion for Skeleton

The model skull, pelvis, thorax, limb bones, hands and feet, together with a series of spheres representing the centers of the spinal joints, were assembled in the basic driving posture depicted in the UMTRI [7] drawings. The model skeleton of the average size adult human male shown in Figures 25 and 26 was thus created.

This geometric computer model of the human skeleton, hereafter referred to as BONEMAN, is capable of performing the tasks for which it was designed. It can simulate any posture attainable by a live human. Figure 27 shows two views of BONEMAN in a typical driving posture, with the left elbow resting on the window ledge, right hand operating a console mounted shift lever, and the left leg splayed outward in a relaxed manner.

Although based on relatively simple geometric shapes, BONEMAN is easily recognizable for what it is, and represents the morphology of the human skeleton well enough to serve as a framework to which models of other organs may be referenced.

The SAE 2-dimensional drafting template currently used by seat designers forces the occupant to assume a forward slumped posture and a flat lumbar spine. Because the comfort of a seat depends greatly on the variety of postures

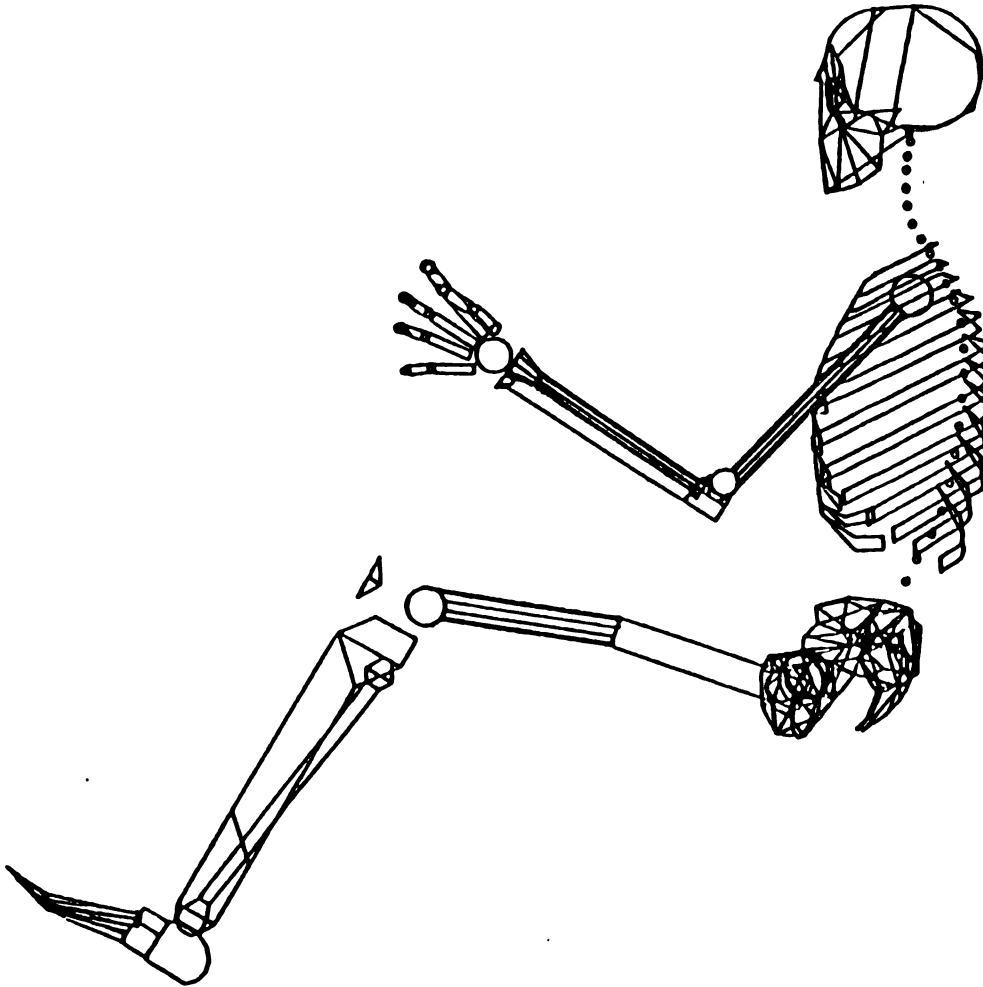


FIGURE 25: FULL SKELETAL MODEL - SIDE VIEW

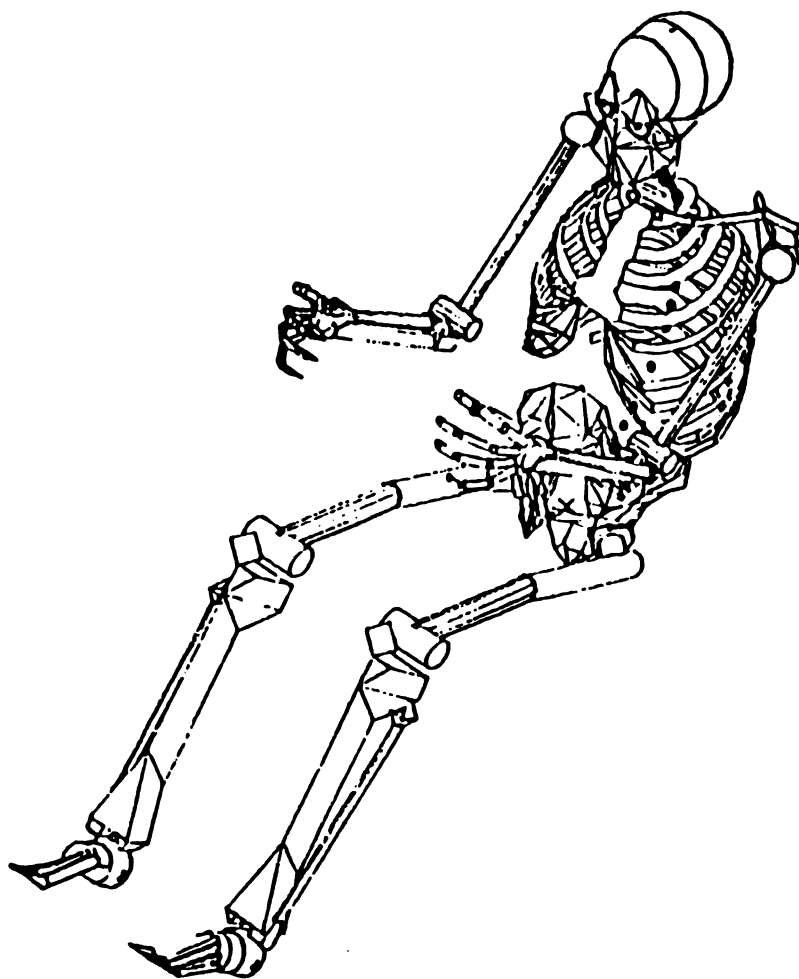
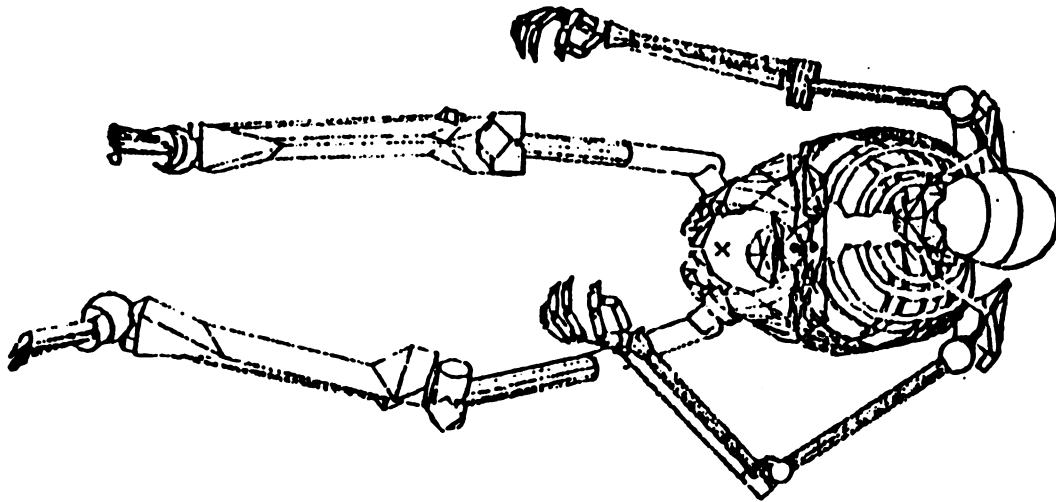
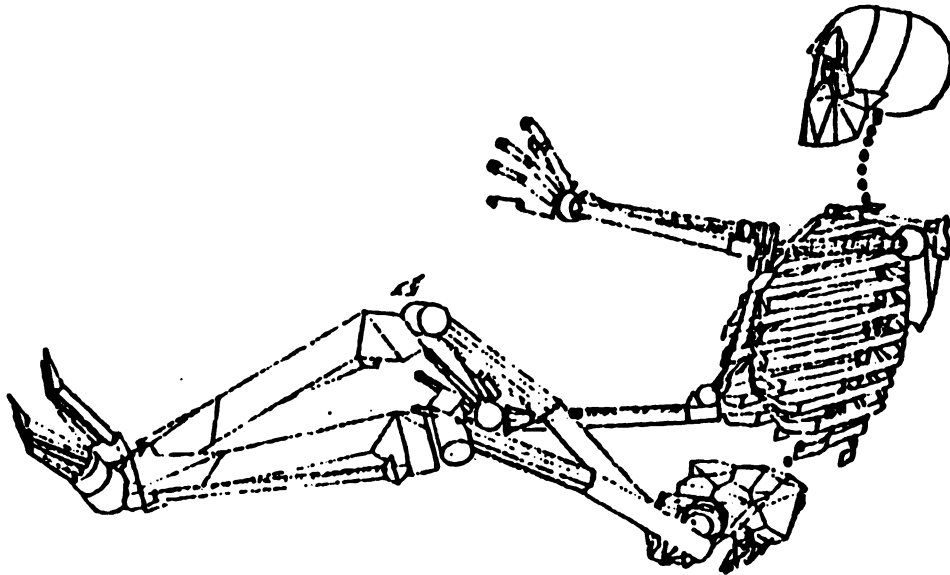


FIGURE 26: FULL SKELETAL MODEL - OBLIQUE VIEW



Top View



Oblique View

FIGURE 27: AN ALTERNATE SKELETAL POSTURE

that can be adopted and the frequency and ease with which they can be altered [18], this fixed lumbar curvature not only results in lower back fatigue and discomfort during long road trips, but also forces the occupant's shoulders to press against the seat back in an unnatural manner (Figure 28). Even when attempts are made to incorporate proper lumbar support into new designs, problems may remain. One study of driver discomfort [19] concluded that although firm, convex lumbar supports were initially rated as very desirable by test subjects, seats so equipped were judged extremely uncomfortable at the conclusion of a three hour driving simulation. Often, the lack of tools which adequately represent the various curvatures assumed by the human spine during changes of position results in a "cut and try" method of seat development in which prototype seats are built and subjectively tested for comfort. Clearly, a more efficient method of occupant depiction is needed by seat designers.

Because of its ability to represent any degree of spinal curvature (Figure 29), BONEMAN will give designers a tool with which they may create seats with anatomically desirable lumbar contours.

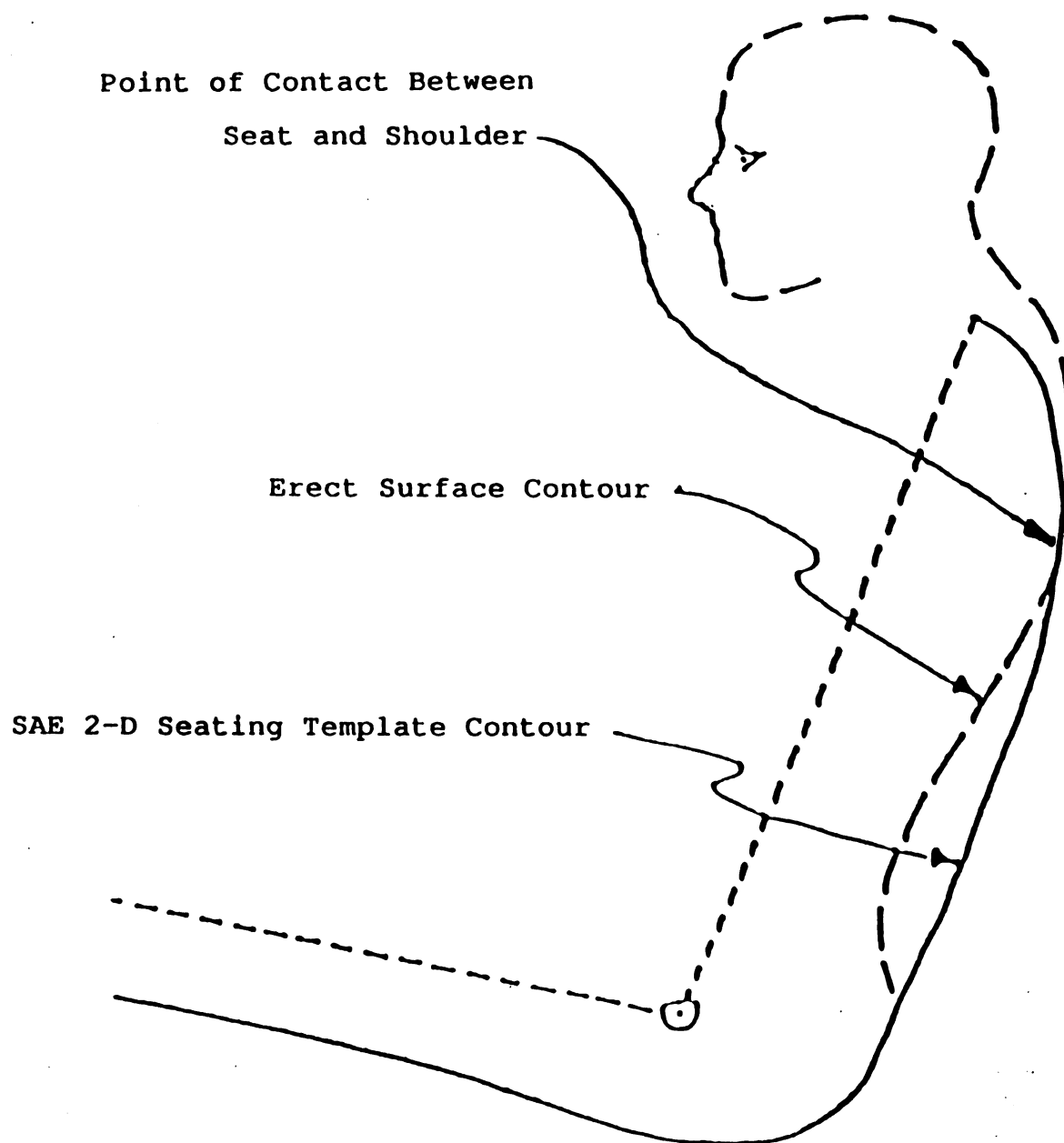
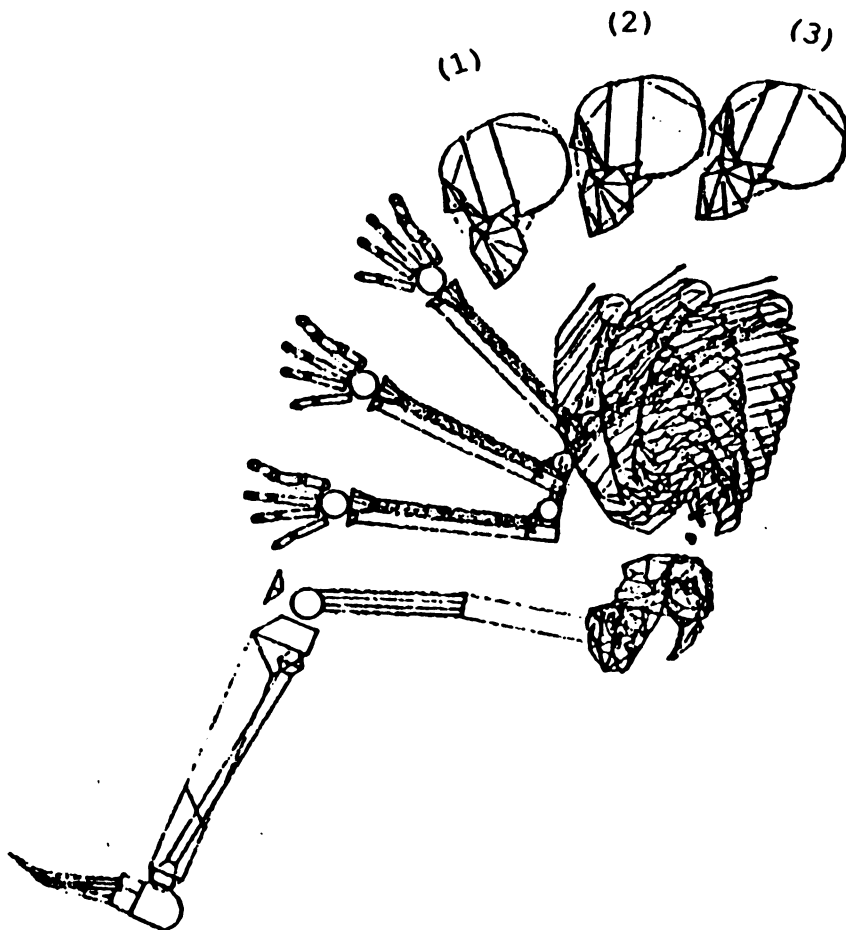


FIGURE 28: POOR LUMBAR CURVATURE IN A SEAT DESIGN



(1) = 20 Degrees of Lumbar Flexion

(2) = Straight Lumbar Spine

(3) = 20 Degrees of Lumbar Extension

FIGURE 29: DEPICTION OF SPINAL MOTION IN THE MODEL

3. MUSCLE MODELING

3.1. Introduction

The complex shape of the human body is, in part, the result of contours generated by hundreds of muscles. The computer model should represent the musculature with geometric simplicity, yet with sufficient fidelity to provide body contours which are useful in representing body interactions with seat contact surfaces. The objective of this section was to explore how the body's muscle masses might best be geometrically represented.

3.2. Methods

3.2.1. The Major Muscle Groups

Once the skeletal components of the model have been positioned in a desired posture, the locations of the boney origins and insertions of the various muscles of interest may be determined. If an accurate representation of body contours is to be developed, models of important muscle groups must be created and positioned relative to the boney structures.

Study of cadavers, anatomical preparations, anatomy texts [10,11,12] and live human subjects was again undertaken to develop an understanding of how the various muscle groups could best be portrayed in the computer model. Tables 1 through 5 list major muscle groups which determine the gross conformation of the human body. The locations, origins, insertions, and functions of individual muscles are

Table 1. Muscles Which Extend the Thigh

Muscle	Origin	Insertion
<u>QUADRACEPS GROUP</u>		
Vastus Medialis	Linea Aspera of Femur	Patellar Tendon
Vastus Lateralis	Greater Trochanter of Femur	Patellar Tendon
Vastus Intermedius	Anterior Surface of Femoral Shaft	Patellar Tendon
Rectus Femoris	Anterior Inferior Illiac Spine (AIIS)	Patellar Tendon
<u>OTHERS</u>		
Sartorius	Anterior Superior Illiac Spine (ASIS)	Medial Surface of Proximal
Tibia		

MOST REPRESENTATIVE ORIGIN: Between ASIS and AIIS

MOST REPRESENTATIVE INSERTION: Patellar Tendon

Note: Patella is to be modeled as an extension of the proximal tibia due to the relatively constant distance between the patella and the tibial crest.

Table 2. Muscles Which Flex the Thigh

Muscle	Origin	Insertion
<u>HAMSTRINGS GROUP</u>		
Biceps Femoris, Short Head	Linea Aspera of Femur	Head of Fibula
Biceps Femoris, Long Head	Ischial Tuberosity	Head of Fibula
SemiMembranosus	Ischial Tuberosity	Medial Condyle of Tibia
SemiTendinosus	Ischial Tuberosity	Proximal, Medial Side of Tibia

MOST REPRESENTATIVE ORIGIN: Ischial Tuberosity

MOST REPRESENTATIVE INSERTION: Proximal Tibia / Fibula,
Midpoint in Lateral View.

Table 3. Muscles Which Flex the Shank

Muscle	Origin	Insertion
Gastrocnemius (both heads)	Femoral Condyles	Calcaneus
Soleus	Proximal Fibula (Lateral Surface)	Calcaneus

RATIONALE FOR MODELING: Since the gastrocnemius is the most powerful of this muscle group, its origin and insertion are used.

Table 4. Muscles Which Erect the Spine
(Sacrospinalis or Erector Spinae Complex)

	Muscle	Origin Insertion
<u>LONGITUDINAL GROUP</u> (Splits at L5)		
<u>Iliocostalis</u>	Illiic Crest and sacrospinal aponeurosis of Ribs 3-12.	Angles of Ribs and Transverse Processes of C4-C7.
Longissimus	Sacrospinal Aponeurosis and Transverse Process C1-L2.	Angles of Ribs 1-7, Transverse Process of C1-T12 and Mastoid of Temporal Bone.
Spinalis	Spines of T11-L2, and C5-T2.	Spines of T2-T4 and C2-C4.
<u>TRANSVERSOSPINAL GROUP *</u>		
<u>SemiSpinalis</u>	Cover 4-6 Vertebral Segments	
Multifidi	Cover 3 Vertebral Segments	
Rotatores	Cover 1 Vertebral Segment	

* This group should be ignored in the modeling process, due to the extremely short length of the muscles, and angles of action at large angles to the plane of the 2-D model.

POSTVERTEBRAL MUSCLES of the NECK

<u>Obliquus Capitus Superior</u>	Atlas	Axis
Obliquus Capitus Inferior	Axis	Atlas
Rectus Capitis Posterior Major	Axis	Occipital Bone
Rectus Capitis Posterior Minor	Atlas	Occipital Bone

RATIONALE FOR MODELING THE ERECTOR SPINAE: This muscle group includes members which originate on the illiac crest and insert all along the spinal column, plus others which originate at various levels along the vertebral column and insert as high as the occipital bone of the skull. It is therefore best modeled as originating at the iliac crest and inserting on the skull, with attachments (pulleys?) to the vertebral column at intervals in between.

Table 5. Muscles Which Flex the Spine

Muscle	Origin	Insertion
Iliacus *	Iliac Fossa	Lesser Trochanter
Psoas Major *	L1-L5 Bodies	Lesser Trochanter
Psoas Minor **	T12-L1 Bodies	Illiopectineal eminence

* These muscles should not be considered in the model as their prime function is to flex the thigh.

** This muscle should not be included in the model because of its small moment arm.

PREVERTEBRAL MUSCLES of the NECK

Rectus Capitis Anterior	Atlas	Occipital Bone
Rectus Capitis Lateralis	Atlas	Occipital Bone
Longus Capitis	Transverse Process C2-C6	Occipital Bone
Longus Colli	Transverse Process of C3-T3	C1-C6

MOST REPRESENTATIVE ORIGIN: C2

MOST REPRESENTATIVE INSERTION: Occipital Bone

ABDOMINAL MUSCLES WHICH SERVE TO FLEX THE SPINE

Rectus Abdominus	Xiphoid Process	Pubic Symphysis and Pubic Crest
External Abdominal Oblique	Lower 8 ribs	Anterior Illiac Crest
Internal Abdominal Oblique	Illiic Crest and Inguinal Ligament	Last 4 Ribs, Linea Alba, and Pubis

RATIONALE FOR MODELING: Since the rectus abdominus is the chief antagonist of the erector spinae group, its origin and insertion should be used.

summarized. Graphical representations of the summarized information are shown in Figure 30.

The following question was asked: Could adequate body contours be generated by the computer if the various leg muscles were modeled in groups? This approach would simplify the modeling and save in development time, computer processing time, and required computer memory.

3.2.2. Alternative Methods of Muscle Depiction

The SDRC IDEAS 3.8 GEOMOD [4] solid modeling software used in development of the skeletal model allowed a choice of two methods for depicting the muscle groups.

The first method was to represent the muscle groups as ellipsoids. Advantages of this method were:

1. Ease of construction.
2. Relatively low required computer memory.
3. A constant volume assumption could be used to predict muscle dimensions following a change in length. It was shown before 1700 A.D. by numerous investigators [20] that muscle volume changes very little during contraction.

The main disadvantage of this method is that only approximate muscle contours can be developed.

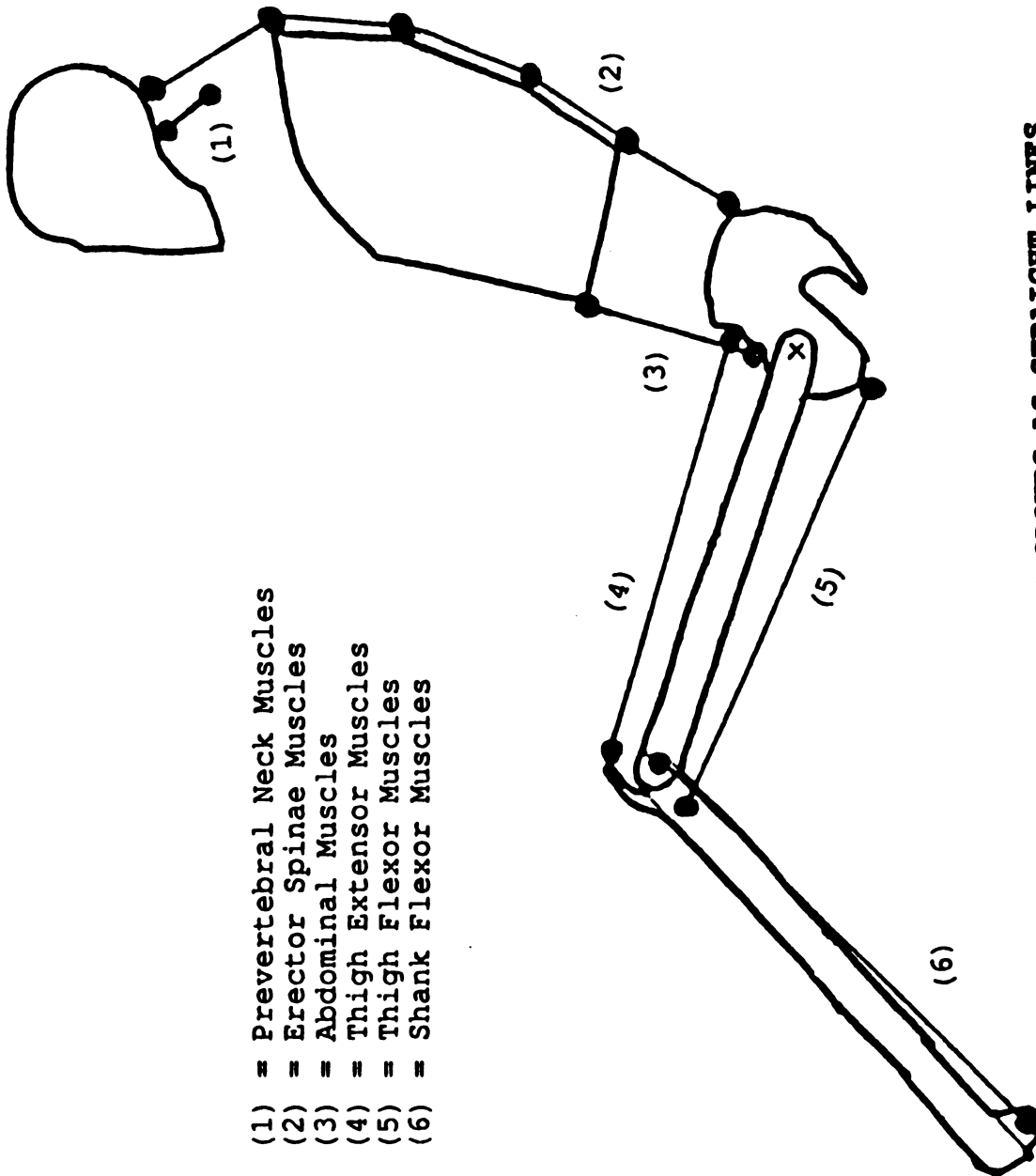


FIGURE 30: MUSCLE GROUPS AS STRAIGHT LINES

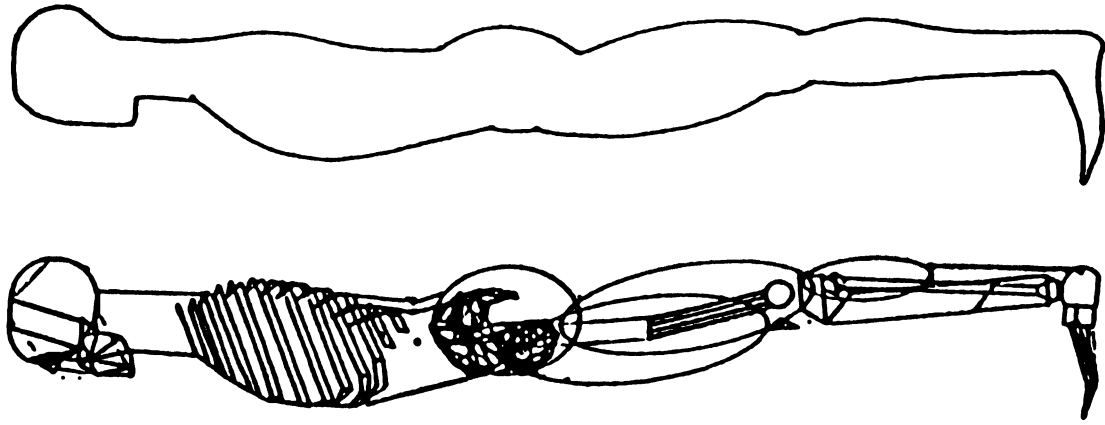
The second available method for modeling the muscle bellies was using a "skinning" technique, in which a series of cross-sectional templates is developed. Spaced at appropriate intervals along an imaginary axis, these templates would then be "covered" by a computer generated skin representing the muscle surface. The shapes thus created could be as detailed as desired, but at the expense of difficult, time-consuming construction and high use of computer memory and time. Figure 31 graphically depicts these two modeling methods. Representation of the muscle groups as ellipsoids was the method chosen for use in the model.

Most researchers investigating joint and muscle forces have assumed that muscles act along straight lines from origin to insertion, as such straight line models are sensitive to both segment position and orientation [21]. Other investigators [22], comparing the accuracy of such straight line models to that of models based on muscle belly centroids, concluded "the numerical data for the particular muscles examined showed a relatively small variation from straight lines...". Therefore, each muscle group in this model is represented by a single ellipsoid, its major axis extending from a representative muscle origin to a representative muscle insertion.

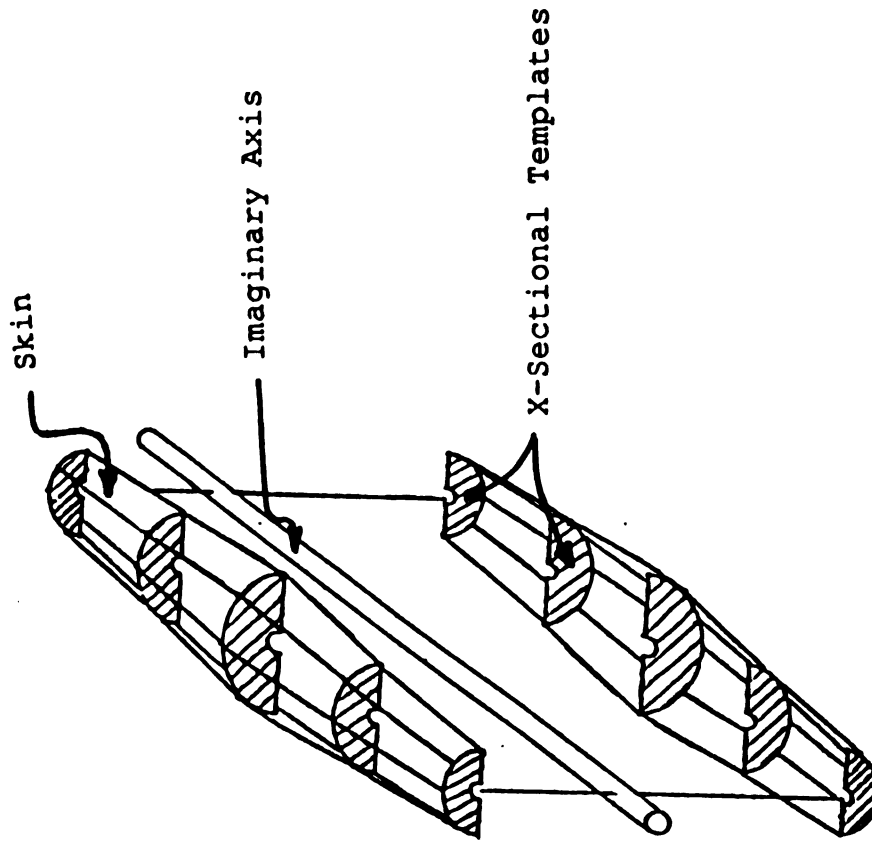
Two assumptions were made:

1. Total muscle volume = $(4/3) (\pi) (R_1) (R_2) (R_3)$ would remain constant, (where R_1 = one half the muscle length, R_2 =

Muscles Modeled as Ellipsoids



Exploded View of "Skinned" Muscle Model

**FIGURE 31: ALTERNATIVE MUSCLE MODELING TECHNIQUES**

one half the muscle width, and $R3 =$ one half the muscle thickness) and,

2. Since seat designers will be most interested in a side view of the model, muscle width (that muscle dimension parallel to the Y axis) should also remain constant. This second assumption is incorrect in a strict biological sense, and may be replaced by a more representative relationship between muscle width and thickness in future versions of the model if deemed necessary by users.

3.3. Muscle Modeling Results and Discussion

As evidenced by Figure 32, muscle modeling with ellipsoids does produce contours easily recognizable as those of the human leg; also, the problem of representing individuals with differing degrees of muscularity is easily handled by simply changing the selected muscle volumes. A muscle volume adjustment was included in the program to facilitate such changes; however, no attempt was made in this study to represent any particular level of muscular development.

Another advantage with this modeling approach is that since muscle volume and width are held constant, anytime a muscle shortens, it also gets thicker, or bulges, in a realistic manner.

The use of ellipsoids (with major axes running between muscle origins and insertions) to model major muscle groups usually generates body contours which look realistic;

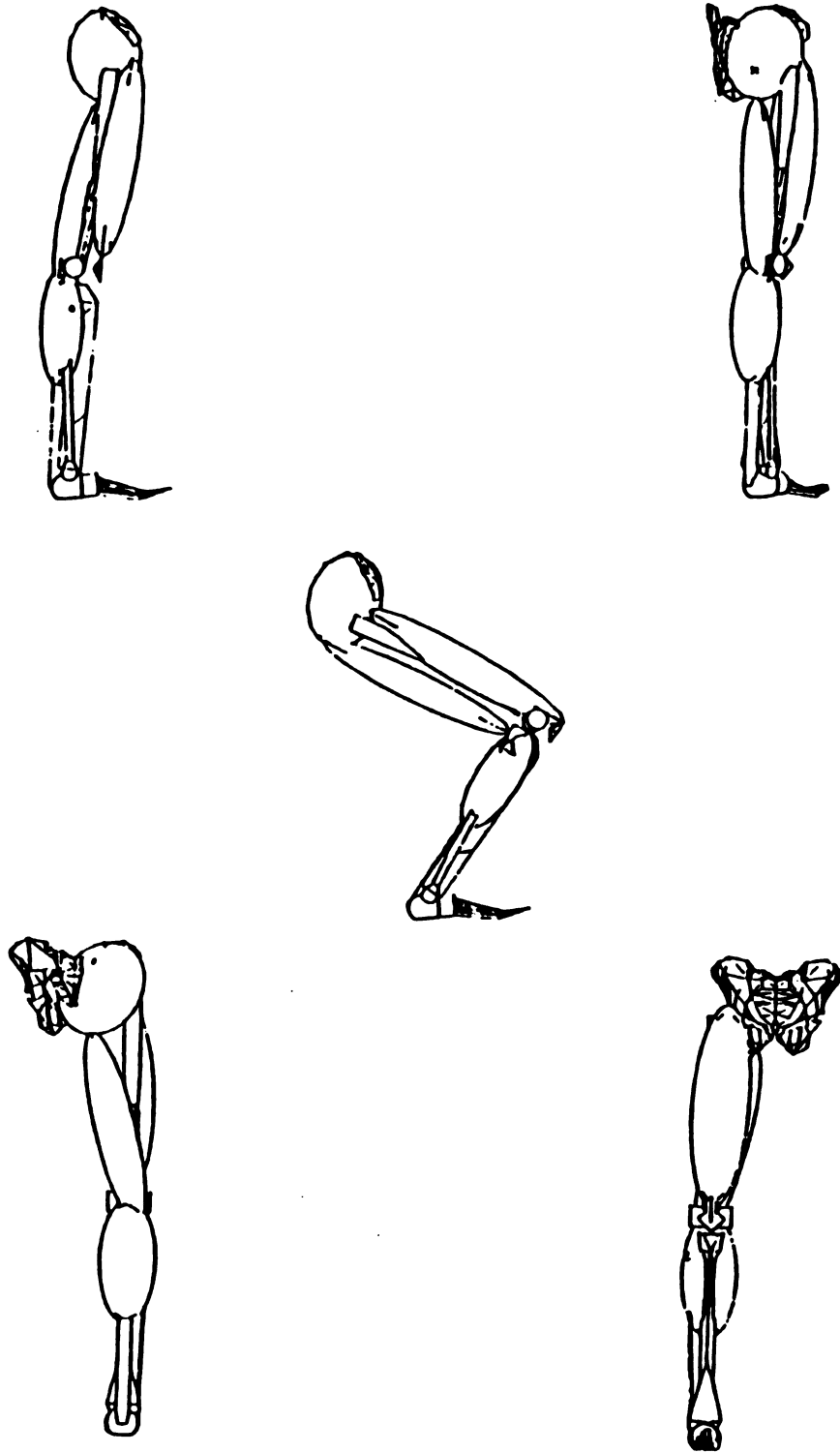


FIGURE 32: VIEWS OF THE MODEL LEG WITH MUSCLES

however, it should be noted that contours thus generated may become distorted in extreme body postures. Because actual tendons of origin and insertion may be forced to bend around boney structures during changes in posture, the relative positions of muscle bellies and skeletal structures change; since a straight line connecting the origin and insertion of a muscle group cannot simulate such tendon deformation [21], modeling results in extreme postures may be compromised.

Figure 33.a is a hidden line plot generated for a posture of extreme hip and knee joint flexion. It can be readily seen that true anatomical relationships are lost in this plot. The use of ellipsoids to represent muscle groups results in the apparent burrowing of the Achille's tendon through the tibia, as well as the passage of the quadriceps muscle group through the distal femur.

Figure 33.b is the same posture as that in Figure 33.a, but with manually simulated curvature in the quadriceps tendon of insertion and the tendon of origin of the gastrocnemius muscle. Clearly, more accurate representation of the anatomy is generated; however, the automation of this tendon curvature would be prohibitive in terms of increased programming complexity and running time. It must therefore be remembered by users of this model that body contours generated in extreme postures may not be satisfactory for seat design purposes.

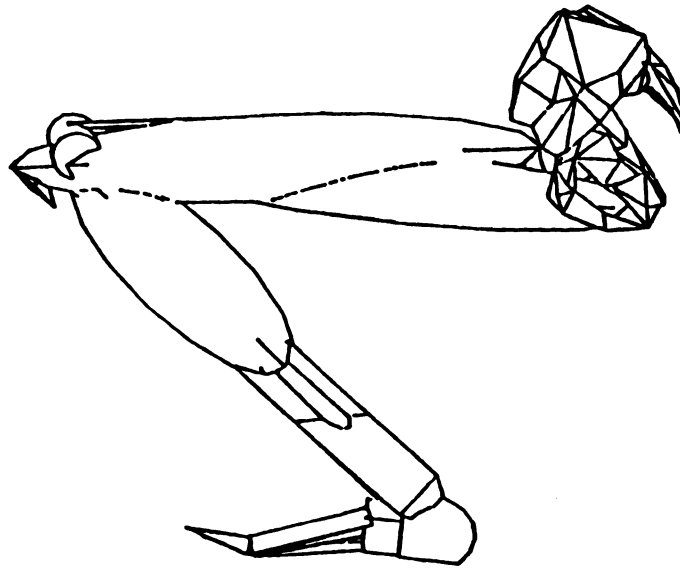


Figure 33(a)

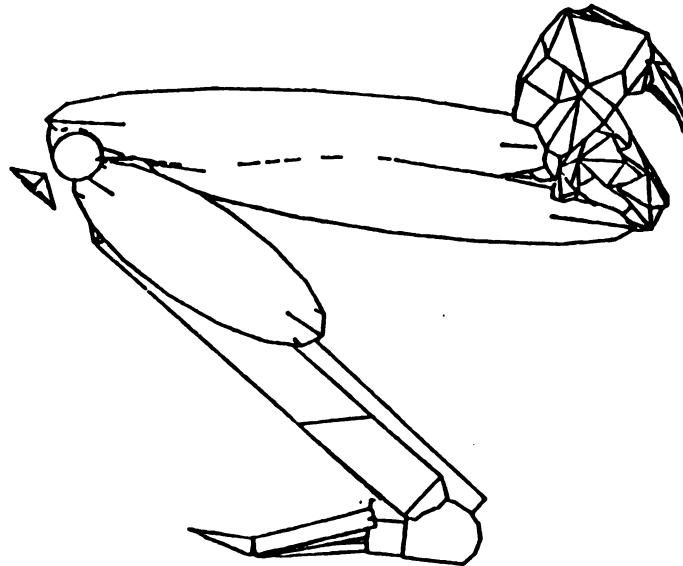


Figure 33(b)

FIGURE 33: A POOR MUSCLE MODELING RESULT

4. MUSCLE LENGTH CONSTRAINT OF SKELETAL MOTION

4.1. Introduction

To be useful in the seating design environment, the geometric model of the human body developed here must be representative both in the configuration of its segments and in the range of motion it permits between segments. In order to assess the acceptability of a selected posture, a method of predicting allowable combinations of joint angles must be found.

The following hypothesis was proposed: Muscle lengths impose limits upon what postures may be assumed by adults, and, within any given individual, regardless of posture, muscle length will not exceed a certain upper limit. The findings of a study by Stokes and Abery [23] are consistent with the hypothesis that the range of hip flexion permitted by the hamstring muscles influences lumbar spine curvature during sitting. Tension in the hamstring muscles necessitates rotation of the pelvis to maintain comfort [19,23]. Thus, if a limiting muscle length condition could be shown to exist for the hamstrings, the mechanism which makes the positions of the upper leg, lower leg, pelvis, and lumbar spine interdependent could be accurately modeled.

A decrease in hamstring length necessitates a more upright seated posture, e.g. people with shortened hamstrings find it awkward to sit in low slung, reclining seats. If the validity of such a limiting hamstring length could be demonstrated experimentally, the computer programs

used to position the geometric model could utilize hamstring muscle length as a criterion to orient the model's pelvis, legs, and lumbar spine, and to judge the appropriateness of any selected posture. Similar methods might also be used to determine acceptable combinations of ankle and knee angles as limited by gastrocnemius length, and to establish the relationship between TLC and pelvic tilt as limited by the length of the lumbar musculature.

The objectives of this investigation of limiting hamstring length were to experimentally determine:

1. what combinations of measured knee and hip angles (Figure 34) are permissible within a given individual;
2. whether or not the range of these permissible angular combinations is limited to a single body posture;
3. if the observed limitations in possible combinations of hip and knee angles are due to a limiting length of the hamstrings; and
4. if a simple four bar linkage might serve as a satisfactory model of the limiting motions of the pelvis, femur, hamstrings, and lower leg.

4.2. Experimental Methods

4.2.1. Biomechanics Evaluation Laboratory

All experimental data were collected at the Biomechanics Evaluation Laboratory (BEL) of Michigan State University. Basic data acquisition systems of the laboratory include three-dimensional motion analysis. All data were collected on a SUN 4/260C workstation. This SUN

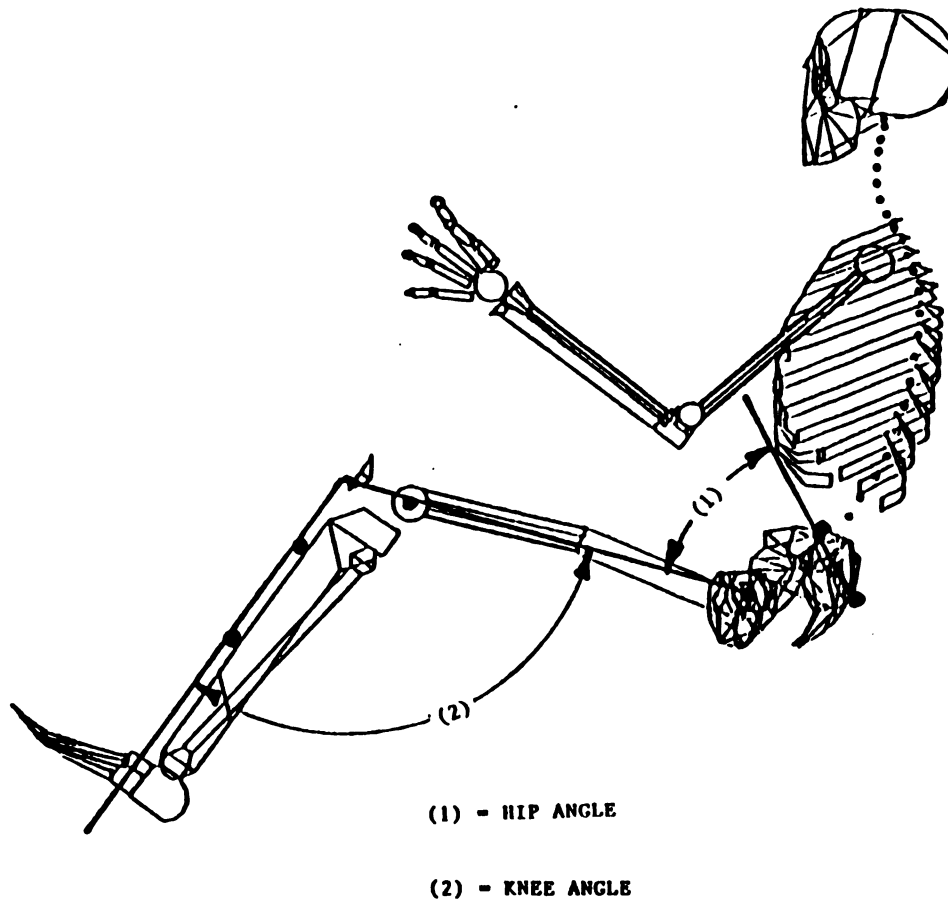


FIGURE 34: HIP ANGLE AND KNEE ANGLE DEFINED

was networked with the A.E. Case Center for Computer-Aided Design in the College of Engineering.

Motion of a body segment was measured by placing retro-reflective spherical targets on anatomical landmarks. A four camera 60 Hz Motion Analysis, Inc. system tracked the trajectories of the targets in space, yielding three-dimensional position data. A video processor identified targets using the light reflected to the cameras. The camera apertures were closed to increase target light intensity relative to ambient light. The video processor digitized target data in pixel space from all four cameras in real time, and then transferred digital position data to the SUN workstation. Direct Linear Transformation routines from "EV3D" software were used to obtain three-dimensional target coordinates. Every tenth frame of collected data was analyzed.

4.2.2. Data Gathering and Analysis

Because the muscle origins and insertions of interest are located on the boney skeleton, for any single skeletal geometry, there can exist only one corresponding muscle length. Therefore, it should be valid to study the skeletal geometry in the limiting postures, which in turn would imply the muscle length. This is not to imply that there can only be one muscle circumference per skeletal posture. For example, one can easily change the circumference of the biceps muscle in the upper arm by contracting it while maintaining a constant elbow angle.

4.2.2.a. Description of Exercises

To experimentally examine the maximum muscle length hypothesis, four human subjects, whose physical characteristics are listed in Table 6., were targeted with adhesive reflective spheres in the following locations:

1. The highest point on the right illiac crest
2. The highest point on the left illiac crest
3. The spine of the first sacral vertebra
4. Right greater trochanter
5. Right lateral femoral epicondyle
6. Right fibular head
7. Anterior surface, proximal right tibia, approximately one third the distance from knee to ankle
8. Anterior surface, distal right tibia, approximately two thirds the distance between the knee and ankle.

Two of the subjects each had an additional target, number 9, placed on the posterior midline of their right calf to facilitate tracking rotation of the lower leg about the tibial axis.

Table 6. Subject Data

	Height (mm)	Weight (Kgm)	Age (years)
Subject 1:	287	82	47
Subject 2:	268	73	22
Subject 3:	264	75	44
Subject 4:	283	77	43

A "standing file" was created for each subject with the subject standing erect, his right foot supported on a chair at a height which produced approximately 90 degrees of hip flexion (Figure 35). Following palpation and compression, an estimate of the depth of soft tissue covering the right ischial tuberosity was made. An additional target, number 10, was then placed on the buttock surface over the right ischial tuberosity, and approximately 3 seconds worth of data was collected while the test subject remained as motionless as possible. The marker on the right ischial tuberosity was then removed. The spatial relationship between the fixed pelvic markers (1,2, and 3) and the right ischial tuberosity was thus determined, making it possible to estimate the spatial position of the tuberosity whenever the locations of the other three pelvic markers are known.

The volunteers performed two exercises which caused them to reach their individual limits of hamstring stretch, while simultaneous determinations of upper leg, lower leg, and pelvis positions were conducted. The first experimental exercise was designed to increase hamstring tension through hip flexion, while the second exercise created hamstring stretch by opening the knee angle. Muscle length would then be estimated from these position studies.

The two experimental exercises were performed as follows (Figure 36):

Exercise I: The test subject began by standing erect. He slumped forward at the waist, keeping his knees

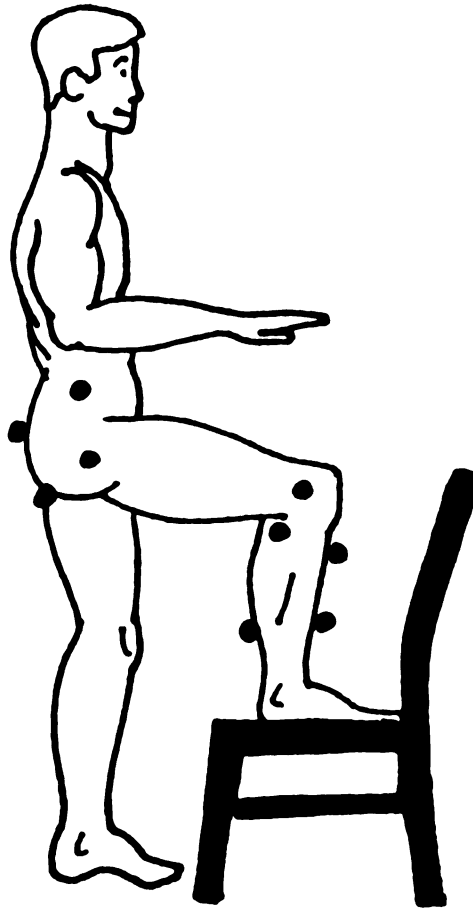


FIGURE 35: CREATION OF A STANDING FILE

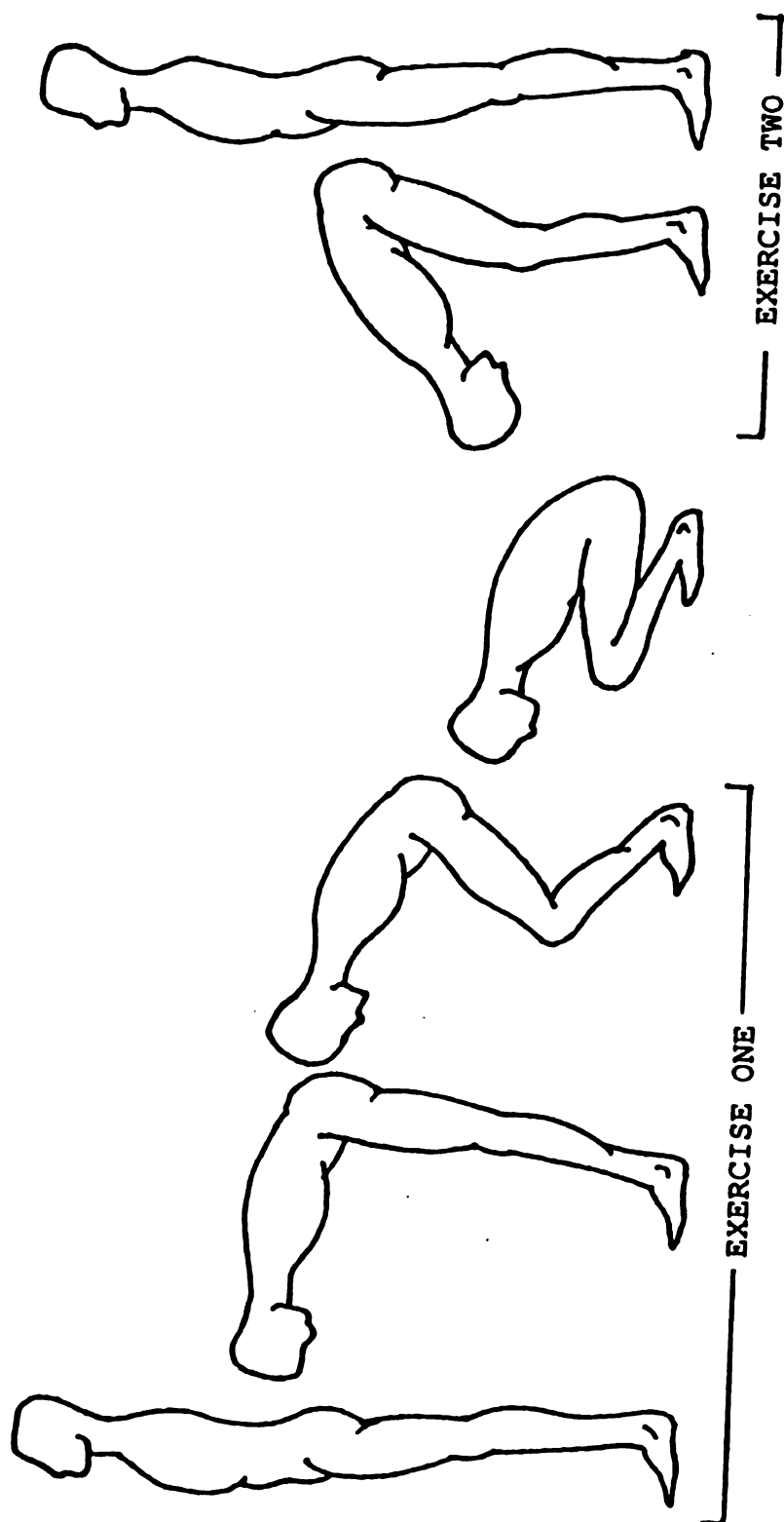


FIGURE 36: THE EXPERIMENTAL EXERCISES

straight, until hamstring tension prevented further motion. The knees were then allowed to slowly bend (the subject maintaining hamstring tension by additional, simultaneous bending at the waist) until the subject reached a "sitting on the heels" posture.

Exercise II: After completing Exercise I, the subject straightened the knees as far as possible without moving his head. After a short pause, the subject maintained hamstring tension for as long as possible while slowly returning to the erect posture.

These exercises were preceded by a period of suitable warmup stretching motions of the hamstrings and lower back muscles to increase repeatability of the test runs. Each of the four test subjects performed the sequence of exercises three times, thus creating twelve sets of experimental results.

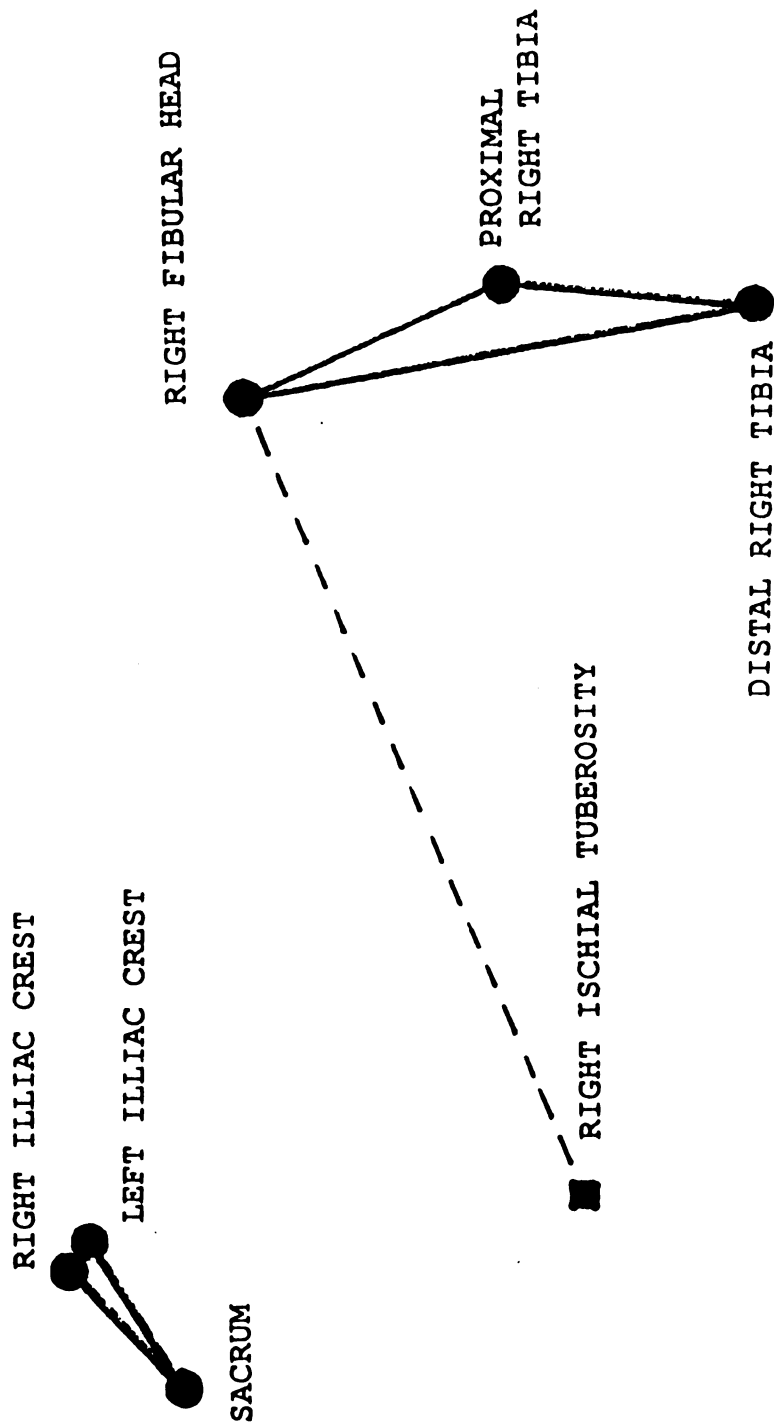
4.2.2.b. Calculation of Muscle Lengths

The long head of the biceps femoris muscle was deemed to be most representative of the hamstring muscle group (Table 2), and its length, defined as the straight line distance between its origin on the right ischial tuberosity and insertion on the right fibular head, was used to estimate the length of the entire right hamstring muscle group.

The distance between the right hamstring origin and insertion (ischial tuberosity and fibular head, respectively) was calculated as follows. Using the 3-D

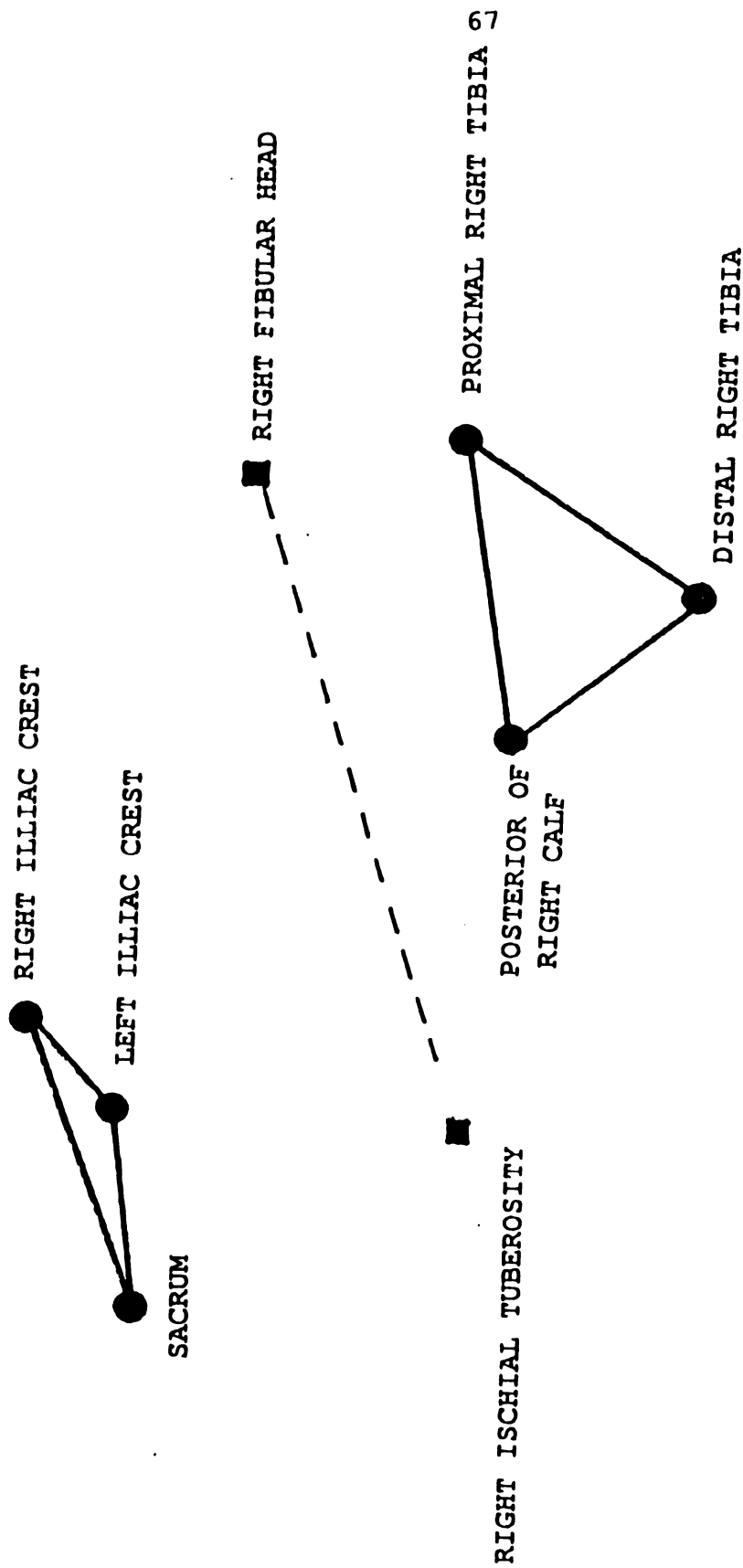
spatial relationship between the right ischeal tuberosity and the other three pelvic markers (1,2,and 3) established in the standing file in conjunction with the known coordinates of pelvic markers 1,2, and 3 during the exercises, the spatial coordinates of the ischeal tuberosity could be computed. Because the right fibular head was targeted, its spatial coordinates were tracked. The trigonometric distance between these two known points (ischial tuberosity and fibular head) represented the hamstring muscle length.

A three dimensional computer representation of each subject's skeletal geometry was constructed by utilizing the spatial coordinates of the skeletal markers developed in the standing files (Figures 37 & 38). The I-DEAS software then was used to manipulate these representations, by using the known coordinates of the live subject's skeletal markers to position the corresponding markers on the representations, through motions duplicating those performed by the live test subjects. In Figures 37 and 38, target locations shown as circles were positioned in computer space using the corresponding subject target coordinates. The locations shown as squares were then calculated using known spatial relationships from the standing files. The software also simultaneously calculated the distance between the estimated location of the ischial tuberosity and the coordinates of the fibular head.



Note: This geometry is for subjects not targeted on the posterior surface of the right calf.

FIGURE 37: COMPUTER REPRESENTATION OF SUBJECT TARGETING GEOMETRY - TYPE ONE



Note: This geometry is for subjects targeted on the posterior surface of the right calf.

FIGURE 38: COMPUTER REPRESENTATION OF SUBJECT TARGETING GEOMETRY - TYPE TWO

4.2.2.c. Calculation of Limb Angles

Angular relationships between various skeletal components were tracked as follows (Refer to Figure 39):

1. Vector A was defined as originating at the target located on the distal right tibia and extending to the target on the proximal right tibia, thus representing the spatial orientation of the lower right leg;
2. Vector B was defined as originating at the right greater trochanter and extending to the right femoral epicondyle, thus representing the spatial orientation of the right thigh;
3. Vector C was defined as originating at the upper midline of the sacrum and extending to a point midway between the high points of the right and left iliac crests, thus creating the ability to track pelvic tilt in the sagittal plane.

It should be noted here that the skeletal tracking was done in a relative sense only - the exact position of the bones in space was unknown due to possible uncertainty in placement of the targets relative to bony landmarks.

Because the locations of the targets on the test volunteers defined the tails and tips of these vectors, both ends of all three vectors were tracked during the experiment, making construction of the vectors possible for each frame of data.

Hip Angle for the live subjects was defined as the angle between Vectors C and B, while Knee Angle was defined

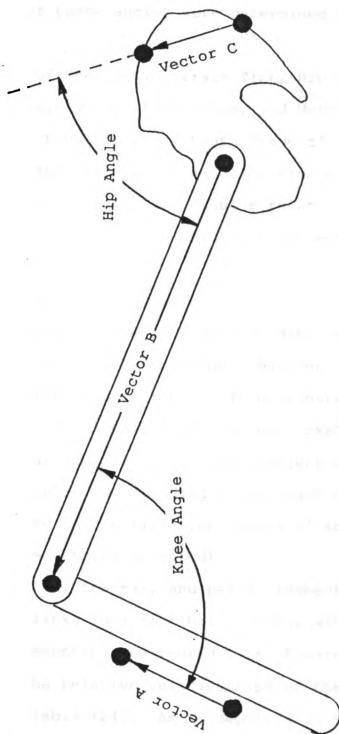


FIGURE 39: VECTOR DEFINITIONS

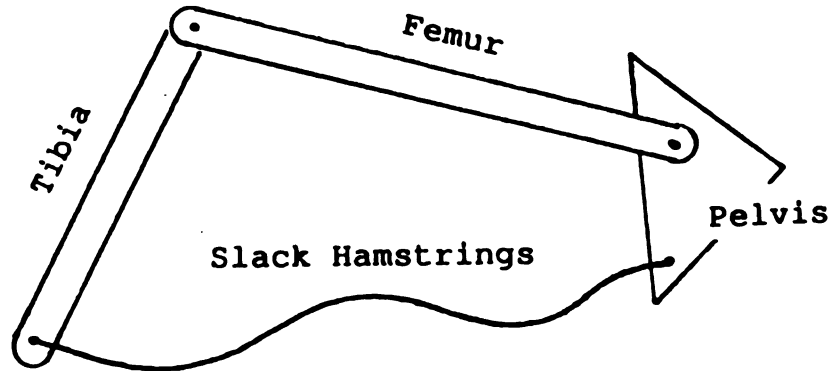
as that angle which existed between Vectors B and A. The magnitudes of these angles were determined using dot products.

Graphs of Knee Angle versus Time, Hip Angle versus Time, Hip Angle versus Knee Angle, and Muscle Length versus Time were plotted for every tenth frame of data. The resulting graphs were examined to determine if similar limiting muscle lengths and angular relationships existed for both exercises, both within each subject and between subjects.

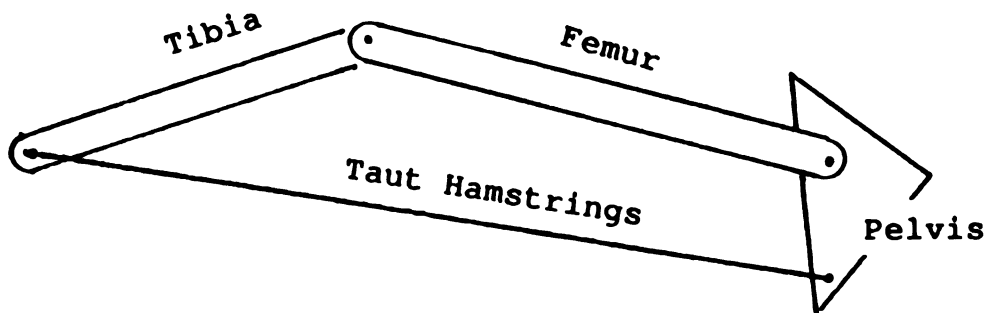
4.2.2.d. Link Length Variations

Examination of the experimental data revealed that the apparent distances between targets mounted on the same boney structure varied considerably. To eliminate this complication, a nominal length for each skeletal segment (femur, tibia, and pelvis) in each subject was determined using the data in the standing files (each segment length was calculated in the first ten frames of standing file data, and the results averaged).

The tibial, femoral, and pelvic segments may be thought of as three links in a four bar linkage, with the hamstring muscles representing the fourth link (Figure 40). Equations predicting the relative relationships of the four links are readily available [24]. As is depicted in Figure 41, the definition of Hip Angle in the linkage equations differs from that used in the laboratory. It was thus necessary to

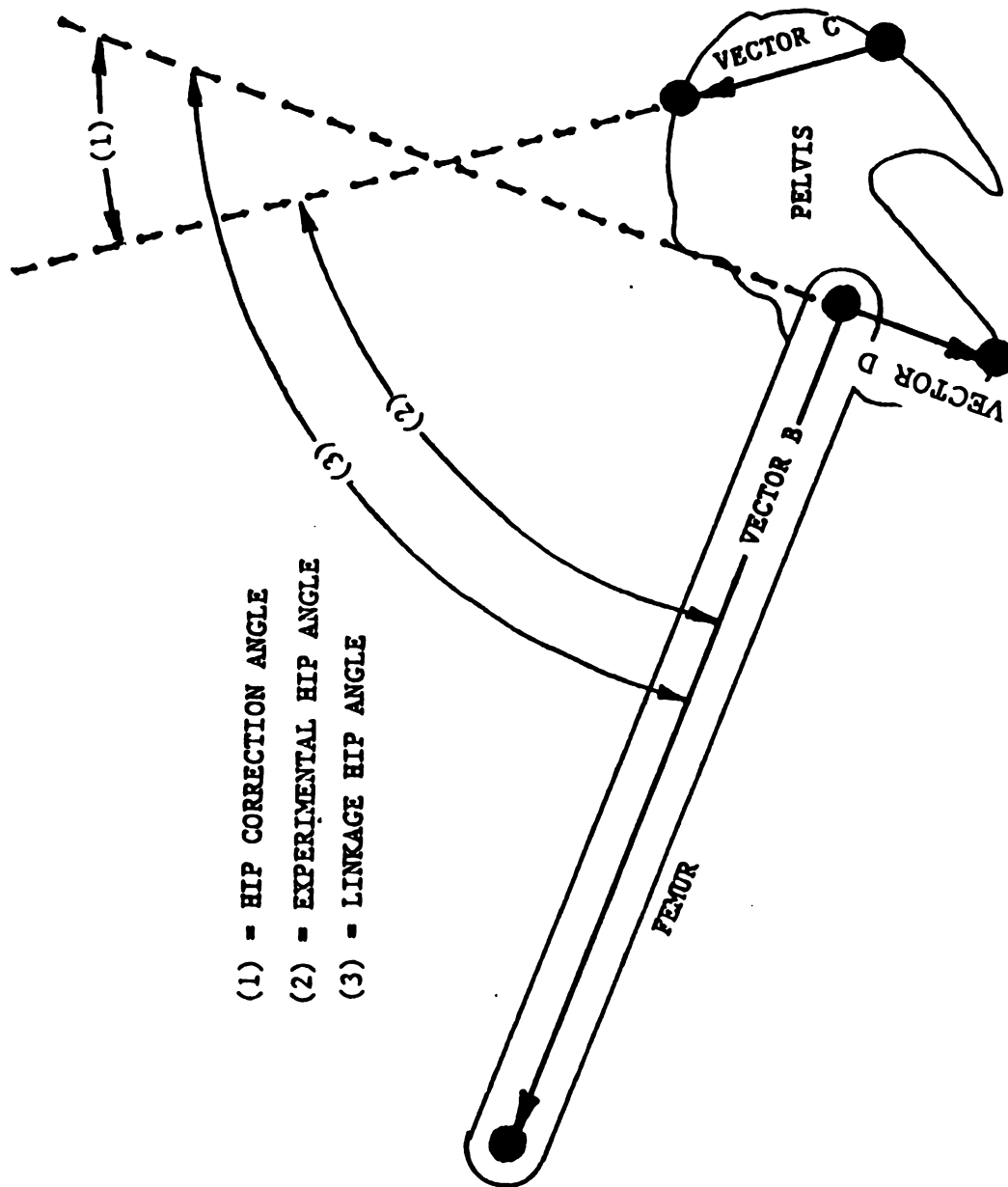


"No Tension Situation"
Linkage Equations Do Not Apply



"Limiting Tension Situation"
Linkage Equations Do Apply as Long
as Limiting Tension is Maintained

FIGURE 40: THE PELVIS AND THIGH AS A FOUR BAR LINKAGE



- (1) - HIP CORRECTION ANGLE
- (2) - EXPERIMENTAL HIP ANGLE
- (3) - LINKAGE HIP ANGLE

FIGURE 41: LINK HIP ANGLE AND LABORATORY HIP ANGLE

convert the Laboratory Hip Angle to equivalent Linkage Hip Angles by using the following relationship:

$$\text{LABORATORY HIP ANGLE} + \text{PELVIC CONSTANT} = \text{LINKAGE HIP ANGLE},$$

where the Pelvic Constant is the angle between Vector C and Vector D, which extends from the right greater trochanter (the greater trochanter of the femur is commonly used in the automotive seating design industry to estimate the location of the hip joint center) to the right ischial tuberosity. The value of the pelvic constant is thus specific to each of the test subjects.

The nominal skeletal segment lengths were utilized along with the experimentally determined knee angles and the converted hip angles as input to a four bar linkage equation (Appendix D) which was used in an iterative manner to predict the length of the fourth segment, that representing the hamstring muscle length. The corrected hamstring lengths thus calculated were plotted against time.

In an attempt to determine the ability of the geometric model developed in the previous sections of this thesis to predict trends in the hamstring lengths of live humans, a computer program (Contained in Appendix E) was written which would cause the model to duplicate the experimental exercises performed by the human volunteers. Because this program uses pelvic, hip, and knee angles as input, it was possible to use the known angular data from the human experimental subjects as input, thereby causing the computer

model to recreate the motions of the live test subjects (Figure 42).

The model's hamstring length (the straight line distance between the model's ischial tuberosity and fibular head) was calculated for each posture of interest, so that trends in the model's hamstring length could be compared to those generated in the human trials. Using the models dimensions in the linkage equations, a composite plot was created which shows what combinations of knee angle and hip angle are possible for a variety of hamstring lengths (Figure 43).

The twelve corrected muscle length versus time graphs were examined to determine what data points corresponded to an approximately constant muscle length. The corresponding data points from the knee angle versus hip angle plots were superimposed on the composite plots in an attempt to gage the correlation between theoretically acceptable angular combinations and those actually observed in the laboratory.

In summary, three different types of hamstring lengths were computed for each set of human subject motion data:

1. Hamstring length for each frame of subject body position data based on target positions on the pelvis and lower leg (hereafter referred to as Muscle Length),
2. Hamstring length for each frame of data based on hip angle, knee angle, and average lengths of the pelvic, femoral, and tibial links, (hereafter referred to as Corrected Muscle Length), and

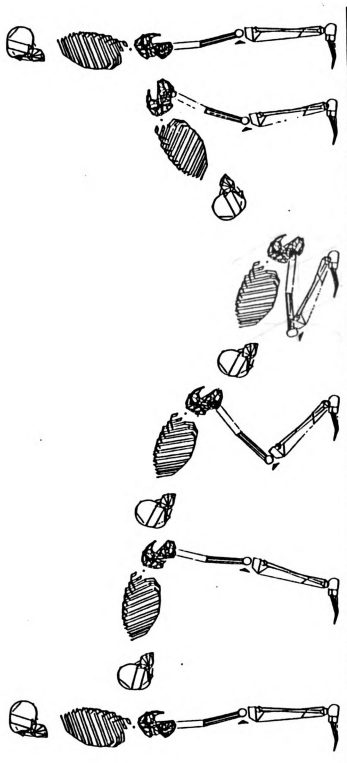


FIGURE 42: THE MODEL DOES THE LABORATORY EXERCISES

Knee Angle
(Degrees)

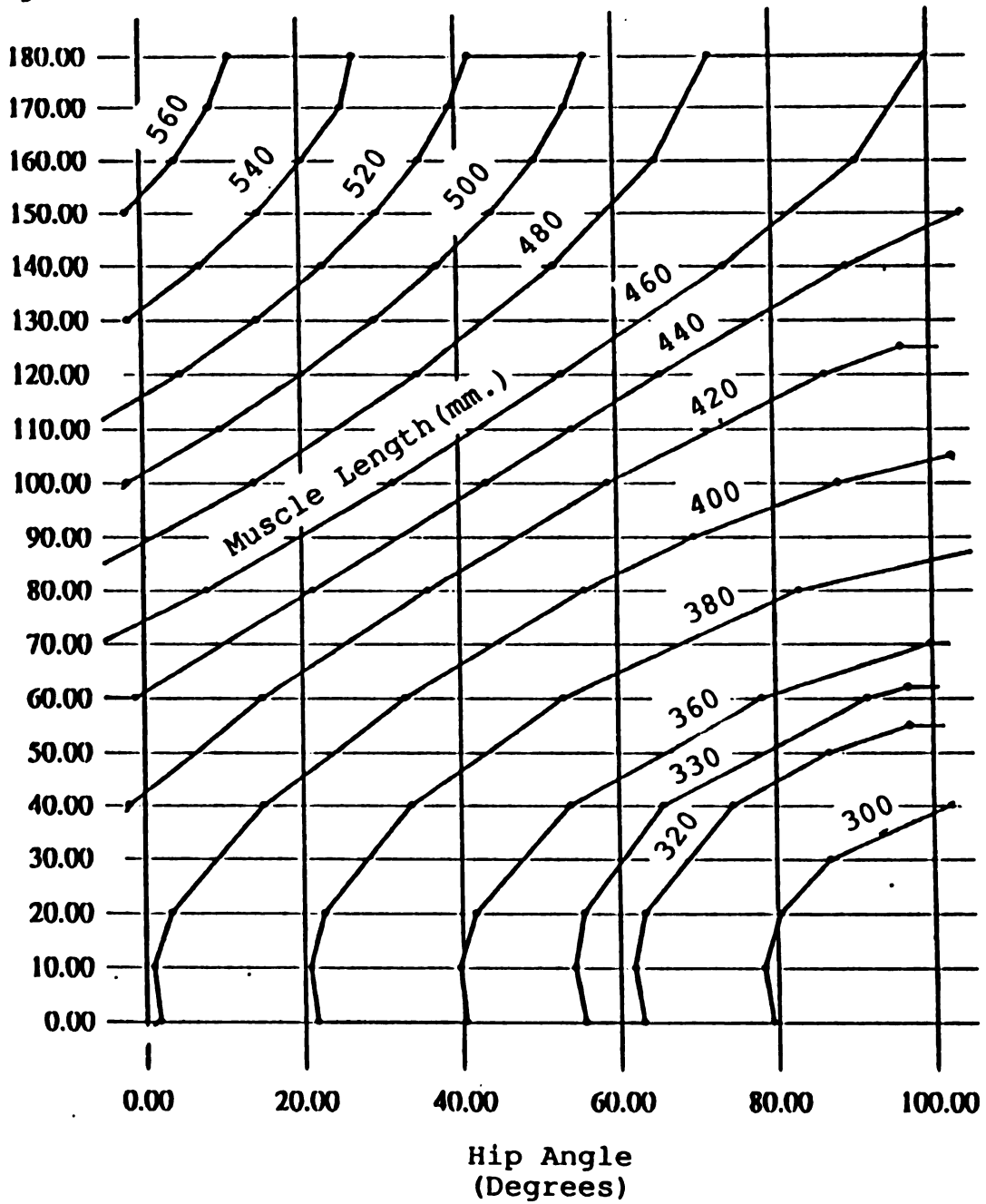


FIGURE 43: HAMSTRING LENGTH RELATED TO JOINT ANGLES

3. Hamstring lengths in the model which correspond to the pelvic and knee angles measured in each frame of subject body position data (hereafter referred to as Model Muscle Length).

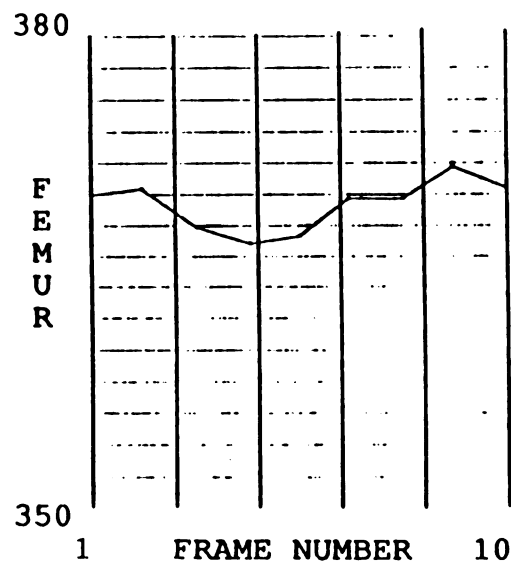
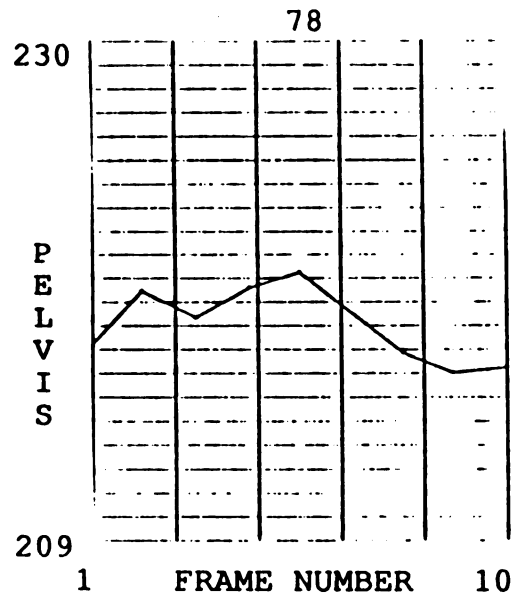
4.3. Muscle Length Results and Discussion

Nominal link lengths and pelvic constants (both defined in Section 4.2.2.), determined using target data from the standing files (Section 4.2.2.) via dot products, were as follows: (Also See Figures 44 through 47).

Table 7: Nominal Link Lengths(mm) and Pelvic Constants(deg)

	Tibia	Femur	Pelvis	Pelvic constant
Subject 1:	53.7	369.3	218.0	68
Subject 2:	48.2	407.4	145.5	59
Subject 3:	47.0	350.7	124.2	73
Subject 4:	87.6	363.4	142.1	79

The fact that the pelvic links were relatively much longer when compared to their corresponding femoral links in the test subjects than they were in either the geometric model or the UMTRI drawings (Table 8), supports the supposition that the method of estimating the depth of soft tissue over the ischial tuberosity probably included some errors. In retrospect, some soft tissue thickness was likely included during the determination of pelvic segment lengths.



Note: all
lengths are
in
millimeters

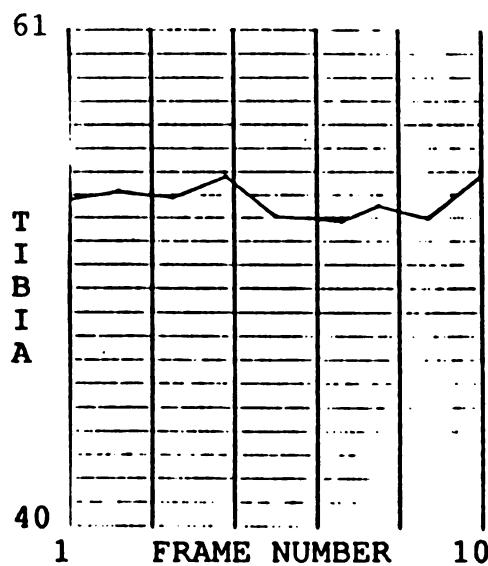
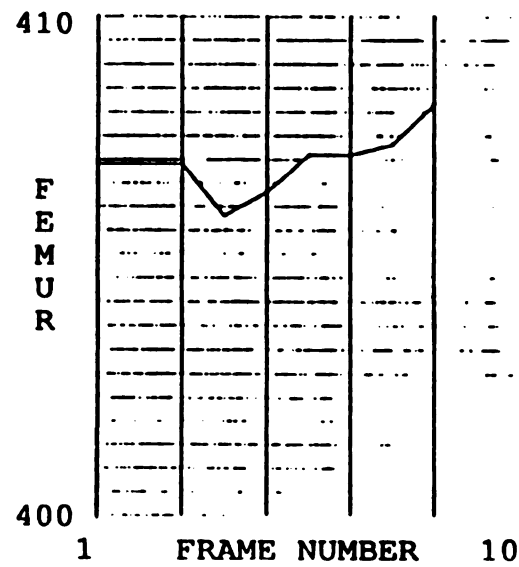
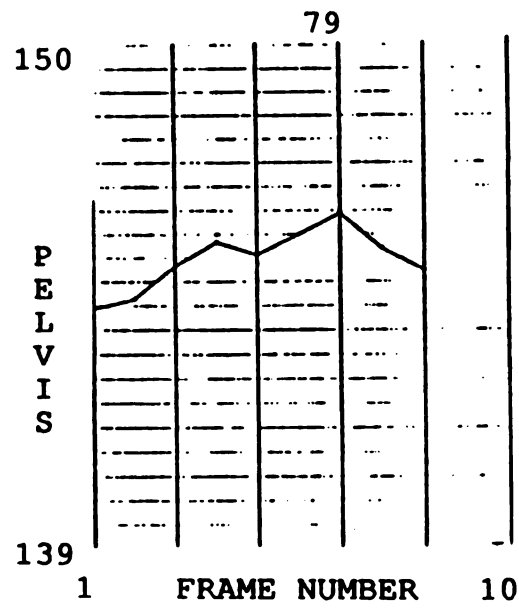


FIGURE 44: VARIATIONS IN SKELETAL LINK LENGTHS, SUBJECT 1



Note: all
lengths are
in
millimeters

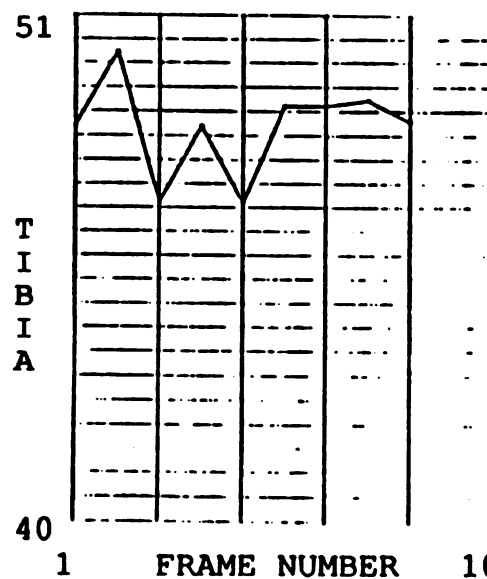
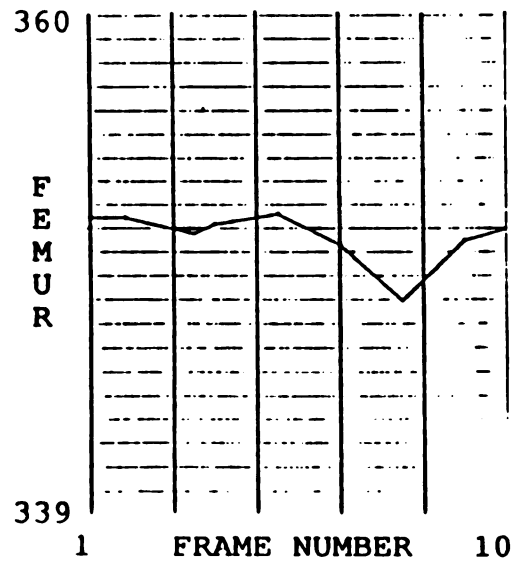
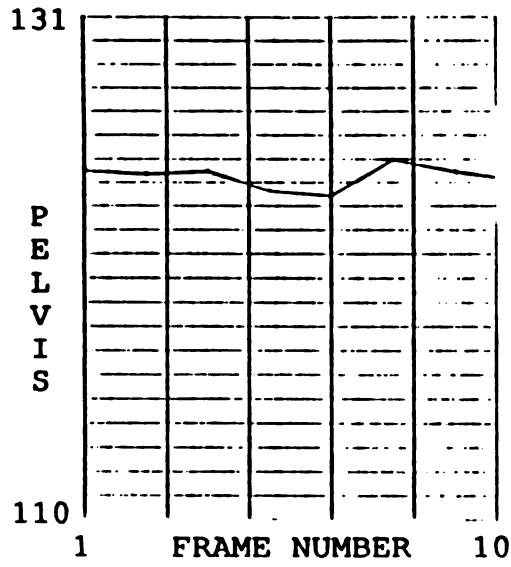


FIGURE 45: VARIATIONS IN SKELETAL LINK LENGTHS, SUBJECT 2

80



Note: all
lengths are
in
millimeters

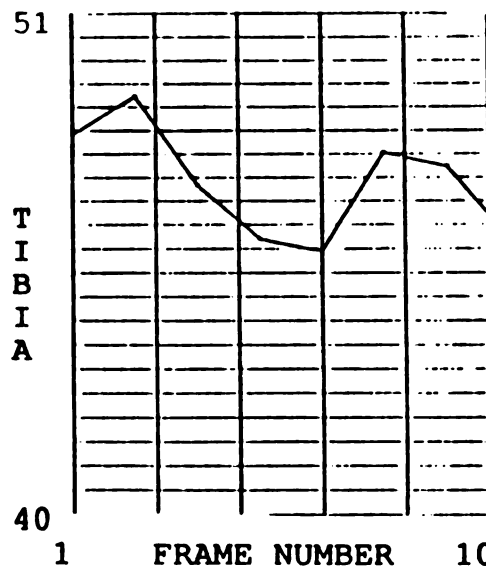
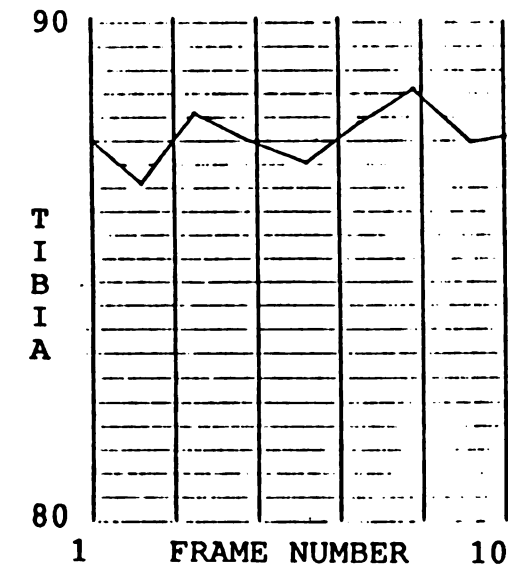
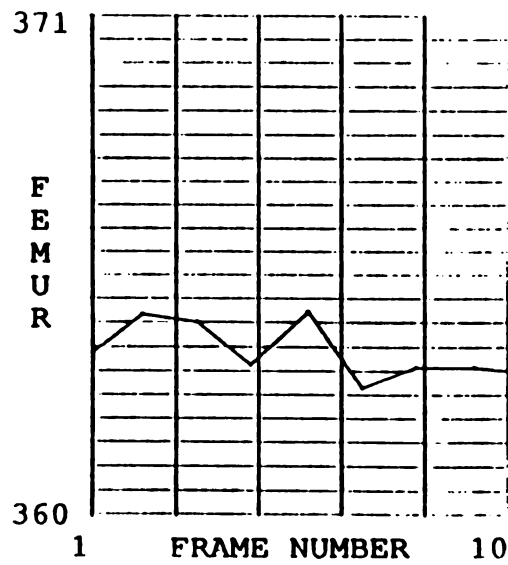
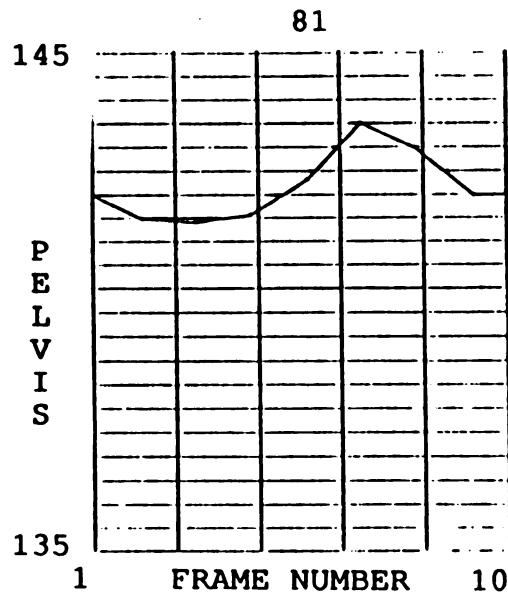


FIGURE 46: VARIATIONS IN SKELETAL LINK LENGTHS, SUBJECT 3



Note: all
lengths are
in
millimeters

FIGURE 47: VARIATIONS IN SKELETAL LINK LENGTHS, SUBJECT 4

Table 8. Link Length Ratios by Subject

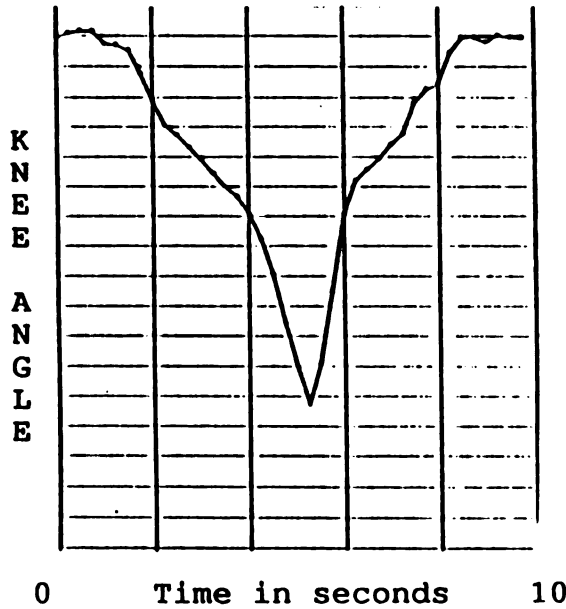
	Tibia/Femur Ratio	Pelvis/Femur Ratio
Subject 1:	.146	.590
Subject 2:	.118	.357
Subject 3:	.134	.354
Subject 4:	.241	.391
Model:	.198	.178
UMTRI:	.119	.224

4.3.1. Experimental Results in Graphical Form

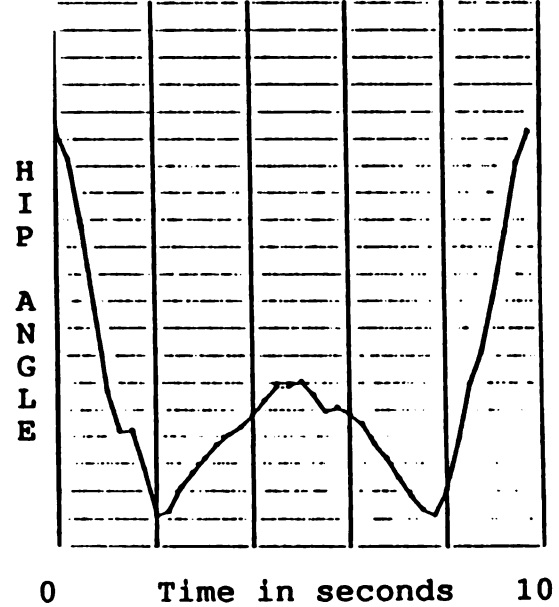
The Knee Angle versus Time, Hip Angle versus Time, Knee Angle versus Hip Angle, and Muscle Length versus Time graphs prepared from the raw laboratory data are presented in Figures 48 through 59.

Using the graphs in Figure 54 as being representative, we see that the following events occurred during a typical pair of exercises. The subject began Exercise One just before data recording began; thus, the hip angle begins at a value smaller than that observed during normal stance at the end of the trial. The hip angle decreased rapidly at the start of Exercise One due to bending at the waist. It continued to do so until hamstring stretch prevented further bending at about 1.5 seconds. The hip angle then remained constant until 3 seconds as the subject discovered he could bend no further at the waist. At 3 seconds, the knees began to bend. The decreasing knee angle relieved hamstring tension, thus allowing the hip angle to again begin

180

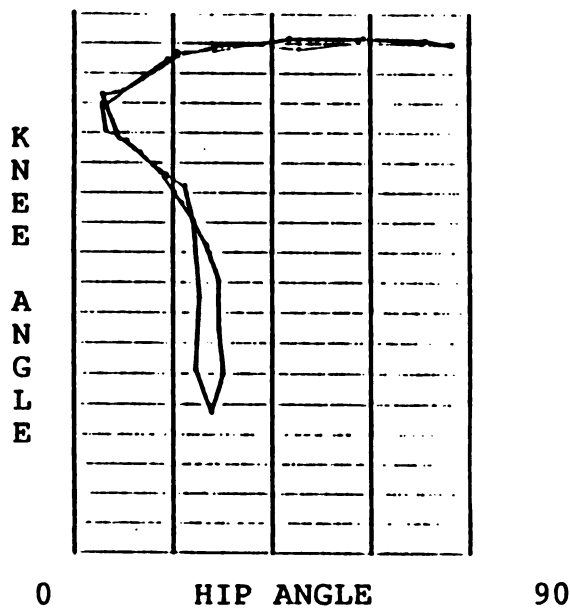


100



Note: Angles in degrees, Length in millimeters

180



600

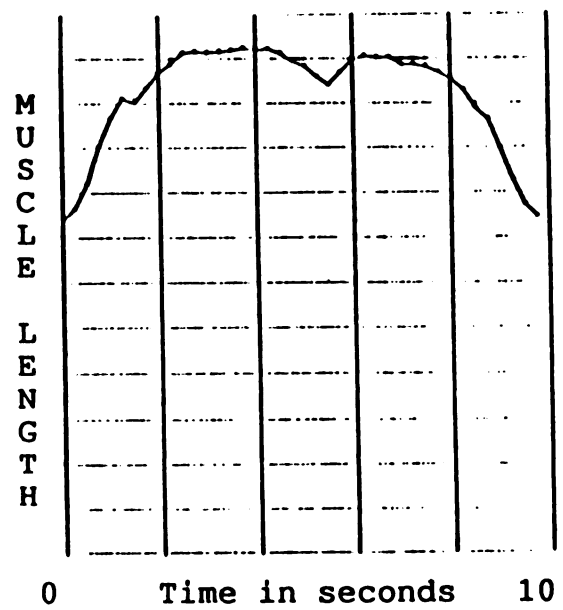
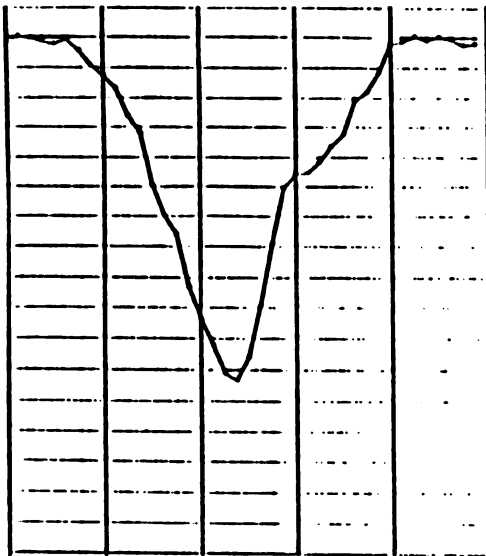


FIGURE 48: UNPROCESSED EXPERIMENTAL DATA, SUBJECT 1, TRIAL 1

180

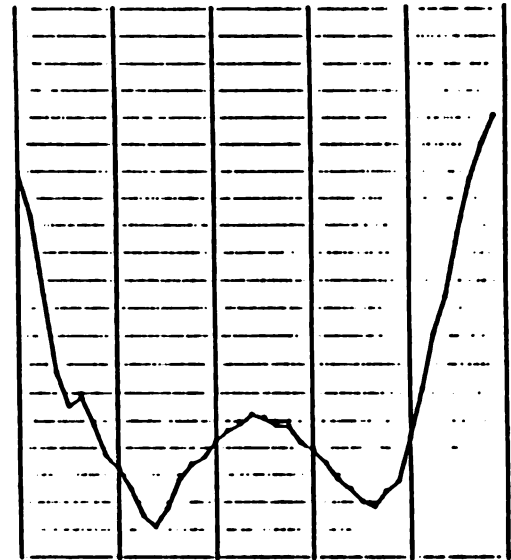
K
N
E
E

A
N
G
L
E

0 Time in seconds 10

100

H
I
P

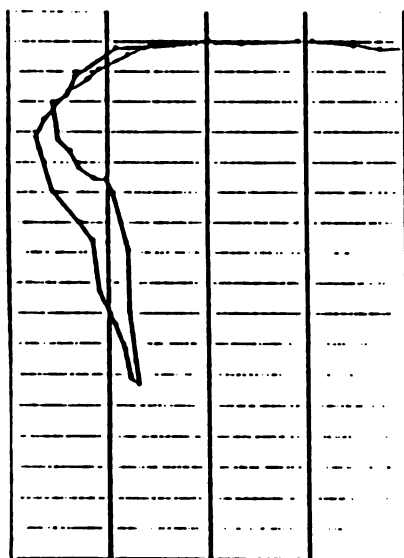
A
N
G
L
E

0 Time in seconds 10

Note: Angles in degrees, Length in millimeters

180

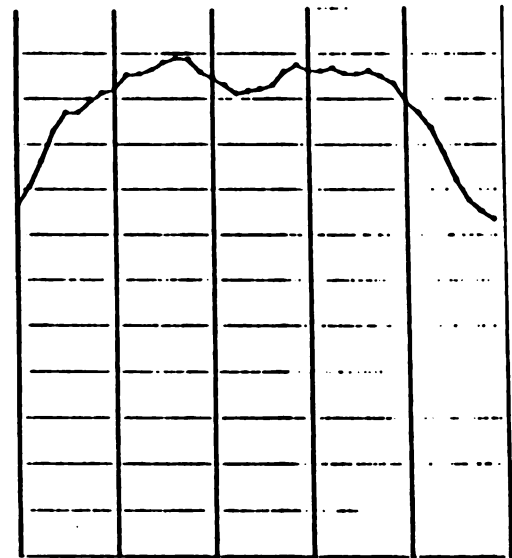
K
N
E
E

A
N
G
L
E

0 HIP ANGLE 90

600

M
U
S
C
L
E

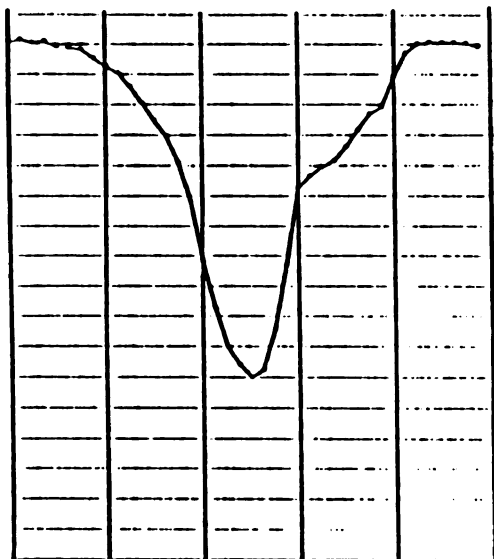
L
E
N
G
T
H

0 Time in seconds 10

FIGURE 49: UNPROCESSED EXPERIMENTAL DATA, SUBJECT 1, TRIAL 2

180

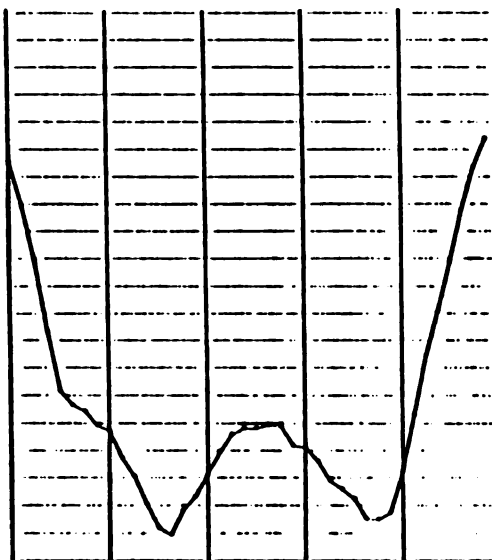
K
N
E
E

A
N
G
L
E

0 Time in seconds 10

100

H
I
P

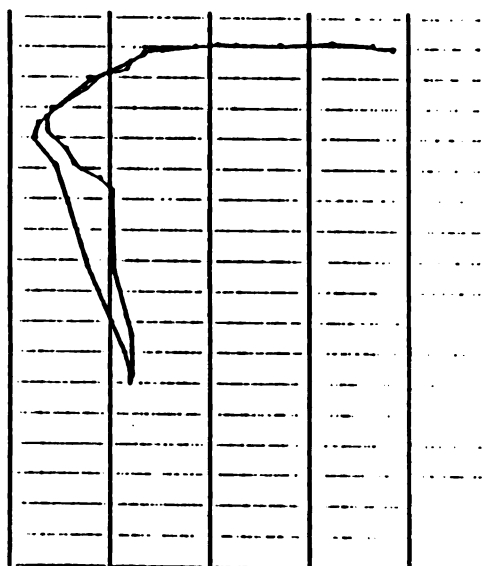
A
N
G
L
E

0 Time in seconds 10

Note: Angles in degrees, Length in millimeters

180

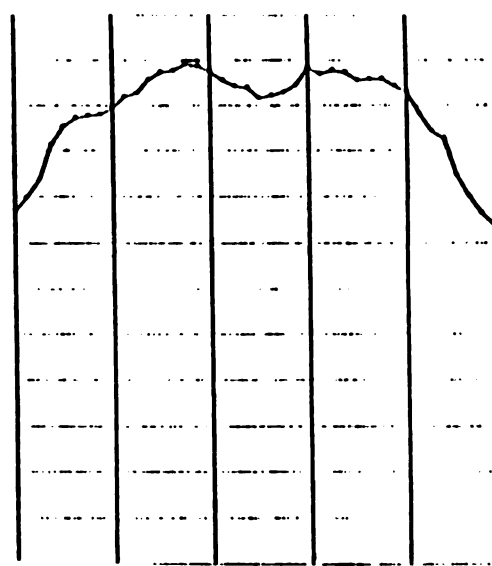
K
N
E
E

A
N
G
L
E

0 HIP ANGLE 90

600

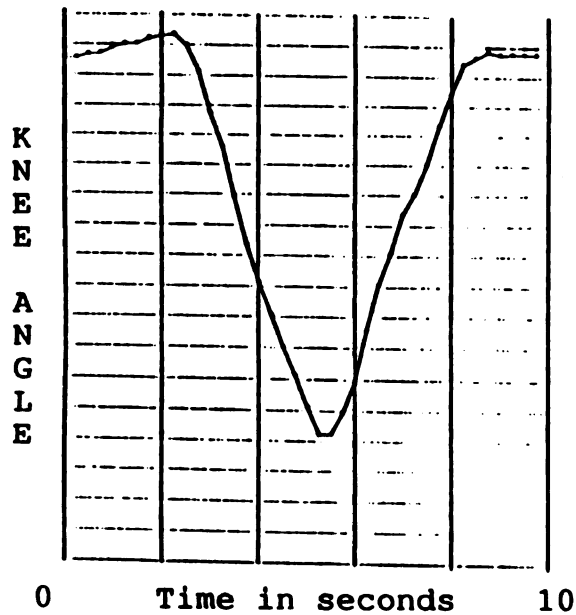
M
U
S
C
L
E

L
E
N
G
T
H

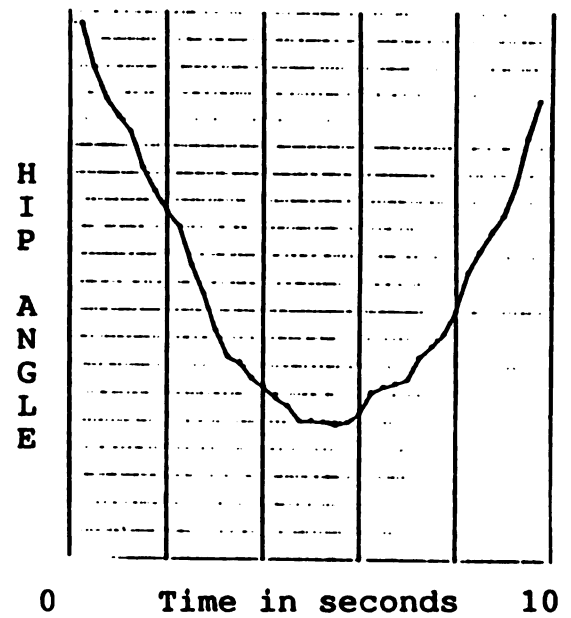
0 Time in seconds 10

FIGURE 50: UNPROCESSED EXPERIMENTAL DATA, SUBJECT 1, TRIAL 3

180

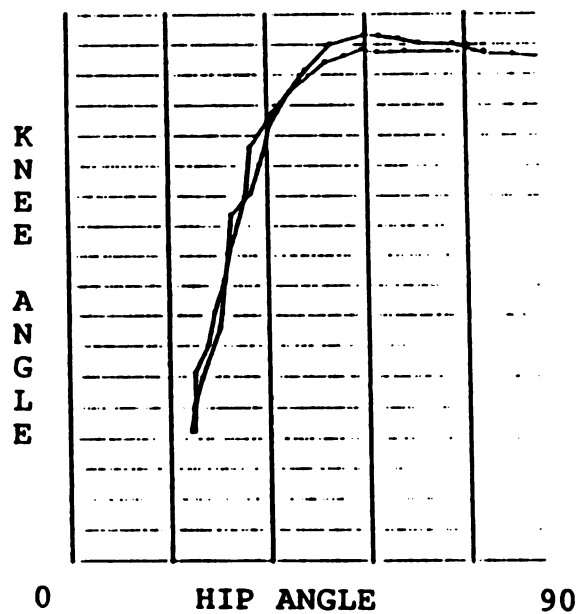


100



Note: Angles in degrees, Length in millimeters

180



600

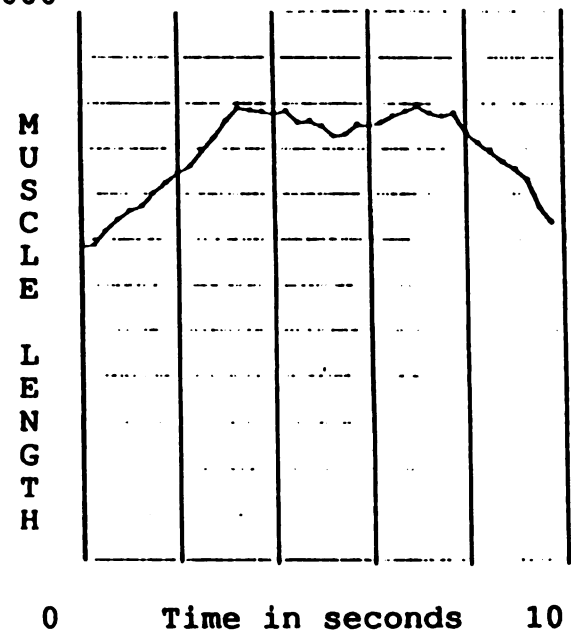
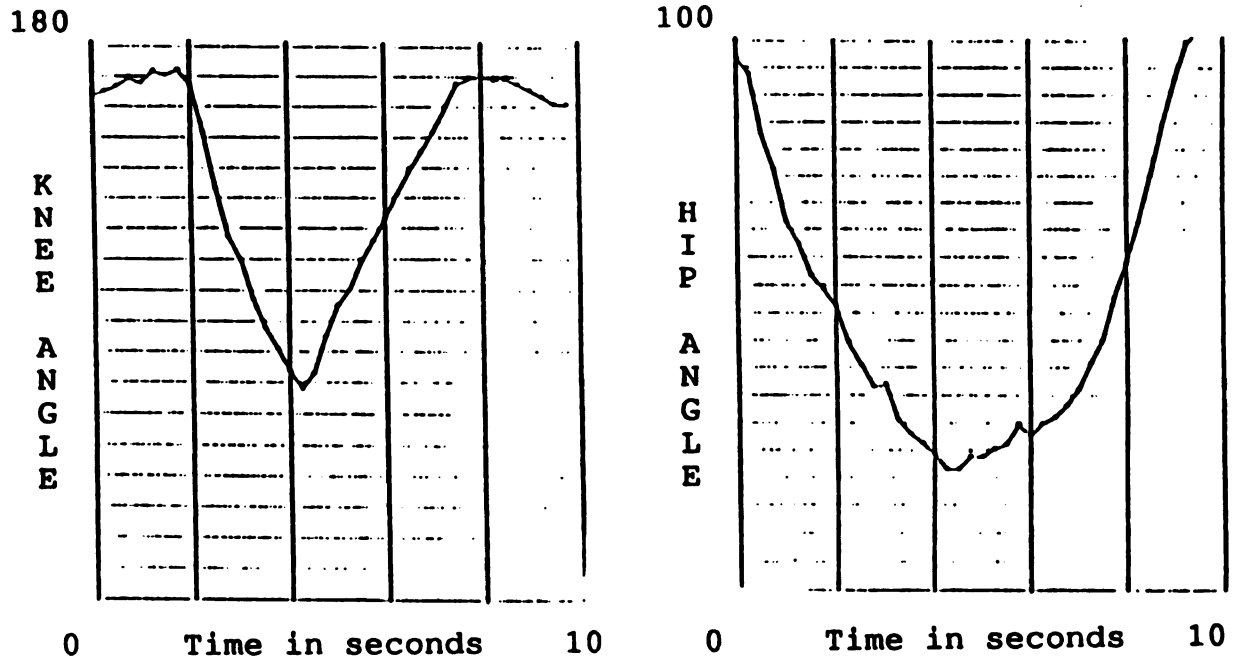


FIGURE 51: UNPROCESSED EXPERIMENTAL DATA, SUBJECT 2, TRIAL 1



Note: Angles in degrees, Length in millimeters

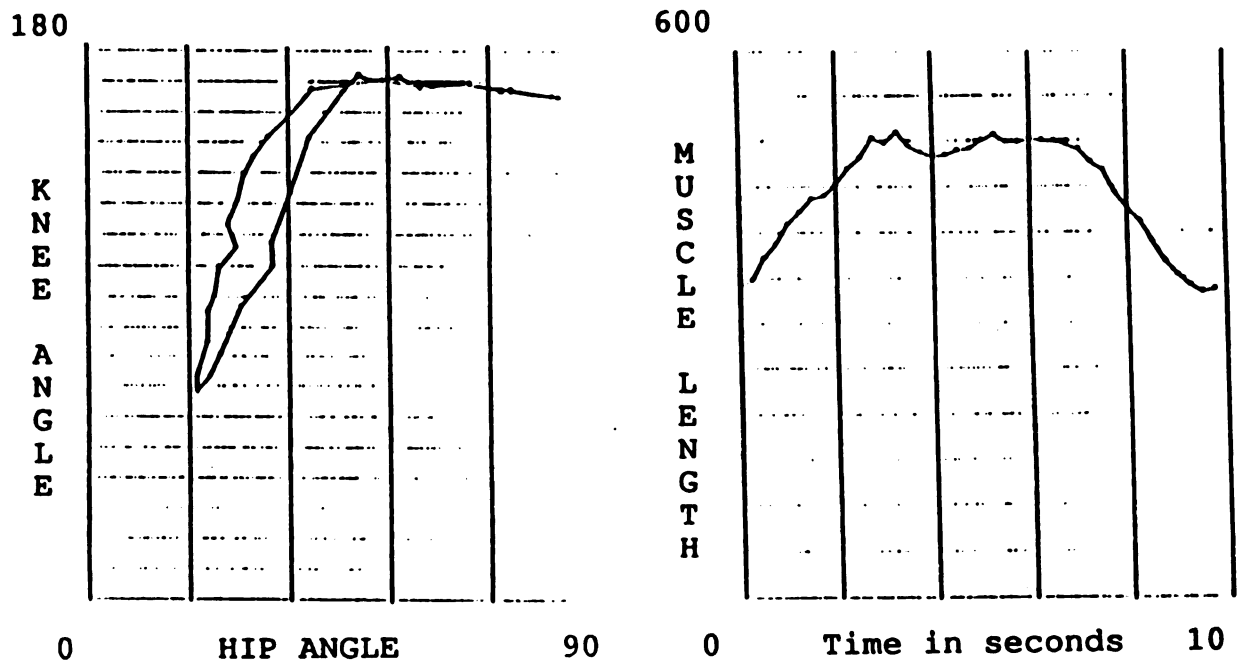
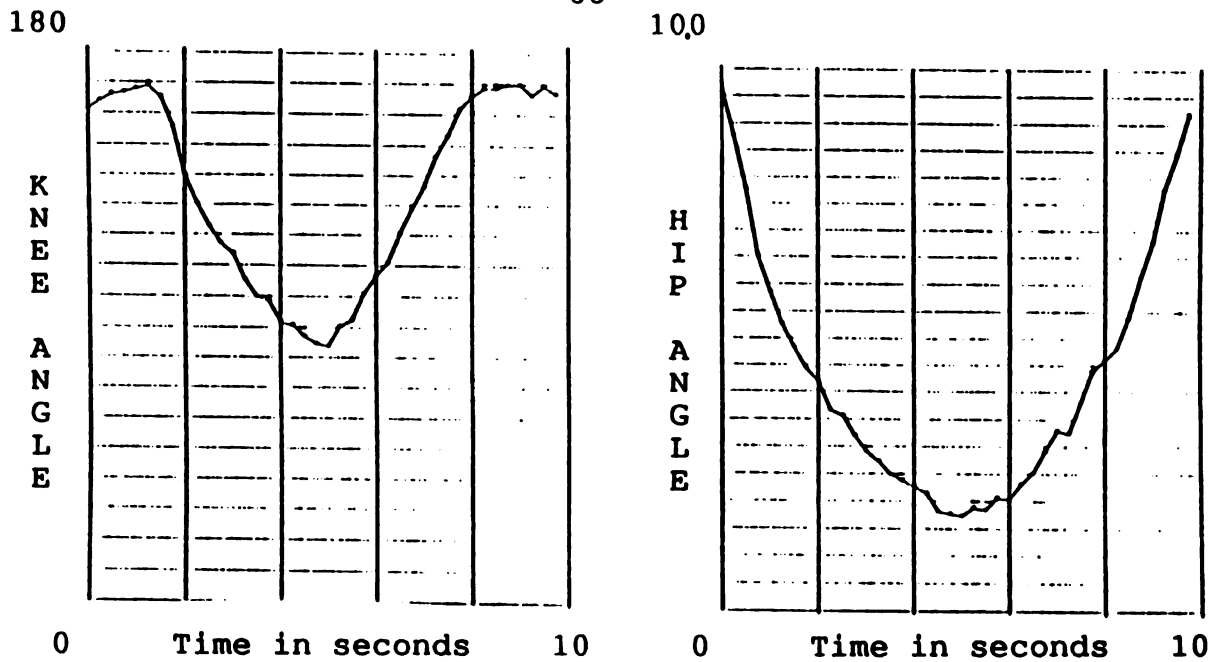


FIGURE 52: UNPROCESSED EXPERIMENTAL DATA, SUBJECT 2, TRIAL 2



Note: Angles in degrees, Length in millimeters

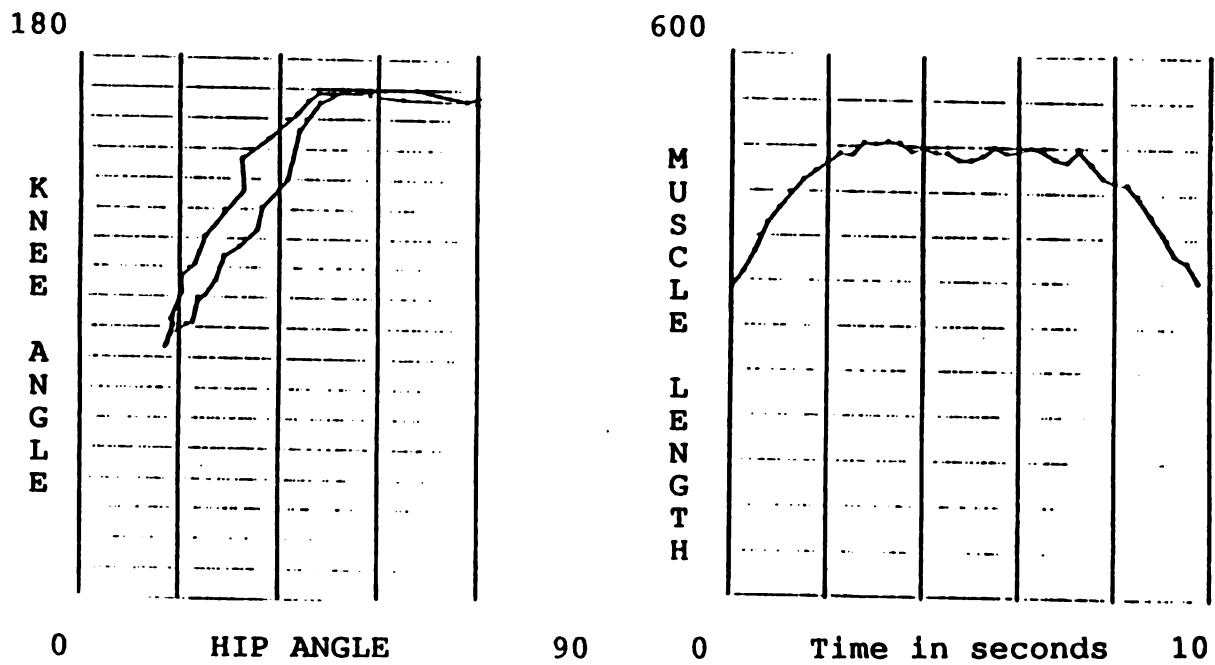
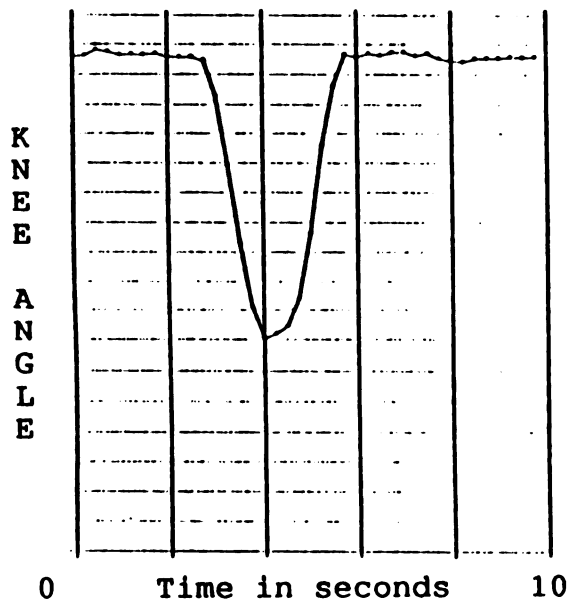
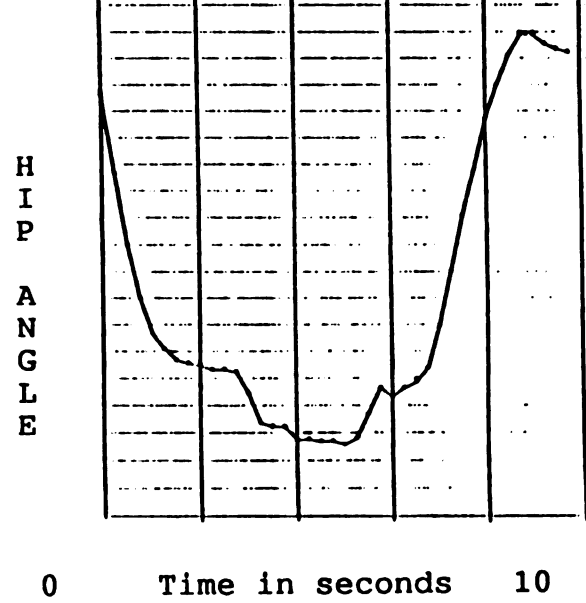


FIGURE 53: UNPROCESSED EXPERIMENTAL DATA, SUBJECT 2, TRIAL 3

180

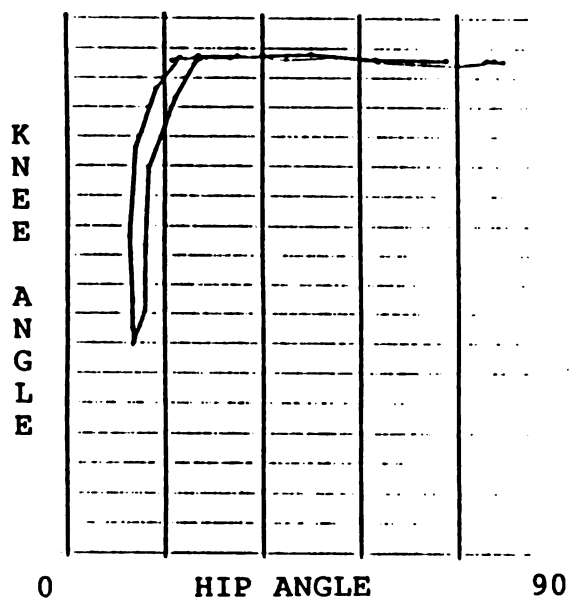


100



Note: Angles in degrees, Length in millimeters

180



600

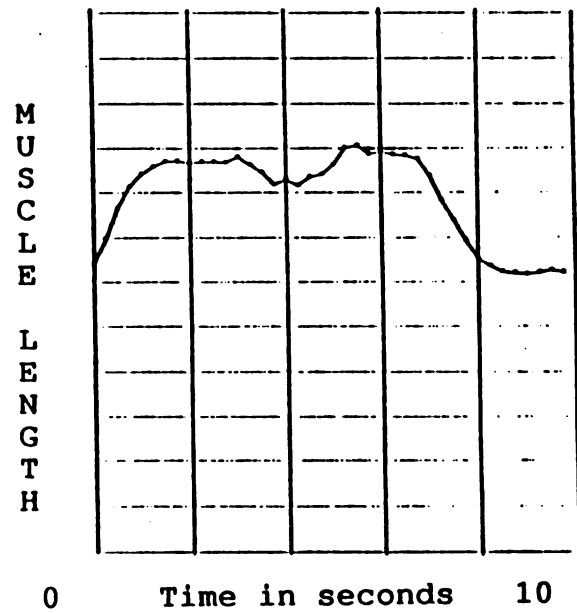
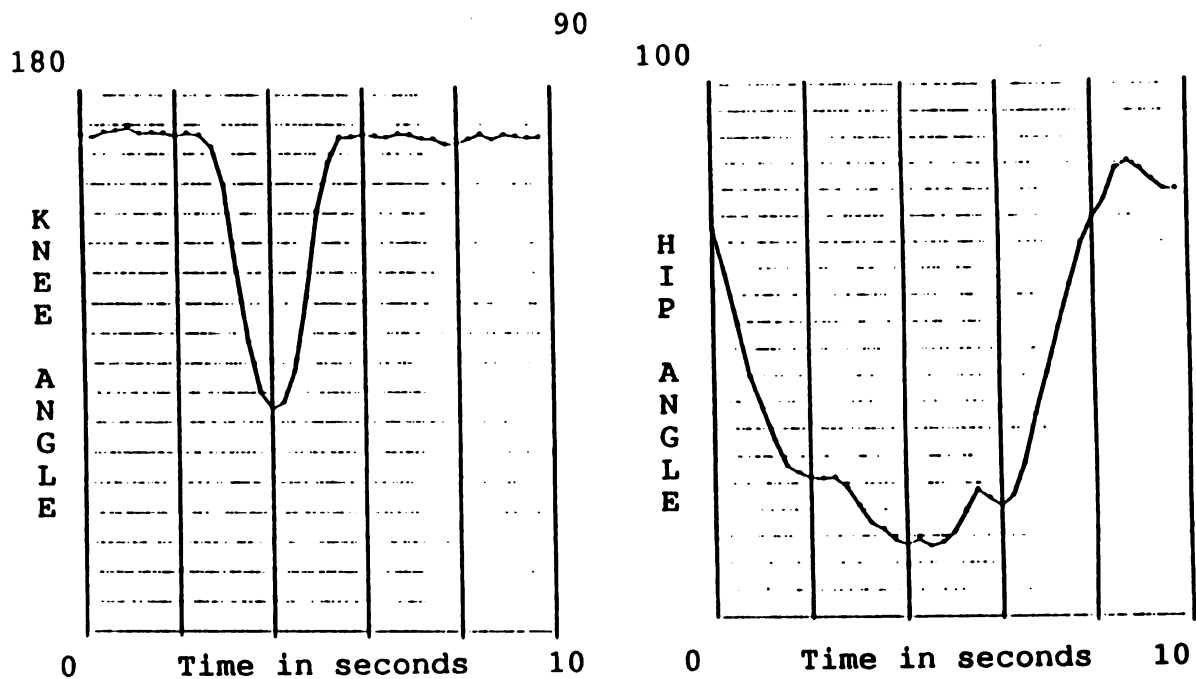


FIGURE 54: UNPROCESSED EXPERIMENTAL DATA, SUBJECT 3, TRIAL 1



Note: Angles in degrees, Length in millimeters

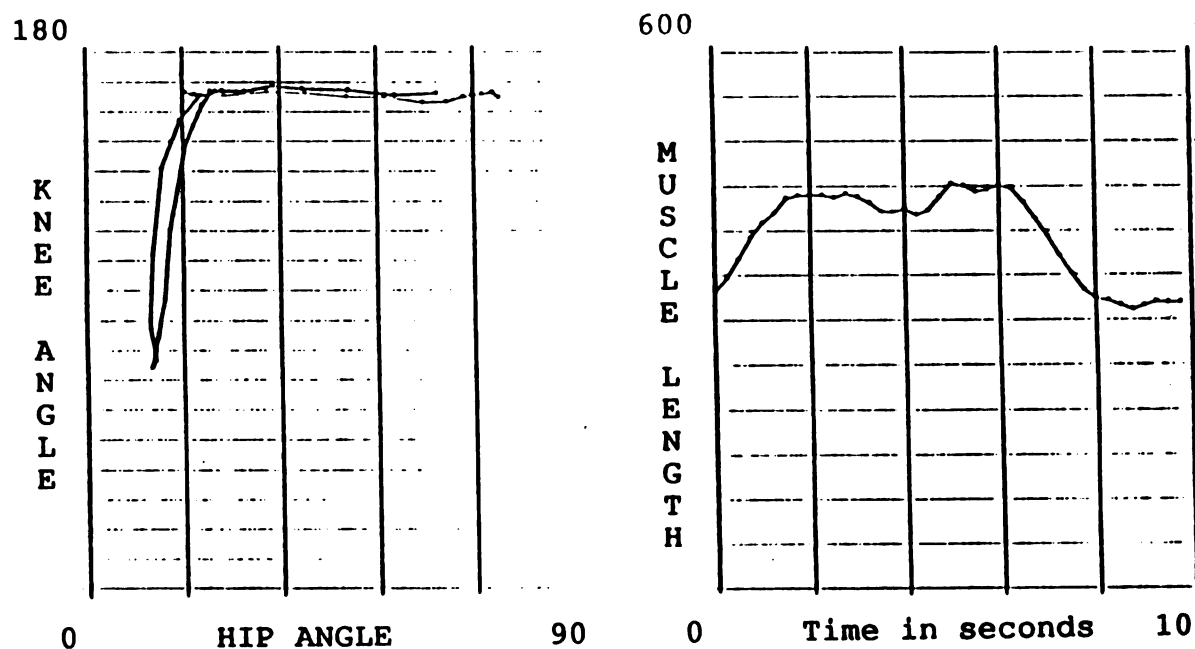
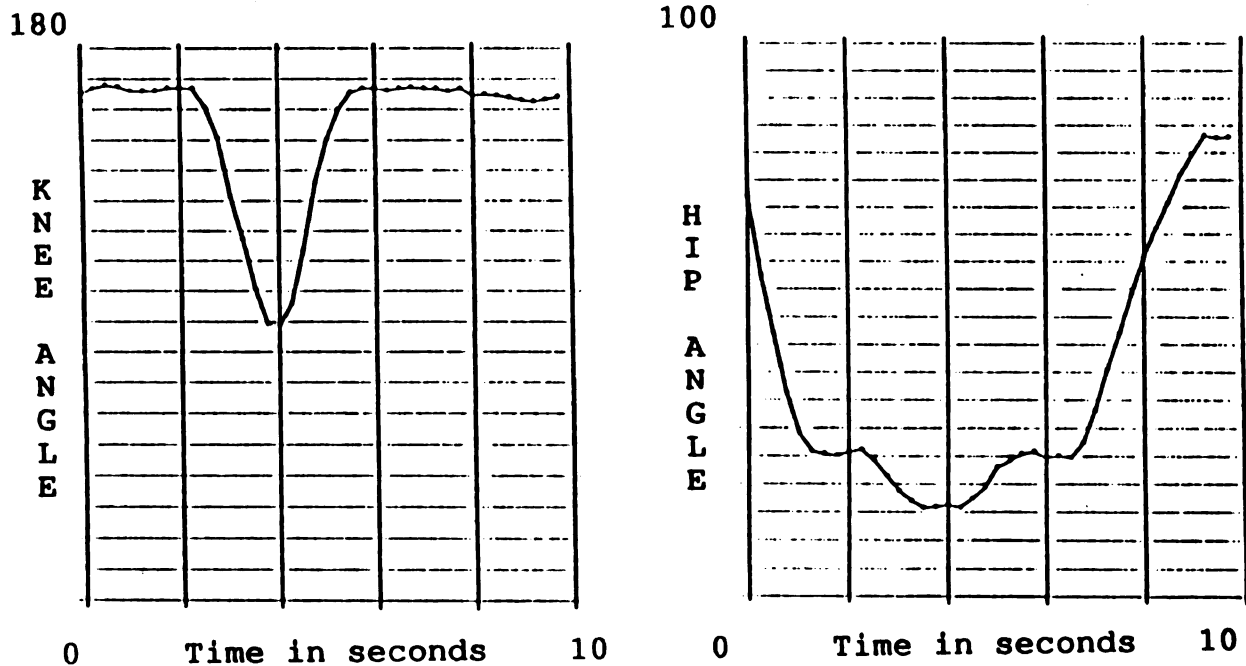


FIGURE 55: UNPROCESSED EXPERIMENTAL DATA, SUBJECT 3, TRIAL 2



Note: Angles in degrees, Length in millimeters

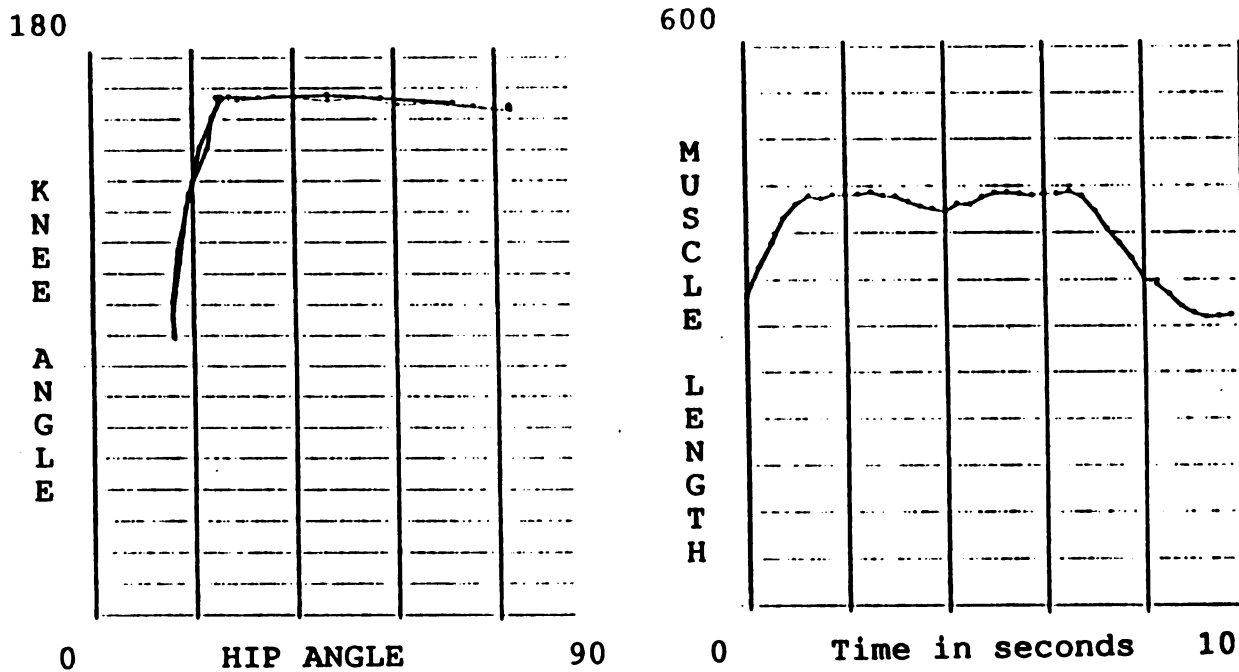
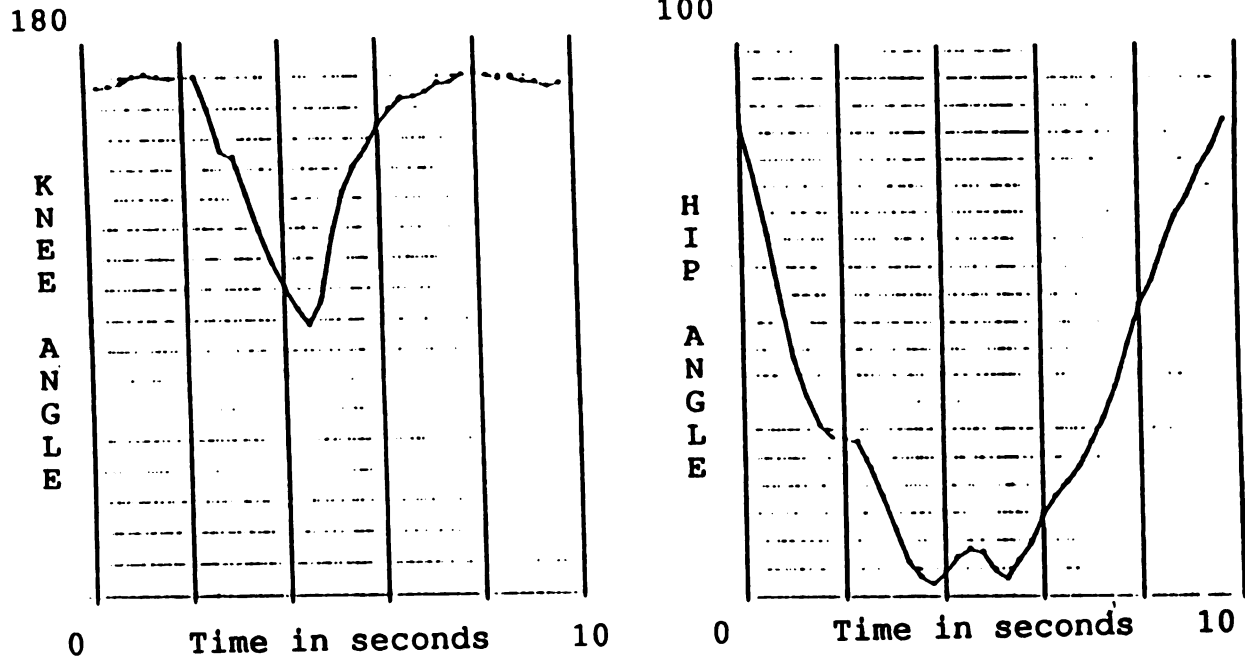


FIGURE 56: UNPROCESSED EXPERIMENTAL DATA, SUBJECT 3, TRIAL 3



Note: Angles in degrees, Length in millimeters

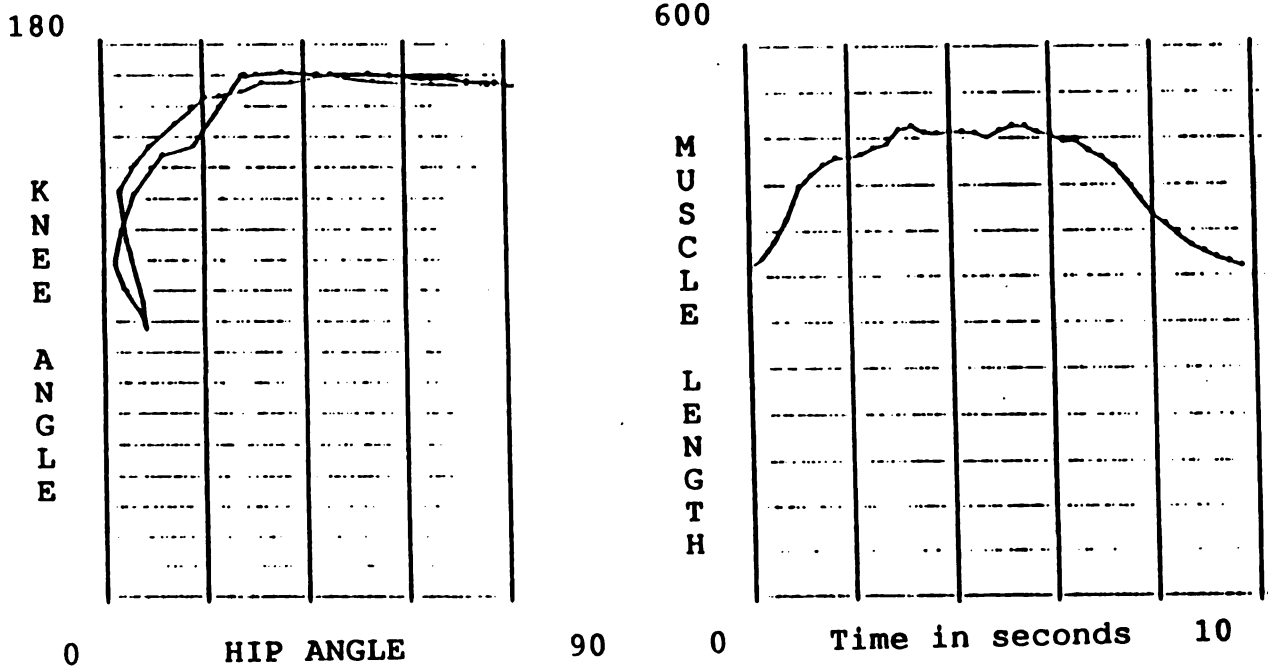
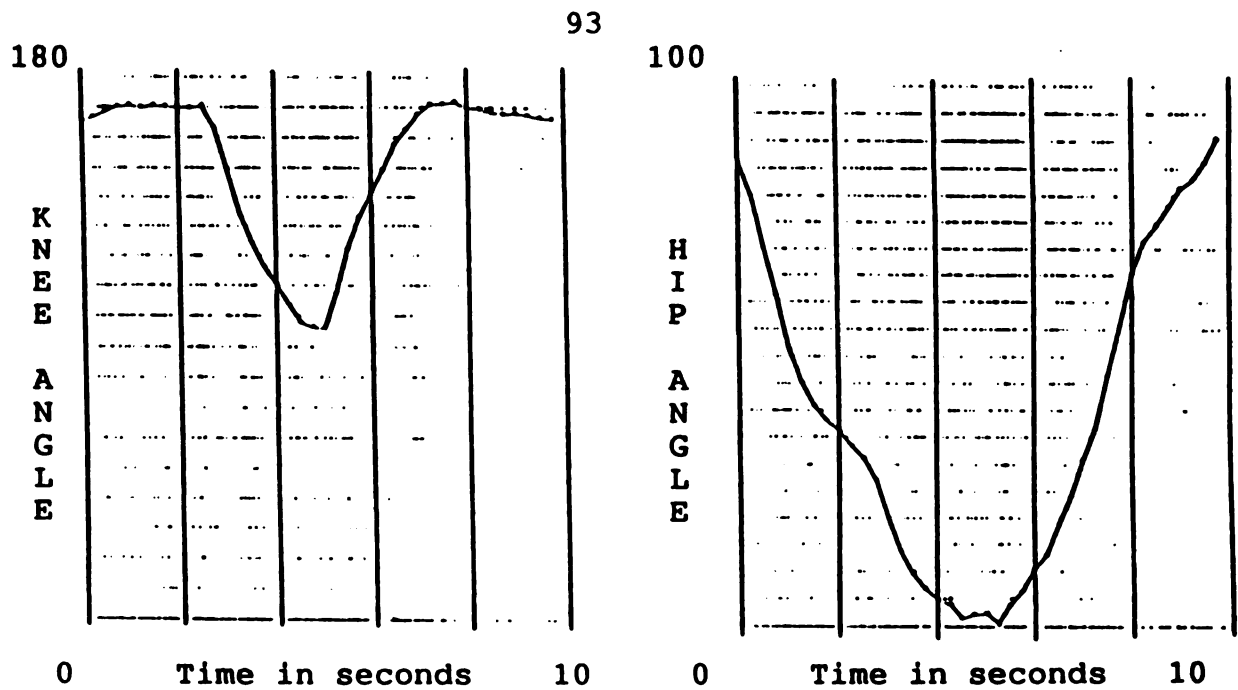


FIGURE 57: UNPROCESSED EXPERIMENTAL DATA, SUBJECT 4, TRIAL 1



Note: Angles in degrees, Length in millimeters

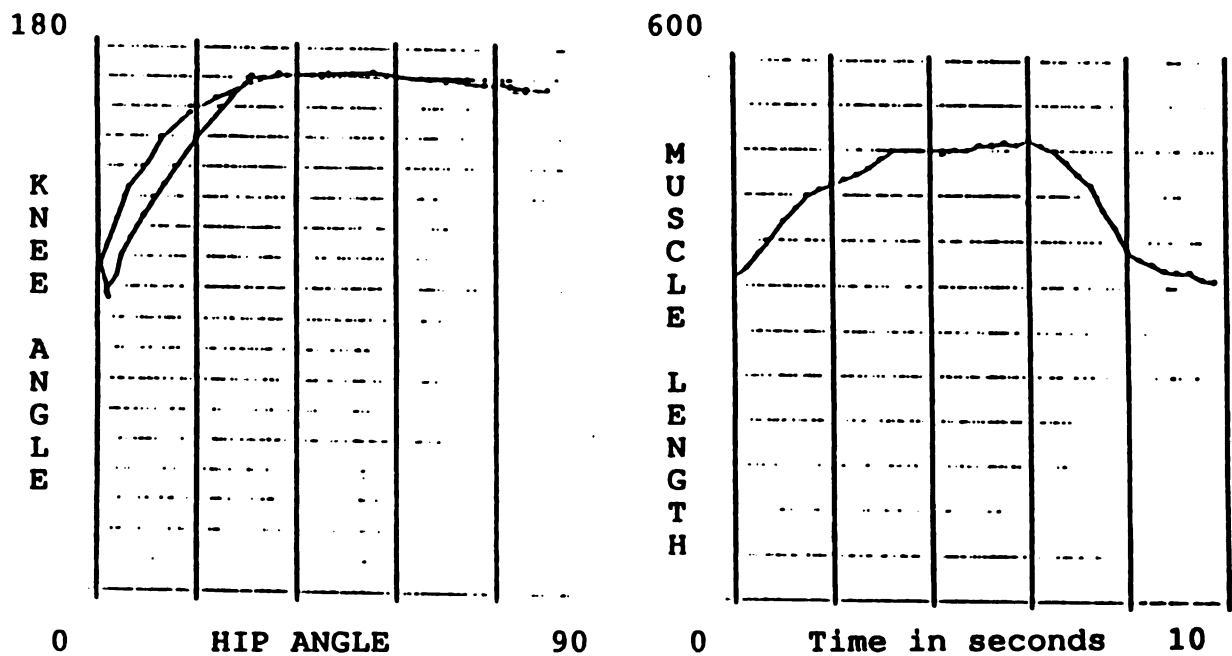
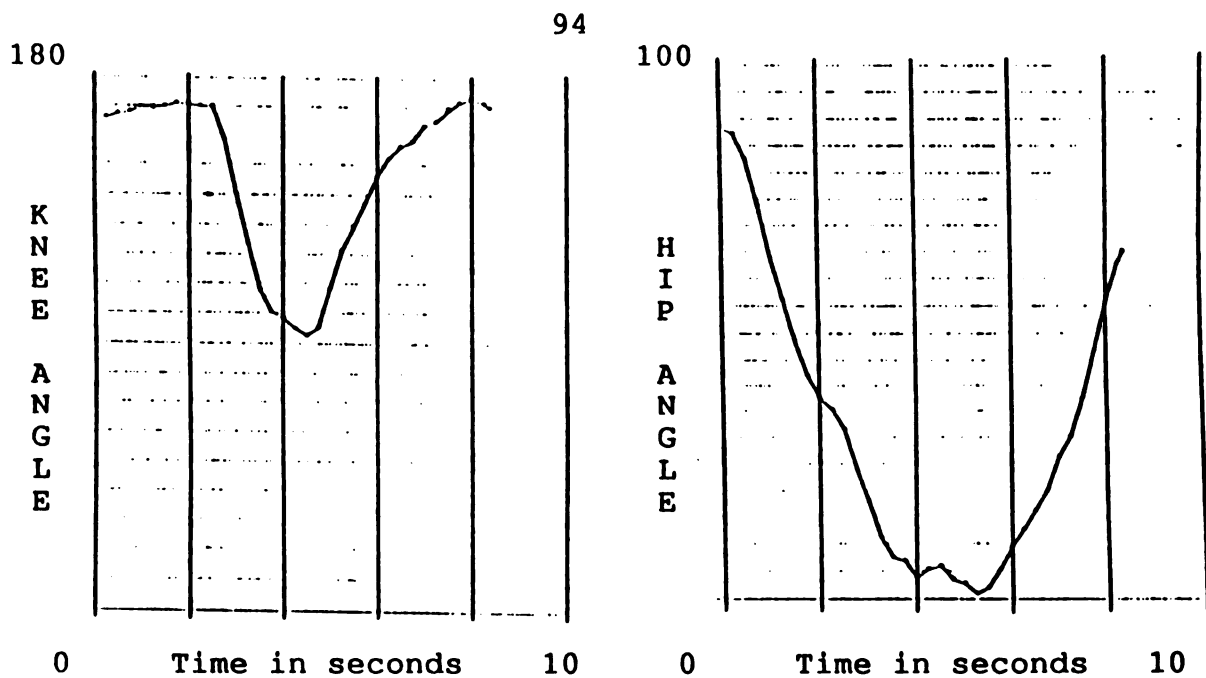


FIGURE 58: UNPROCESSED EXPERIMENTAL DATA, SUBJECT 4, TRIAL 2



Note: Angles in degrees, Length in millimeters

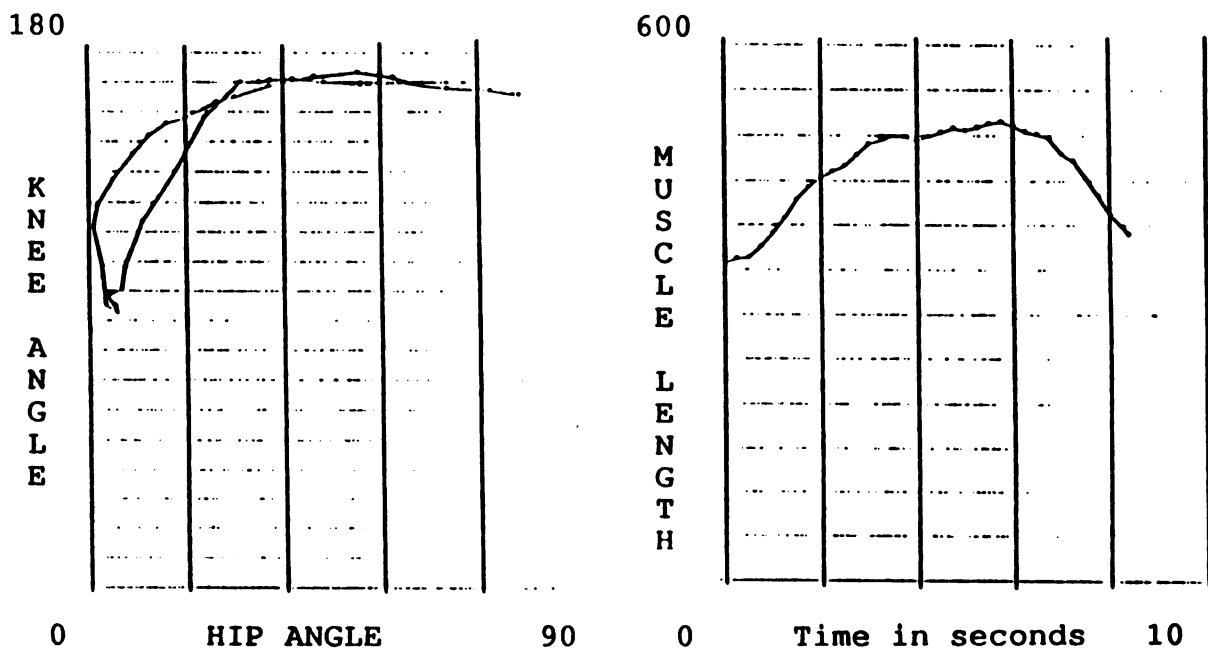


FIGURE 59: UNPROCESSED EXPERIMENTAL DATA, SUBJECT 4, TRIAL 3

decreasing as the subject bent forward at the waist while attempting to maintain a constant hamstring tension. Both knee and hip angle continued to decrease simultaneously until minima were reached at approximately 4 seconds, when Exercise Two was begun. Between 4 and 5 seconds, the knees straightened while hip angle remained approximately constant, again producing a limiting tension in the hamstrings. The subject now was forced, due to this hamstring tension, to increase hip angle as he straightened his knees, reaching the straight knee position at just under 6 seconds. At this time, the subject made a small effort to again decrease his hip angle, but, finding he was close to his limit, quickly stood up and arched his back, thereby overshooting his standing posture. This overshoot caused the hip angle to reach its maximum value approximately 9 seconds into the test, after which it slowly decreased to its value in normal stance.

The Knee Angle versus Hip Angle graph, beginning at the upper right and moving left, shows that the hip angle decreased independently of knee angle during the early parts of the trial. Hip angle and knee angle then become coupled, as is evidenced by the change from a horizontal line to the section with an almost linear slope. The two vertical portions of the graph indicate that knee angle was independent of hip angle during the middle of the trial. The two angles again became coupled for a time, after which hip angle varies independently until trial's end.

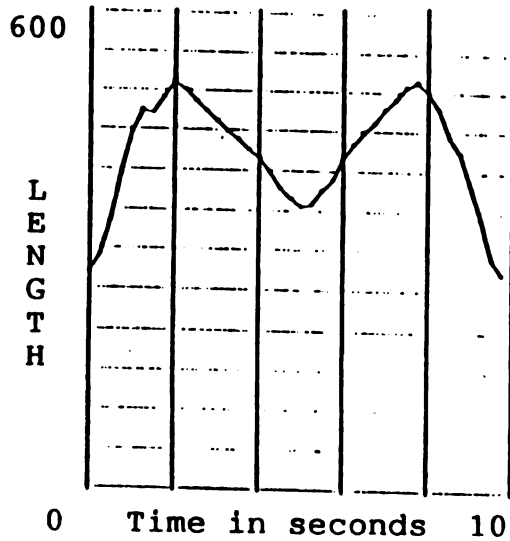
The Muscle Length versus Time graph shows that the muscle length computed from target locations did, indeed, reach a maximum during each exercise, the second maximum being slightly longer than the first.

The Corrected Muscle Length versus Time graphs, prepared from the data after correction for apparent variations in segment lengths, are presented in Figures 60.a through 63.a.

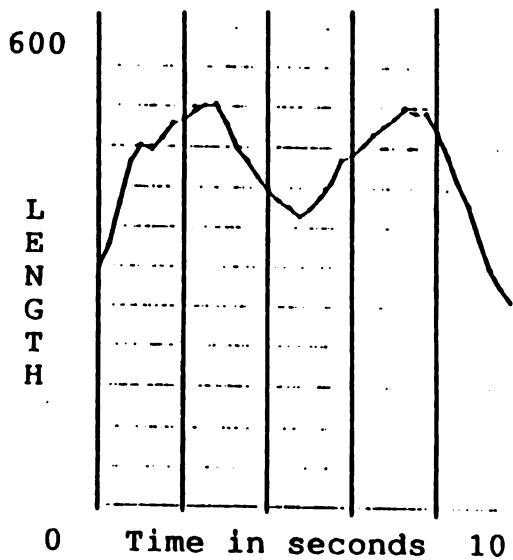
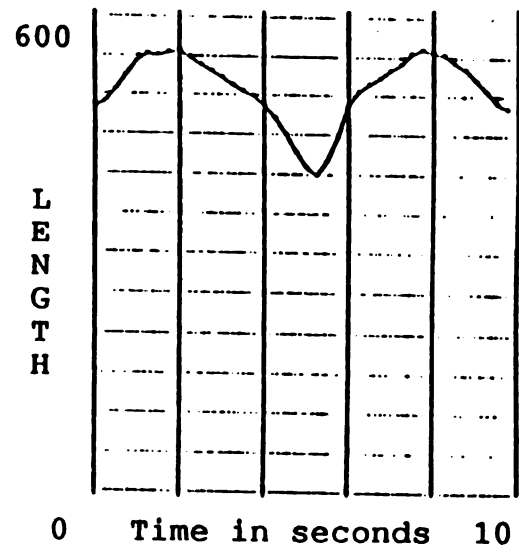
4.3.2. Error Estimation

Since the angular data generated by the live test subjects was used to drive BONEMAN, any error in the angle calculations would directly affect the accuracy of the model's performance. Because the vectors used to measure the desired angles were based upon the target locations, the most likely source of angular error would be inaccurate position estimates for the targets. A technique for estimating the largest likely error for the knee and hip angles is presented in Appendix F. The result of such error analysis is that the largest probable error in Hip Angle and Knee Angle are 1.9 degrees and 2.5 degrees, respectively.

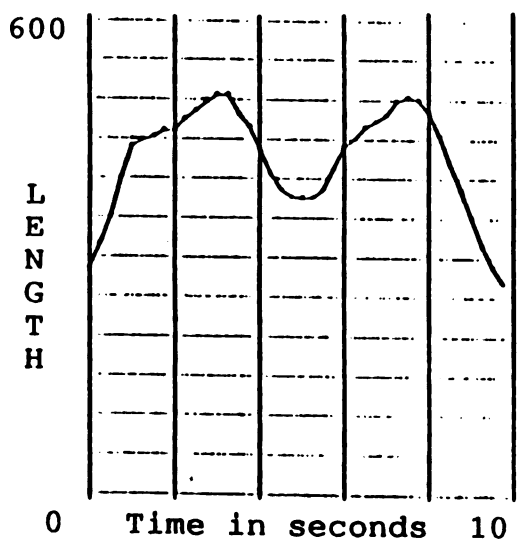
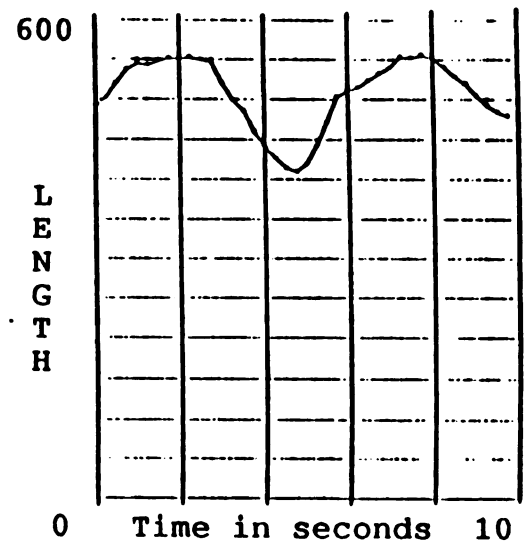
Examination of the Corrected Hamstring Lengths presented in Figures 60.a through 63.a shows that each subject reached two local maxima in muscle length during each trial. The first maximum occurred due to hamstring stretch created by pelvic tilt during Exercise One; the second resulted from hamstring stretch caused by knee extension during Exercise Two. This suggests that there



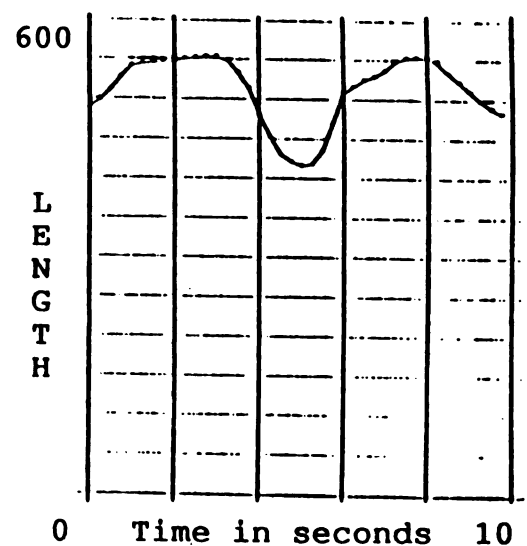
Trial One



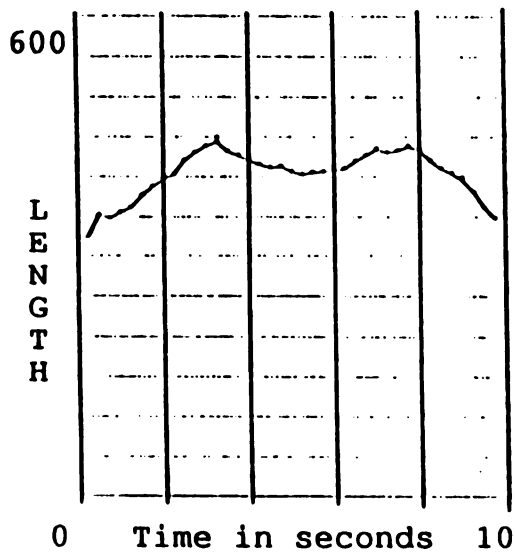
Trial Two



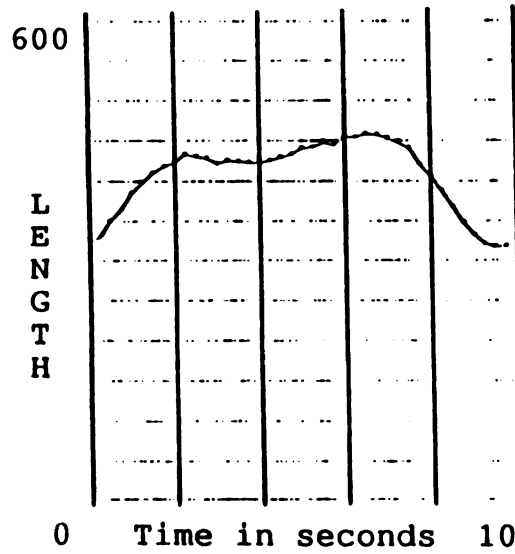
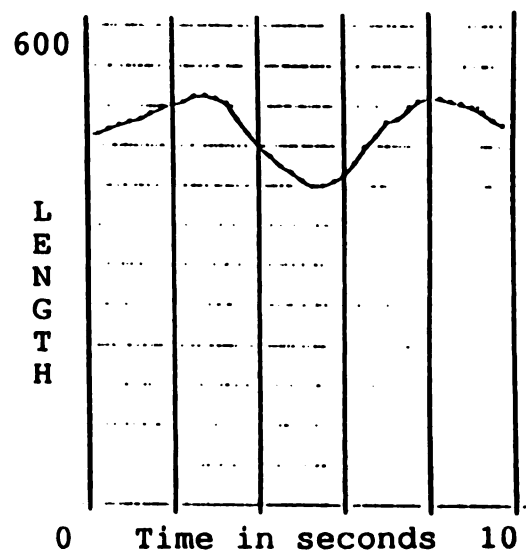
Trial Three



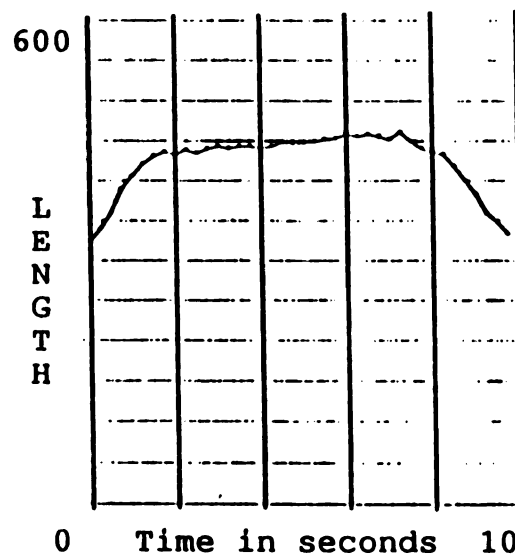
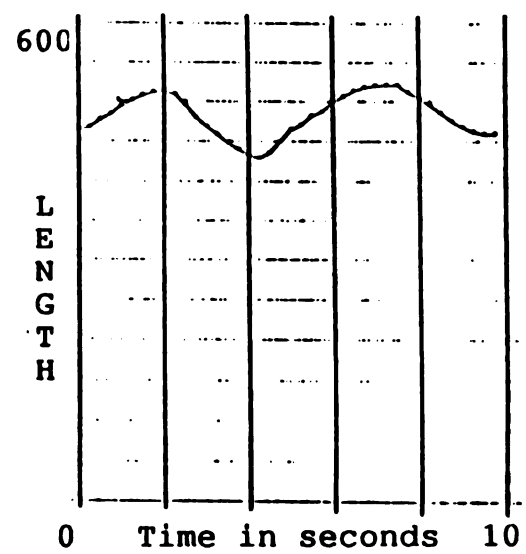
(a) Corrected Muscle Lengths (b) Model Muscle Lengths
 Note: Muscle lengths are in millimeters
FIGURE 60: CORRECTED VRS. MODEL MUSCLE LENGTHS, SUBJECT 1



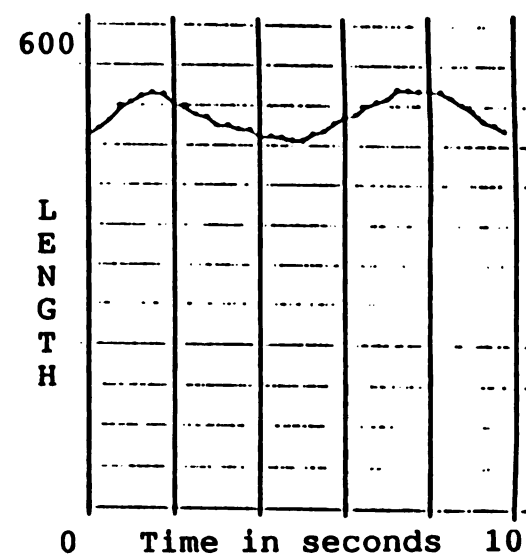
Trial One



Trial Two



Trial Three

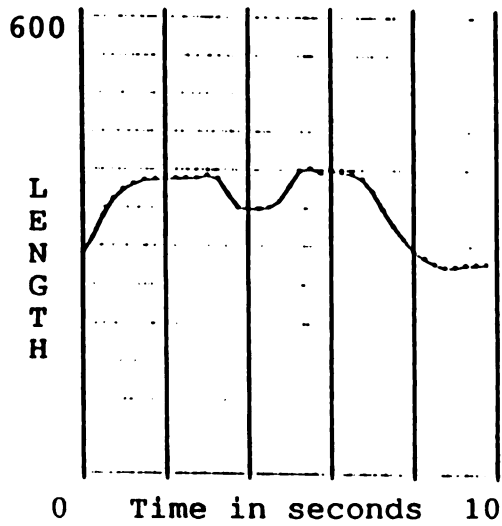


(a) Corrected Muscle Lengths

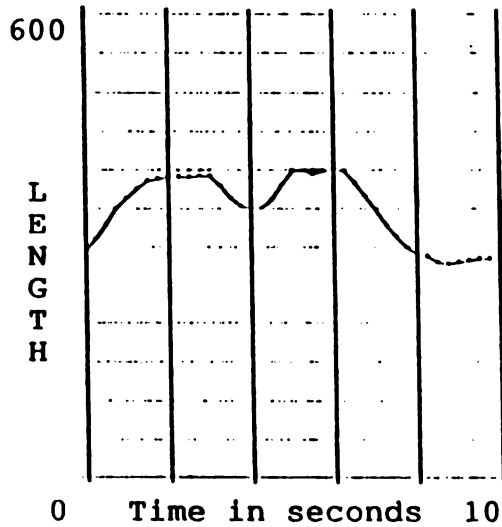
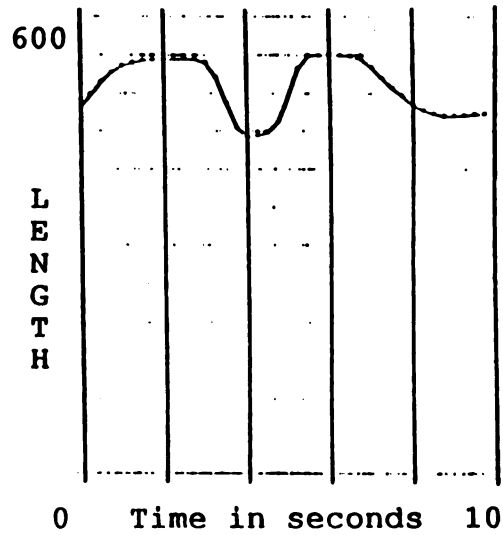
(b) Model Muscle Lengths

Note: Muscle lengths are in millimeters

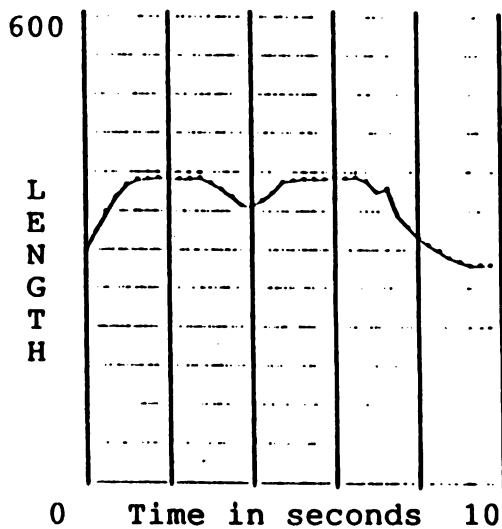
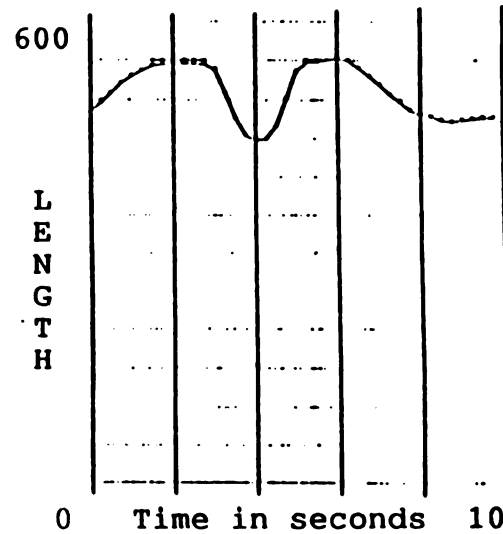
FIGURE 61: CORRECTED VRS. MODEL MUSCLE LENGTHS, SUBJECT 2



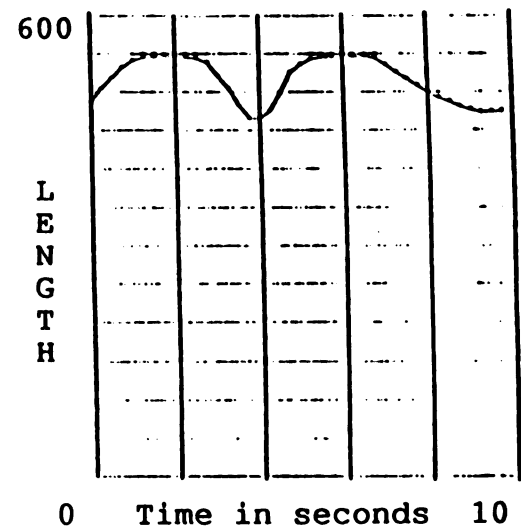
Trial One



Trial Two



Trial Three

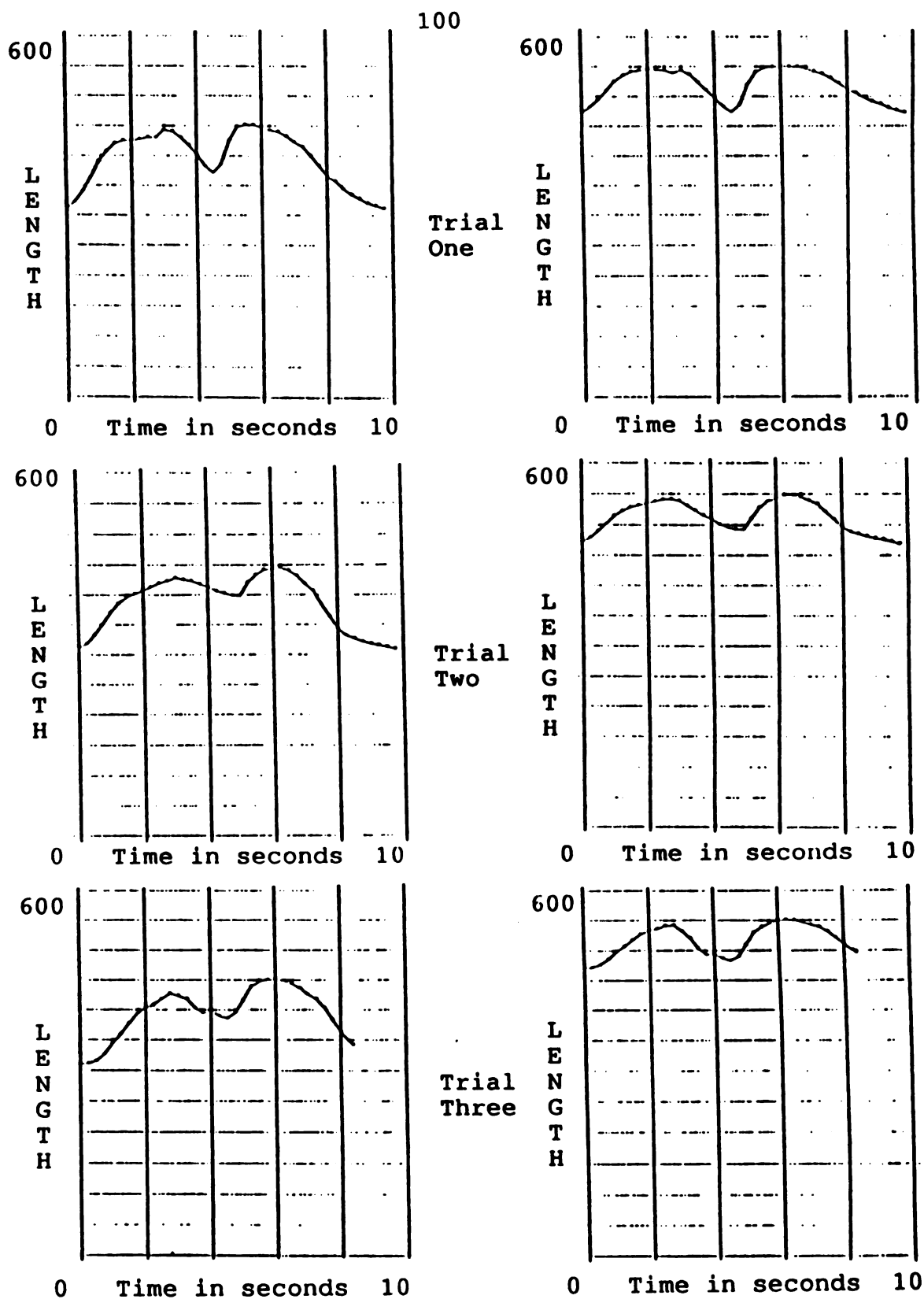


(a) Corrected Muscle Lengths

(b) Model Muscle Lengths

Note: Muscle lengths are in millimeters

FIGURE 62: CORRECTED VRS. MODEL MUSCLE LENGTHS, SUBJECT 3



(a) Corrected Muscle Lengths

(b) Model Muscle Lengths

Note: Muscle lengths are in millimeters

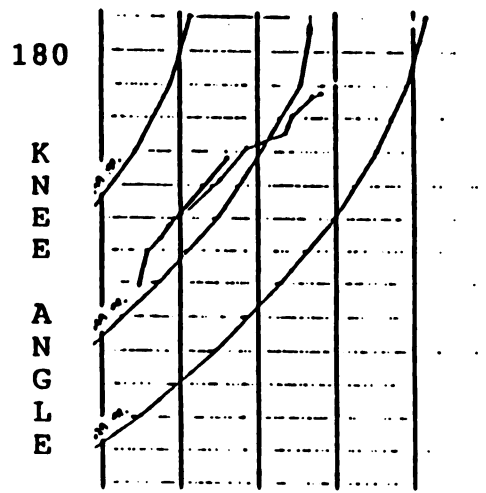
FIGURE 63: CORRECTED VRS. MODEL MUSCLE LENGTHS, SUBJECT 4

was, indeed, a limiting muscle length reached by each of the test subjects. In most instances, the second local maximum was higher than the first, making it clear that this limiting muscle length is not strictly constant within a given individual, but one that can change not only between exercises, but also during the same exercise. This observation is consistent with Atha and Wheatly [25] who found that repeated performance of a similar test improved the range of hip flexion.

4.3.3. Model Predictions Evaluated

Comparison of Corrected Muscle Length data generated by the live subjects with the corresponding Model Muscle Length predictions (Figures 60.b through 63.b) shows that in the majority of exercises, the trends in muscle length of the live subjects are closely followed by the computer predictions. The local maxima and minima, inflection points and overall shape of the curves generated by the test subjects are reflected in the curves generated by the model. The conclusion is that, given adequate angular input, the model will qualitatively duplicate what actually happens to muscle length in live subjects. It will not, however, because of differences between subject and model link lengths, predict actual muscle length. This shortcoming will not prevent the model from performing its primary duty, which is the generation of lifelike body contours.

Figures 64 through 67 are composed of appropriate sections of the composite plot described in Section 4.2.2.,

TRIAL 1

Note: All
angles in
degrees.

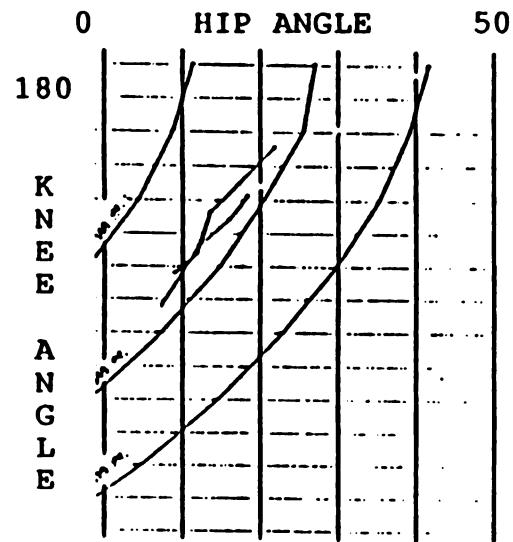
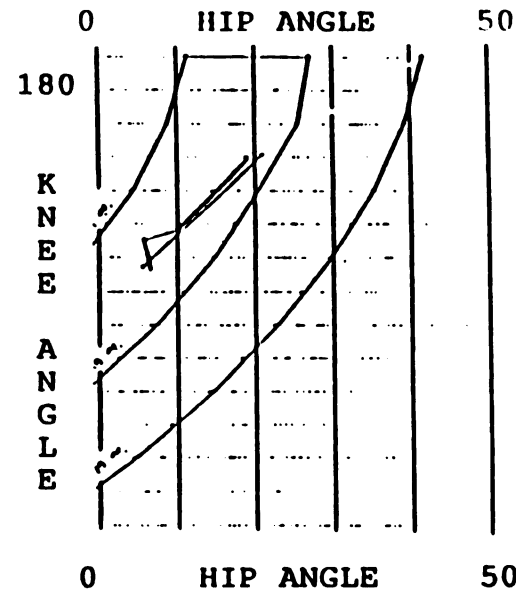
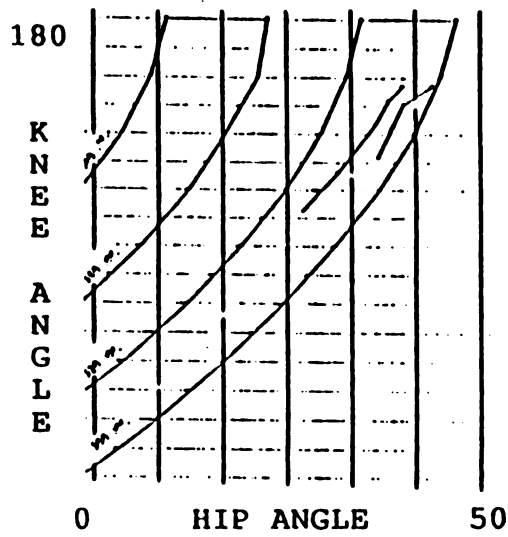
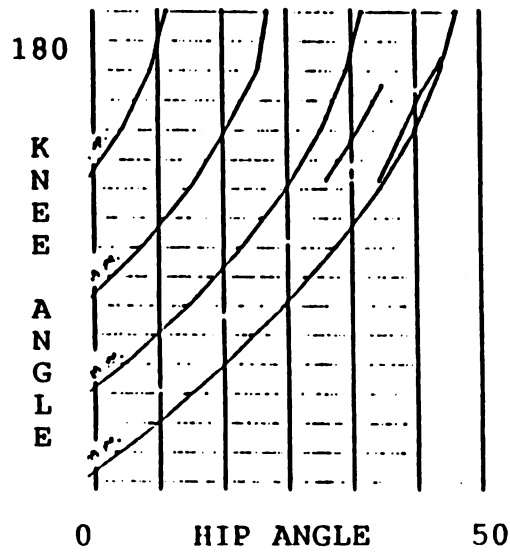
TRIAL 2TRIAL 3

FIGURE 64: EXPERIMENTAL ANGLES COMPARED TO THEORY, SUBJECT 1

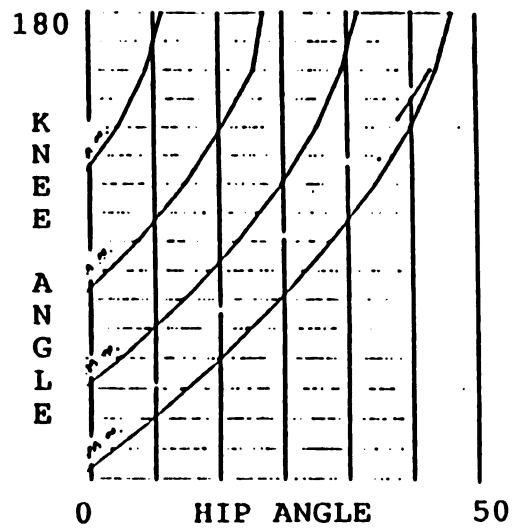


TRIAL 1

Note: All
angles in
degrees.

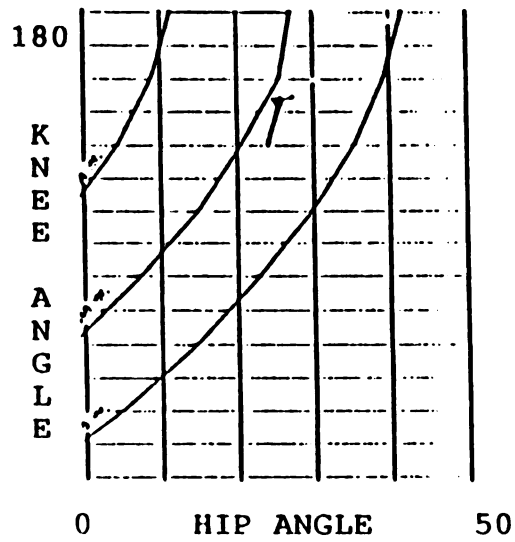


TRIAL 2



TRIAL 3

FIGURE 65: EXPERIMENTAL ANGLES COMPARED TO THEORY, SUBJECT 2

TRIAL 1

Note: All angles in degrees.

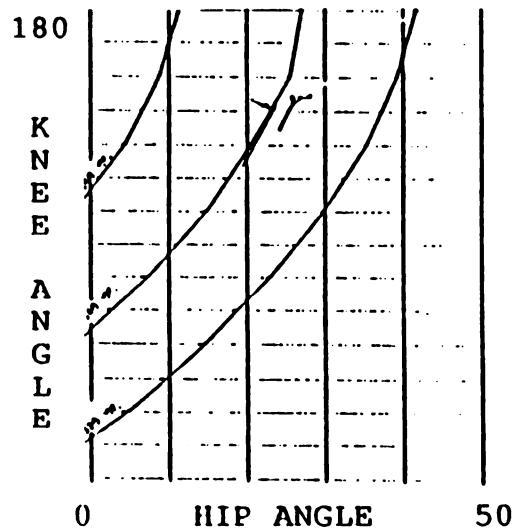
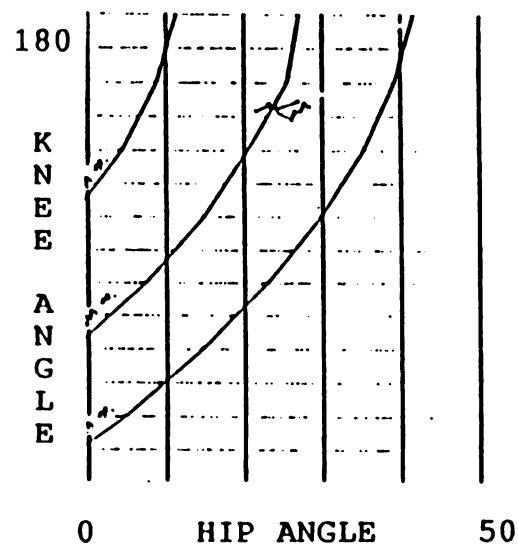
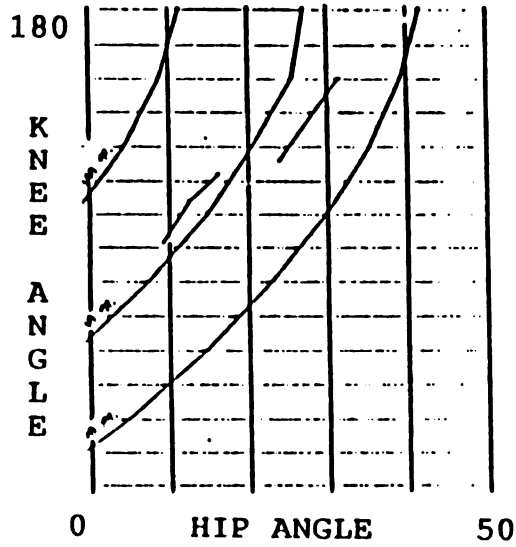
TRIAL 2TRIAL 3

FIGURE 66: EXPERIMENTAL ANGLES COMPARED TO THEORY, SUBJECT 3

TRIAL 1

Note: All
angles in
degrees.

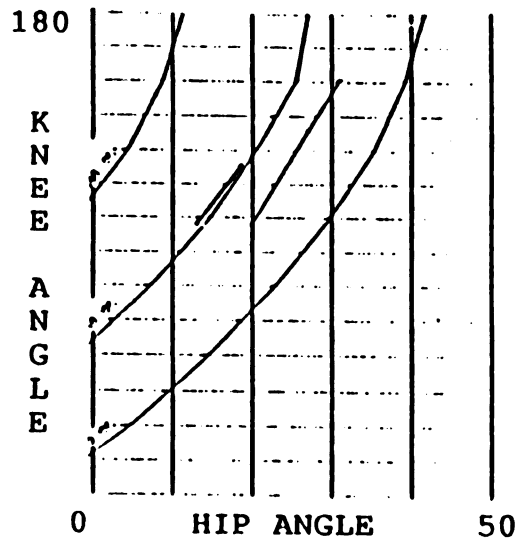
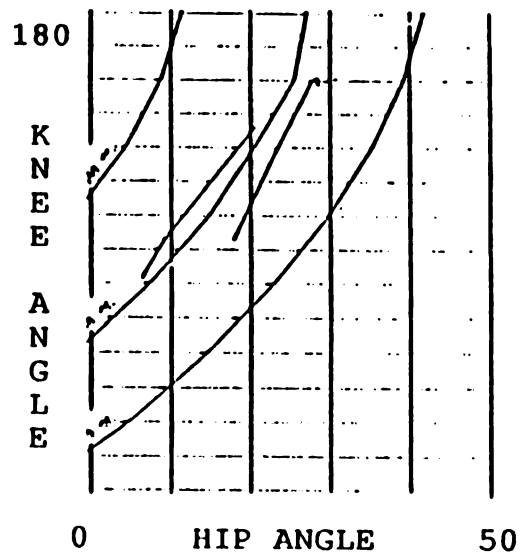
TRIAL 2TRIAL 3

FIGURE 67: EXPERIMENTAL ANGLES COMPARED TO THEORY, SUBJECT 4

upon which have been superimposed those portions of the live subjects' Knee Angle versus Hip Angle graphs which correspond to the times during which approximately constant muscle lengths were observed. Since each trial consisted of two exercises, and one period of "constant" muscle length occurred during each exercise, two segments of interest were generated during each of the twelve trials. It can be seen that there is a consistent tendency for the superimposed portions to parallel the lines of the composite plot, leading to the conclusion that the combinations of Knee Angle and Hip Angle observed in the laboratory were, indeed, the result of a limiting constant length of the hamstring musculature. Because of this, it should be possible to use such a composite plot to determine permissible angular combinations for any given hamstring length, or conversely, to predict what muscle lengths will allow a given combination of knee and hip angles. Thus, this composite plot does much to explain the limits on human flexibility.

4.3.4. Discussion

Knowledge of the relationship between Knee Angle, Hip Angle, and Hamstring length will allow designers to work in the following ways to predict the adequacy of a new seat design before expensive prototypes are built. If the product is intended for a certain target market, i.e., purchasers of luxury cars, compact cars, or sports cars, consideration of factors such as age and physical condition of the typical person purchasing that class of vehicle may

be used to predict the range of hamstring stretch and joint angle combinations likely to be found desirable by the buyer. If the goal is to accomodate as many people as possible, the model could be used to predict whether or not the new seat would be comfortable for a large segment of the population. Considerable variation in the range of hamstring-limited hip flexion, unrelated to sex, age, work, or leisure activities [18] exists in the healthy adult population. Consistent use of the model in this manner should contribute to a more complete understanding of such variations in hip flexibility.

5. CONCLUSION

The three specific goals of this work have been accomplished.

A skeletal model (BONEMAN) has been developed which incorporates torso mobility as developed by Haas [3] and adds legs, shoulders, and arms which can be positioned to represent all body postures of an average adult male. Thus, BONEMAN will be useful in the representation of driving postures.

Addition of muscles to BONEMAN has been studied, and the use of ellipsoids to model muscle groups will, when properly used in conjunction with the skeletal model, produce computer simulated body contours useful to designers of automobile seats.

The role played by the hamstring muscle group in the limitation and interdependence of knee angle and hip angle has been described in this thesis. Because the straightening or reversal of lumbar lordosis during sitting is also related to hamstring tightness [18], with tight hamstrings limiting the amount of lordosis attainable for a specified knee angle, an immediate goal for future research should be the determination of the relationship which exists between TLC and hamstring length.

The level of constraint placed by other muscle groups upon joint ranges of motion throughout the body, such as gastrocnemius length limiting combinations of knee and ankle

angles, or the lumbar muscles and fascia influencing lumbar curvature, should be explored in future work.

The area of deflection of body contours by surface contact forces must be investigated if the model is ever to predict body/seat interface contours. All this information must also be applied to models of other sizes of people, such as the small woman and large man.

The tasks completed in this thesis, i.e., the representation of skeletal and muscle geometry, and the description of the influence of hamstring muscle length on body position, are important steps in the development of new representations of humans for use in product design.

APPENDICES

APPENDIX A

Spinal Joint Center Coordinates

For the coordinates, cp() indicates a cervical point. Each interspace is represented by three numbers. The first number is the X coordinate, the second number is the Y coordinate, and the third number is the Z coordinate.

ALL COORDINATES ARE IN MM

These are the coordinates for the C1/SKULL interspace (occipital condylar axis)

cp(1)=-213

cp(2)=0

cp(3)=612

These are the coordinates for the C1/C2 interspace

cp(4)=-213

cp(5)=0

cp(6)=602

These are the coordinates for the C2/C3 interspace

cp(7)=-207

cp(8)=0

cp(9)=586

These are the coordinates for the C3/C4 interspace

cp(10)=-204

cp(11)=0

cp(12)=571

These are the coordinates for the C4/C5 interspace

cp(13)=-201

cp(14)=0

cp(15)=551

These are the coordinates for the C5/C6 interspace

cp(16)=-200

cp(17)=0

cp(18)=532

These are the coordinates for the C6/C7 interspace

cp(19)=-203

cp(20)=0

cp(21)=511

These are the coordinates for the C7/T1 interspace

cp(22)=-210

cp(23)=0

cp(24)=493

For the coordinates, tp() indicates a torso point. Each interspace is represented by three numbers. The first number is the X coordinate, the second number is the Y coordinate, and the third number is the Z coordinate.

ALL COORDINATES ARE IN MM

These are the coordinates for the C7/T1 interspace

tp(1)=-210

tp(2)=0

tp(3)=493

These are the coordinates for the T1/T2

tp(4)=-218

tp(5)=0

tp(6)=476

These are the coordinates for the T2/T3

tp(7)=-226

tp(8)=0

tp(9)=459

These are the coordinates for the T3/T4

tp(10)=-231

tp(11)=0

tp(12)=440

These are the coordinates for the T4/T5

tp(13)=-237

tp(14)=0

tp(15)=421

These are the coordinates for the T5/T6

tp(16)=-242

tp(17)=0

tp(18)=395

These are the coordinates for the T6/T7

tp(19)=-241

tp(20)=0

tp(21)=367

These are the coordinates for the T7/T8

tp(22)=-238

tp(23)=0

tp(24)=339

These are the coordinates for the T8/T9

tp(25)=-232

tp(26)=0

tp(27)=311

These are the coordinates for the T9/T10

tp(28)=-225

tp(29)=0

tp(30)=281

These are the coordinates for the T10/T11

tp(31)=-217

tp(32)=0

tp(33)=251

These are the coordinates for the T11/T12

tp(34)=-207

tp(35)=0

tp(36)=219

These are the coordinates for the T12/L1 interspace

tp(37)=-194.1

tp(38)=0

tp(39)=189.2

For the spinous process points, stp() represents a spinous process point. The first number is the X coordinate, the second number is the Y coordinate, and the third number is

the Z coordinate.

ALL COORDINATES ARE IN MM

These are the coordinates for T1

stp(1)=-270

stp(2)=0

stp(3)=462

These are the coordinates for T2

stp(4)=-277

stp(5)=0

stp(6)=437

These are the coordinates for T3

stp(7)=-285

stp(8)=0

stp(9)=410

These are the coordinates for T4

stp(10)=-293

stp(11)=0

stp(12)=380

These are the coordinates for T5

stp(13)=-297

stp(14)=0

stp(15)=352

These are the coordinates for T6

stp(16)=-300

stp(17)=0

stp(18)=325

These are the coordinates for T7

stp(19)=-295

stp(20)=0

stp(21)=285

These are the coordinates for T8
stp(22)=-284
stp(23)=0
stp(24)=253
These are the coordinates for T9
stp(25)=-277
stp(26)=0
stp(27)=225
These are the coordinates for T10
stp(28)=-265
stp(29)=0
stp(30)=192
These are the coordinates for T11
stp(31)=-255
stp(32)=0
stp(33)=165
These are the coordinates for T12
stp(34)=-246
stp(35)=0
stp(36)=146

For the coordinates, lp() indicates a lumbar point. Each interspace is represented by three numbers. The first number is the X coordinate, the second number is the Y coordinate, and the third number is the Z coordinate.

ALL COORDINATES ARE IN MM

These are the coordinates for the T12/L1 interspace

lp(1)=-194.1

lp(2)=0

lp(3)=189.2

The coordinates for the L1/L2 interspace

lp(4)=-173.7

lp(5)=0

lp(6)=160

The coordinates for the L2/L3 interspace

lp(7)=-152.9

lp(8)=0

lp(9)=130.3

The coordinates for the L3/L4 interspace

lp(10)=-130.8

lp(11)=0

lp(12)=98.7

The coordinates for the L4/L5 interspace

lp(13)=-110

lp(14)=0

lp(15)=69

The coordinates for the L5/S1 interspace

lp(16)=-89

lp(17)=0

lp(18)=39

APPENDIX B

Lumbar Spinal Motion Program

This program produces the desired lumbar curvature in the 50% male model, using total lumbar curvature as input. Spinal flexion is negative, extension is positive. Curvature is equally divided among the relevant spinal joints.

```
C : .....
C : declare variables & read in total lumbar curvature:
C : .....
K : #echo none
K : #declare angle(1)
K : #input "What is desired TLC?" angle
K : #angle=angle/6
C : .....
C : rotate components about T12-L1:
C : .....
K : /
K : O
K : R
K : I
K : H
C : 29
C : 28
C : 27
C : 26
C : 25
C : 24
C : 23
C : 22
C : 21
C : 20
K : 19
K : 6
K : 7
K : 8
K : 9
K : 10
K : 11
K : 12
K : 13
K : 5
K : 3
K : D
K :
K : K
K : -194.1 0 189.2
K : 0 -angle 0
```

```

C : .....
C : rotate components about L1-L2:
C : .....
K : R
K : I
K : H
K : 18
C : 29
C : 28
C : 27
C : 26
C : 25
C : 24
C : 23
C : 22
C : 21
C : 20
K : 19
K : 6
K : 7
K : 8
K : 9
K : 10
K : 11
K : 12
K : 13
K : 5
K : 3
K : D
K :
K : K
K : -173.7 0 160
K : 0 -angle 0
P :
C : .....
C : rotate components about L2-L3:
C : .....
K : R
K : I
K : H
K : 17
K : 18
C : 29
C : 28
C : 27
C : 26
C : 25
C : 24
C : 23
C : 22
C : 21
C : 20
K : 19
K : 6
K : 7

```

```

K : 8
K : 9
K : 10
K : 11
K : 12
K : 13
K : 5
K : 3
K : D
K :
K : K
K : -152.9 0 130.3
K : 0 -angle 0
C : rotate components about L3-L4:
C : .....
K : R
K : I
K : H
K : 16
K : 17
K : 18
C : 29
C : 28
C : 27
C : 26
C : 25
C : 24
C : 23
C : 22
C : 21
C : 20
K : 19
K : 6
K : 7
K : 8
K : 9
K : 10
K : 11
K : 12
K : 13
K : 5
K : 3
K : D
K :
K : K
K : -130.8 0 98.7
K : 0 -angle 0
P :
C : .....
C : rotate components about L4-L5:
C : .....
K : R
K : I
K : H
K : 15

```

```

K : 16
K : 17
K : 18
C : 29
C : 28
C : 27
C : 26
C : 25
C : 24
C : 23
C : 22
C : 21
C : 20
K : 19
K : 6
K : 7
K : 8
K : 9
K : 10
K : 11
K : 12
K : 13
K : 5
K : 3
K : D
K :
K : K
K : -110 0 69
K : 0 -angle 0
P :
C : .....
C : rotate components about L5-S1:
C : .....
K : R
K : I
K : H
K : 14
K : 15
K : 16
K : 17
K : 18
C : 29
C : 28
C : 27
C : 26
C : 25
C : 24
C : 23
C : 22
C : 21
C : 20
K : 19
K : 6
K : 7
K : 8

```

```
K : 9
K : 10
K : 11
K : 12
K : 13
K : 5
K : 3
K : D
K :
K : K
K : -89 0 39
K : 0 -angle 0
C : .....
C : reconfigure and finish program:
C : .....
K : echo all
K : /
E :
```

APPENDIX C

Limb Positioning Program

This program positions the limbs of the 50% male model in 3-D space, using as inputs: a) the desired heel and hand coordinates, and b) any desired splay angles for the extremities. Hamstring length and knee angle are provided as output.

```
K : #echo none
C : .....
C : declare variables to move the right leg:
C : .....
K : #Declare RHeel(3)
K : #Declare Rendpoint(3)
K : #Declare RHip(3)
K : #Declare Rlength(1)
K : #Declare RInsert(3)
K : #Declare Rstretch(1)
K : #Declare RAng7(1)
K : #Declare RSplayang(1)
K : #Declare Rell(1)
K : #Declare RAng1(1)
K : #Declare RAng3(1)
K : #Declare RAng4(1)
K : #Declare RAng6(1)
K : #Declare RKnee(3)
K : #Declare Ra(1)
K : #Declare Rb(1)
K : #Declare Rc(1)
K : #Declare Rd(1)
K : #Declare Re(1)
K : #Declare Rangle(1)
K : #Declare Rhand(3)
K : #Declare Rarmsplay(1)
C : Input for the rite side of the body
K : #Input"Enter desired right hand coordinates" Rhand
K : #Input"Enter desired right heel point coordinates" RHeel
K : #Input"Enter desired right leg splay angle" Rsplayang
K : #Input"Enter desired right arm splay angle" Rarmsplay
C : .....
C : Crunch the numbers to locate the right knee :
C : ( Other "crunch" sections below follow same logic ) :
C : .....
C : Convert heel position to ankle joint position
K : #RHeel(1)=RHeel(1)-15.03
K : #RHeel(2)=RHeel(2)+.6
K : #RHeel(3)=RHeel(3)+60.67
```

```

C : Initialize hip joint coordinates
K : #RHip(1)=0
K : #RHip(2)=-81
K : #RHip(3)=0
C : Determine distance between hip and ankle
K : #Ra=Rheel(1)-RHip(1)
K : #Ra=Ra*Ra
K : #Rb=Rheel(2)-Rhip(2)
K : #Rb=Rb*Rb
K : #Rc=Rheel(3)-Rhip(3)
K : #Rc=Rc*Rc
K : #Rel1=sqrt(Ra+Rb+Rc)
C : If the specified heel is to far from the hip, abort the run
K : #If (Rel1 GT 870) then GOTO abort
C : Use law of cosines to determine knee coordinates
K : #Rang3=asin((RHip(3)-Rheel(3))/Rel1)
K : #Rang1=acos((-19229.6+(Rel1*Rel1))/(852.4*Rel1))
K : #Rang4=Rang1-Rang3
K : #Rang6=asin((Rheel(2)-Rhip(2))/Rel1)
K : #Rang7=90-Rang6
K : #RKnee(1)=(426.24*cos(Rang4)*cos(Rang6))+Rhip(1)
K : #RKnee(2)=(426.24*cos(Rang4)*sin(Rang6))+Rhip(2)
K : #RKnee(3)=(426.24*sin(Rang4))+Rhip(3)
C : Locate the insertion of the hamstrings
K : #Rd=Rknee(3)-Rheel(3)
K : #Rang5=asin(Rd/439.8)
K : #RInsert(1)=Rheel(1)-((375*cos(Rang5))*sin(Rang7))
K : #Re=(375*cos(Rang5))
K : #RInsert(2)=Rheel(2)-(Re*cos(RAng7))
K : #RInsert(3)=Rheel(3)+(375*sin(Rang5))
K : /
K : cg
C : .....
C : Translate the rite tibia & f ibula:
C : .....
K : /
K : o
K : mt
K : h
K : 58
K : k
K : 706.95 -119.0 -201.33
K : k
K : RHeel(1) RHeel(2) RHeel(3)
C : .....
C : Pivot the rite femur into position:
C : .....
K : /
K : o
K : p
K : h
K : 57
K : k
K : Rhip(1) Rhip(2) Rhip(3)
K : k

```

```

K : 404.1 -122.47 129.1
K : k
K : Rknee(1) Rknee(2) Rknee(3)
C : .....
C : Rotate the rite tibia & fibula:
C : .....
K : p
K : h
K : 58
K : k
K : RHeel(1) RHeel(2) RHeel(3)
K : k
K : (RHeel(1)-302.85) (Rheel(2)-3.47) (Rheel(3)+330.43)
K : k
K : RKnee(1) Rknee(2) Rknee(3)
C : .....
C : Translate the rite foot:
C : .....
K : /
K : o
K : mt
K : h
K : 5
K : k
K : 706.95 -119.00 -201.33
K : k
K : Rheel(1) Rheel(2) Rheel(3)
C : .....
C : Splay the rite leg :
C : .....
P :
K : /
K : o
K : ab
K : h
K : 57
K : p
K : k
K : Rhip(1) Rhip(2) Rhip(3)
K : k
K : Rheel(1) Rheel(2) Rheel(3)
K : k
K : Rhip(1) Rhip(2) Rhip(3)
K : r
K : Rsplayang
K : ab
K : h
K : 58
K : p
K : k
K : Rhip(1) Rhip(2) Rhip(3)
K : k
K : Rheel(1) Rheel(2) Rheel(3)
K : k
K : Rheel(1) Rheel(2) Rheel(3)
K : r
K : Rsplayang

```

```

C : .....
C : Declare variables to move the left leg:
C : .....
P :
K : #Declare Lheel(3)
K : #Declare Lendpoint(3)
K : #Declare Lhip(3)
K : #Declare Llength(1)
K : #Declare Linsert(3)
K : #Declare Lstretch(1)
K : #Declare Lang7(1)
K : #Declare Lsplayang(1)
K : #Declare Lell(1)
K : #Declare Lang1(1)
K : #Declare Lang3(1)
K : #Declare Lang4(1)
K : #Declare Lang6(1)
K : #Declare Lknee(3)
K : #Declare La(1)
K : #Declare Lb(1)
K : #Declare Lc(1)
K : #Declare Ld(1)
K : #Declare e(1)
K : #Declare Langle(1)
K : #Declare Lhand(3)
K : #Declare Larmsplay(1)
C : Input for the left side of the body
K : #Input"Enter desired left hand coordinates" Lhand
K : #Input"Enter desired left heel coordinates" Lheel
K : #Input"Enter desired left leg splay angle" Lsplayang
K : #Input"Enter desired left arm splay angle" Larmsplay
C : .....
C : Crunch the numbers to locate the left knee:
C : .....
K : #LHeel(1)=LHeel(1)-10
K : #LHeel(3)=LHeel(3)+60
K : #Lhip(1)=0
K : #Lhip(2)=81
K : #Lhip(3)=0
K : #La=Lheel(1)-Lhip(1)
K : #La=La*La
K : #Lb=Lheel(2)-Lhip(2)
K : #Lb=Lb*Lb
K : #Lc=Lheel(3)-Lhip(3)
K : #Lc=Lc*Lc
K : #Lell=sqrt(La+Lb+Lc)
K : #If (Lell GT 900) then GOTO abort
K : #Lang3=asin((Lhip(3)-Lheel(3))/Lell)
K : #Lang1=acos((19217+(Lell*Lell))/(922.26*Lell))
K : #Lang4=Lang1-Lang3
K : #Lang6=asin((Lheel(2)-Lhip(2))/Lell)
K : #Lang7=90-Lang6
K : #Lknee(1)=(461*cos(Lang4)*cos(Lang6))+Lhip(1)
K : #Lknee(2)=(461*cos(Lang4)*sin(Lang6))+Lhip(2)
K : #Lknee(3)=(461*sin(Lang4))+Lhip(3)

```

```

K : #Ld=Lknee(3)-Lheel(3)
K : #Lang5=asin(Ld/439.8)
K : #Linsert(1)=Lheel(1)-(375*cos(Lang5))
K : #e=(330*cos(Lang5))
K : #Linsert(2)=Lheel(2)-(e*cos(Lang7))
K : #Linsert(3)=Lheel(3)+(375*sin(Lang5))
C : .....
C : Translate the left tibia and fibula :
C : .....
K : /
K : o
K : mt
K : h
K : 56
K : k
K : 714 119.6 -206
K : k
K : Lheel(1) Lheel(2) Lheel(3)
C : .....
C : Pivot the left femur into position:
C : .....
K : /
K : o
K : p
K : h
K : 55
K : k
K : Lhip(1) Lhip(2) Lhip(3)
K : k
K : (Lhip(1)+440) 122.5 (Lhip(3)+138)
K : k
K : Lknee(1) Lknee(2) Lknee(3)
C : .....
C : Rotate Left tibia and fibula:
C : .....
K : p
K : h
K : 56
K : k
K : Lheel(1) Lheel(2) Lheel(3)
K : k
K : (Lheel(1)-274) (Lheel(2)+3.5) (Lheel(3)+344)
K : k
K : Lknee(1) Lknee(2) Lknee(3)
C : .....
C : Translate the left foot:
C : .....
K : /
K : o
K : mt
K : h
K : 8
K : k
K : 714 119.6 -206
K : k
K : Lheel(1) Lheel(2) Lheel(3)

```

```

C : #GOTO stop2
C : #stop:
C : #arm:
C : .....
C : Splay the left leg :
C : .....
K : /
K : o
K : ab
K : h
K : 55
K : p
K : k
K : Lhip(1) Lhip(2) Lhip(3)
K : k
K : Lheel(1) Lheel(2) Lheel(3)
K : k
K : Lhip(1) Lhip(2) Lhip(3)
K : r
K : -1*(Lsplayang)
K : ab
K : h
K : 56
K : p
K : k
K : Lhip(1) Lhip(2) Lhip(3)
K : k
K : Lheel(1) Lheel(2) Lheel(3)
K : k
K : Lheel(1) Lheel(2) Lheel(3)
K : r
K : -1*(Lsplayang)
C : .....
C : Declare variables to move the rite arm:
C : .....
K : #Declare Rshlder(3)
K : #Declare Rwrist(3)
K : #Declare Relbow(3)
K : #Declare Rf(1)
K : #Declare Rg(1)
K : #Declare Rh(1)
K : #Declare Ri(1)
K : #Declare Rj(1)
K : #Declare Rk(1)
K : #Declare Rl(1)
K : #Declare RAng14(1)
K : #Declare RAng11(1)
K : #Declare RAng13(1)
K : #Declare RAng16(1)
K : #Declare RHand(3)
C : .....
C : Crunch the numbers to locate the rite elbow:
C : .....
K : #Rshlder(1)=-214
K : #Rshlder(2)=-179
K : #Rshlder(3)=418

```

```

K : #Rwrist(1)=Rhand(1)-63
K : #Rwrist(2)=Rhand(2)
K : #Rwrist(3)=Rhand(3)-30
K : #Rf=Rwrist(1)-Rshlder(1)
K : #Rg=Rwrist(2)-Rshlder(2)
K : #Rh=Rwrist(3)-Rshlder(3)
K : #Rl=sqrt(Rf*Rf+Rg*Rg+Rh*Rh)
K : #If (Rl GT 585 ) then GOTO abort
K : #Ri=Rshlder(3)-Rwrist(3)
K : #Rangl4=asin(Ri/Rl)
K : #Rj=296*296-293*293-Rl*Rl
K : #Rj=Rj/(-2*293*Rl)
K : #Rangl1=acos(Rj)
K : #Rangl3=Rangl1-Rangl4
K : #Rangl6=90
K : #Relbow(1)=Rwrist(1)-293*cos(Rangl3)*sin(Rangl6)
K : #Relbow(2)=Rwrist(2)-293*cos(Rangl3)*cos(Rangl6)
K : #Relbow(3)=Rwrist(3)-293*sin(Rangl3)
C : .....
C : Pivot rite humerus :
C : .....
K : /
K : o
K : p
K : h
K : 12
K : k
K : -214 -179 419
K : k
K : 19 -179 236
K : k
K : Relbow(1) Relbow(2) Relbow(3).
K : /
C : .....
C : Translate the right radius and ulna:
C : .....
K : o
K : mt
K : h
K : 3
K : k
K : 19 -179 236
K : k
K : Relbow(1) Relbow(2) Relbow(3)
K : mt
K : h
K : 2
K : k
K : 19 -179 236
K : k
K : Relbow(1) Relbow(2) Relbow(3)
C : .....
C : Rotate the rite radius and ulna:
C : .....
K : p
K : h
K : 3
K : k

```

```

K : Relbow(1) Relbow(2) Relbow(3)
K : k
K : (Relbow(1)+237) (Relbow(2)-5) (Relbow(3)+172)
K : k
K : Rwrist(1) Rwrist(2) Rwrist(3)
K : p
K : h
K : 2
K : k
K : Relbow(1) Relbow(2) Relbow(3)
K : k
K : (Relbow(1)+237) (Relbow(2)-5) (Relbow(3)+172)
K : k
K : Rwrist(1) Rwrist(2) Rwrist(3)
C : .....
C : Translate rite hand:
C : .....
K : mt
K : h
K : 4
K : k
K : 256 -184 408
K : k
K : Rwrist(1) Rwrist(2) Rwrist(3)
C : .....
C : Splay the rite arm :
C : .....
K : /
K : o
K : ab
K : h
K : 12
K : p
K : k
K : Rshlder(1) Rshlder(2) Rshlder(3)
K : k
K : Rwrist(1) Rwrist(2) Rwrist(3)
K : k
K : Rshlder(1) Rshlder(2) Rshlder(3)
K : r
K : -1*Rarmsplay
K : ab
K : h
K : 3
K : p
K : k
K : Rshlder(1) Rshlder(2) Rshlder(3)
K : k
K : Rwrist(1) Rwrist(2) Rwrist(3)
K : k
K : Rwrist(1) Rwrist(2) Rwrist(3)
K : r
K : -1*Rarmsplay
K : ab
K : h
K : 2
K : p

```

```

K : k
K : Rshlder(1) Rshlder(2) Rshlder(3)
K : k
K : Rwrist(1) Rwrist(2) Rwrist(3)
K : k
K : Rwrist(1) Rwrist(2) Rwrist(3)
K : r
K : -1*Rarmsplay
K : /
K : au
P :
C : .....
C : Declare variables to move the left arm:
C : .....
K : #Declare Lshlder(3)
K : #Declare Lwrist(3)
K : #Declare Lelbow(3)
K : #Declare Lf(1)
K : #Declare Lg(1)
K : #Declare Lh(1)
K : #Declare Li(1)
K : #Declare Lj(1)
K : #Declare Lk(1)
K : #Declare Ll(1)
K : #Declare Langl4(1)
K : #Declare Langl1(1)
K : #Declare Langl3(1)
K : #Declare Langl6(1)
K : #Declare Lhand(3)
C : .....
C : Crunch the numbers to locate the left elbow:
C : .....
K : #Lshlder(1)=-214
K : #Lshlder(2)=179
K : #Lshlder(3)=418
K : #Lwrist(1)=Lhand(1)-63
K : #Lwrist(2)=Lhand(2)
K : #Lwrist(3)=Lhand(3)-30
K : #Lf=Lwrist(1)-Lshlder(1)
K : #Lg=Lwrist(2)-Lshlder(2)
K : #Lh=Lwrist(3)-Lshlder(3)
K : #Ll=sqrt(Lf*Lf+Lg*Lg+Lh*Lh)
K : #If ( Ll GT 585 ) then GOTO abort
K : #Li=Lshlder(3)-Lwrist(3)
K : #Langl4=asin(Li/Ll)
K : #Lj=296*296-293*293-Ll*Ll
K : #Lj=Lj/(-2*293*Ll)
K : #langl1=acos(Lj)
K : #Langl3=Langl1-Langl4
K : #Langl6=90
K : #Lelbow(1)=Lwrist(1)-293*cos(Langl3)*sin(Langl6)
K : #Lelbow(2)=Lwrist(2)-293*cos(Langl3)*cos(Langl6)
K : #Lelbow(3)=Lwrist(3)-293*sin(Langl3)
C : .....
C : Pivot left humerus:
C : .....

```

```

K : /
K : o
K : p
K : h
K : 13
K : k
K : -214 179 419
K : k
K : 19 179 236
K : k
K : Lelbow(1) Lelbow(2) Lelbow(3)
K : /
C : .....
C : Translate the left radius and ulna:
C : .....
K : o
K : mt
K : h
K : 52
K : k
K : 19 179 236
K : k
K : Lelbow(1) Lelbow(2) Lelbow(3)
K : mt
K : h
K : 51
K : k
K : 19 179 236
K : k
K : Lelbow(1) Lelbow(2) Lelbow(3)
C : .....
C : Rotate the left radius and ulna:
C : .....
K : p
K : h
K : 52
K : k
K : Lelbow(1) Lelbow(2) Lelbow(3)
K : k
K : (Lelbow(1)+237) (Lelbow(2)+5) (Lelbow(3)+172)
K : k
K : Lwrist(1) Lwrist(2) Lwrist(3)
K : p
K : h
K : 51
K : k
K : Lelbow(1) Lelbow(2) Lelbow(3)
K : k
K : (Lelbow(1)+237) (Lelbow(2)+5) (Lelbow(3)+172)
K : k
K : Lwrist(1) Lwrist(2) Lwrist(3)
C : .....
C : Translate the left hand:
C : .....
K : mt
K : h

```

```

K : 9
K : k
K : 256 184 408
K : k
K : Lwrist(1) Lwrist(2) Lwrist(3)
C : .....
C : Splay the left arm:
C : .....
K : /
K : o
K : ab
K : h
K : 13
K : p
K : k
K : Lshlder(1) Lshlder(2) Lshlder(3)
K : k
K : Lwrist(1) Lwrist(2) Lwrist(3)
K : k
K : Lshlder(1) Lshlder(2) Lshlder(3)
K : r
K : Larmsplay
K : ab
K : h
K : 52
K : p
K : k
K : Lshlder(1) Lshlder(2) Lshlder(3)
K : k
K : Lwrist(1) Lwrist(2) Lwrist(3)
K : k
K : Lwrist(1) Lwrist(2) Lwrist(3)
K : r
K : Larmsplay
K : ab
K : h
K : 51
K : p
K : k
K : Lshlder(1) Lshlder(2) Lshlder(3)
K : k
K : Lwrist(1) Lwrist(2) Lwrist(3)
K : k
K : Lwrist(1) Lwrist(2) Lwrist(3)
K : r
K : Larmsplay
K : /
C : .....
C : Measure angle of left knee:
C : .....
K : /
K : l
K : me
K : a
K : k
K : Lhip(1) Lhip(2) Lhip(3)

```

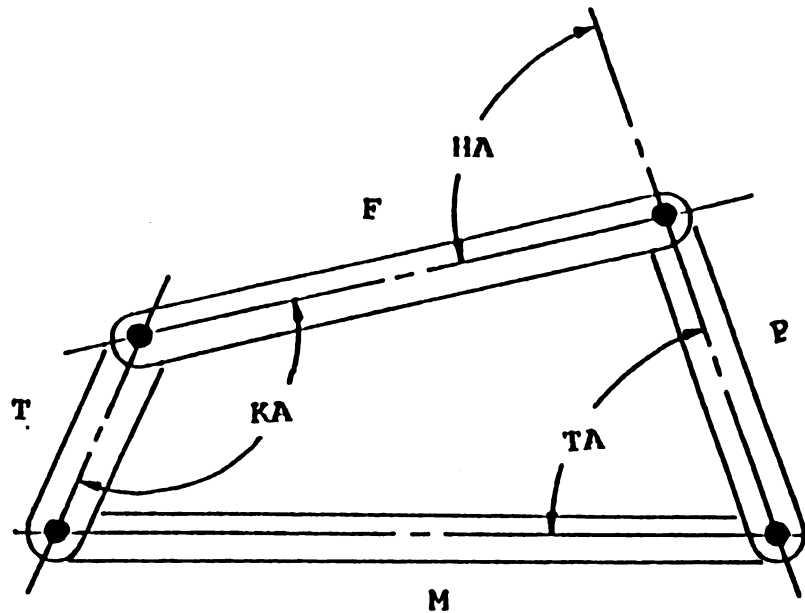
```

K : k
K : Lknee(1) Lknee(2) Lknee(3)
K : k
K : Lheel(1) Lheel(2) Lheel(3)
K : #Langle=Z_LIST(1)
C : .....
C : Measure length of the left hamstring:
C : .....
K : /
K : l
K : me
K : po
K : k
K : 21 60 -65
K : k
K : Linsert(1) Linsert(2) Linsert(3)
K : #Llength=Z_LIST(1)
K : #output"The left hamstring length is "Llength" mm."
K : #output"The left knee angle is "Langle"degrees"
C : .....
C : Measure angle of rite knee :
C : .....
K : /
K : l
K : me
K : a
K : k
K : Rhip(1) Rhip(2) Rhip(3)
K : k
K : Rknee(1) Rknee(2) Rknee(3)
K : k
K : Rheel(1) Rheel(2) Rheel(3)
K : #Rangle=Z_LIST(1)
C : .....
C : Measure length of rite hamstring :
C : .....
K : /
K : l
K : me
K : po
K : k
K : 21 -60 -65
K : k
K : Rinsert(1) Rinsert(2) Rinsert(3)
K : #Rlength=Z_LIST(1)
K : #output"The right hamstring length is "Rlength"mm."
K : #output"The right knee angle is "Rangle" degrees"
K : #WAIT 10
K : au
K : #Wait 30
K : /
K : v
K : rm
K : 0 0 90
K : #abort:
K : #output"Location abort."
K : #Echo all
E :

```

APPENDIX D

Linkage Equations



- F = Femoral Link Length
- T = Tibial Link Length
- P = Pelvic Link Length
- M = Hamstring Muscle Length
- HA = Hip Angle
- KA = Knee Angle
- TA = Transmission Angle

The solution of this four bar linkage may be found using the following formulas:

$$TA = \arccos((M^2 + P^2 - F^2 - T^2 + 2FT\cos KA) / 2MP)$$

$$HA = 2\arctan((T\sin KA - M\sin TA) / (P - F + T\cos KA - M\cos TA))$$

FIGURE 68: THE LINKAGE

APPENDIX E

The Exercise Program

This program uses angular information supplied by the user to position a partial model of the 50th percentile human male skeleton in a desired posture. Once this has been accomplished, the program simulates and orients the major muscle groups of the right leg.

During muscle fabrication, muscle volume and lateral dimensions are assumed to remain constant. Muscle thickness and length are allowed to vary as necessary. The muscularity of the individual may be varied by changing the magnitude of a multiplier of the nominal muscle volumes. (As written, the program recreates the musculature of a slight individual.)

This program supplies as output the final lengths of the major muscle groups it has modeled.

C : Regain straight lumbar spine if so desired.

K : Echo none

C : GOTO HERE

K : /

K : o

K : r

K : h

K : 6

K : k

K : -23.22 0 214.25

K : 0 25 0

K : r

K : h

K : 23

K : k

K : -23.22 0 214.25

K : 0 25 0

K : r

K : h

K : 53

K : -23.22 0 214.25

K : 0 25 0

K : r

K : h

K : 17

K : k

K : -23.22 0 214.25

K : 0 25 0

K : r

K : h

K : 6

```

K : k
K : -11.15 0 156.4
K : 0 25 0
K : r
K : h
K : 23
K : k
K : -11.15 0 156.4
K : 0 25 0
K : r
K : h
K : 53
K : k
K : -11.15 0 156.4
K : 0 25 0
K : r
K : h
K : 17
K : k
K : -11.15 0 156.4
K : 0 25 0
K : r
K : h
K : 46
K : k
K : -11.15 0 156.4
K : 0 25 0
C : rotate all segments around ankle to maintain balance
K : r
K : h
K : 2
K : k
K : -97.8 -120.7 -858
K : 0 -8 0
K : r
K : h
K : 3
K : k
K : -97.8 -120.7 -858
K : 0 -8 0
K : r
K : h
K : 5
K : k
K : -97.8 -120.7 -858
K : 0 -8 0
K : r
K : h
K : 48
K : k
K : -98.7 -120.7 -858
K : 0 -8 0
K : r
K : h
K : 46
K : k
K : -98.7 -120.7 -858

```

```

K : 0 -8 0
K : r
K : h
K : 17
K : k
K : -98.7 -120.7 -858
K : 0 -8 0
K : r
K : h
K : 53
K : k
K : -98.7 -120.7 -858
K : 0 -8 0
K : r
K : h
K : 23
K : k
K : -98.7 -120.7 -858
K : 0 -8 0
K : r
K : h
K : 6
K : k
K : -98.7 -120.7 -858
K : 0 -8 0
C : rotate pelvis & torso about hips
K : #Declare Delta(1)
K : #Input "What is pelvic rotation?" Delta(1)
K : r
K : h
K : 6
K : k
K : -124 -81 5.95
K : 0 Delta 0
K : r
K : h
K : 23
K : k
K : -124 -81 5.95
K : 0 Delta 0
K : r
K : h
K : 53
K : k
K : -124 -81 5.95
K : 0 Delta 0
K : r
K : h
K : 17
K : k
K : -124 -81 5.95
K : 0 Delta 0
K : r
K : h
K : 46
K : k

```

```

K : -124 -81 5.95
K : 0 Delta 0
K : r
K : h
K : 48
K : k
K : -124 -81 5.95
K : 0 Delta 0
K : r
K : h
K : 5
K : k
K : -124 -81 5.95
K : 0 Delta 0
C : rotate about ankles to keep balance
K : r
K : h
K : 2
K : k
K : -97.8 -120.7 -858
K : 0 (-Delta/4) 0
K : r
K : h
K : 3
K : k
K : -97.8 -120.7 -858
K : 0 (-Delta/4) 0
K : r
K : h
K : 5
K : k
K : -97.8 -120.7 -858
K : 0 (-Delta/4) 0
K : r
K : h
K : 48
K : k
K : -97.8 -120.7 -858
K : 0 (-Delta/4) 0
K : r
K : h
K : 46
K : k
K : -97.8 -120.7 -858
K : 0 (-Delta/4) 0
K : r
K : h
K : 17
K : k
K : -97.8 -120.7 -858
K : 0 (-Delta/4) 0
K : r
K : h
K : 53
K : k
K : -97.8 -120.7 -858
K : 0 (-Delta/4) 0

```

```

K : r
K : h
K : 23
K : k
K : -97.8 -120.7 -858
K : 0 (-Delta/4) 0
K : r
K : h
K : 6
K : k
K : -97.8 -120.7 -858
K : 0 (-Delta/4) 0
C : Calculate knee and hip locations, using Law of Cosines
K : #Declare Alpha(1)
K : #Declare Beta(1)
K : #Declare Gamma(1)
K : #Declare Knee(3)
K : #Declare Hip(3)
K : #Input "What is anterior tibial angle with floor?" Alpha
K : #Input "What is knee angle?" Beta
K : #echo none
K : #Gamma=Beta-Alpha
K : #Knee(1)=(440.6*cos(Alpha))+(-97.8)
K : #Knee(2)=-120.7
K : #Knee(3)=(440.6*sin(Alpha))+(-858)
K : #Hip(1)=Knee(1)-(436.94*cos(Gamma))
K : #Hip(2)=-81
K : #Hip(3)=Knee(3)+(436.94*sin(Gamma))
C : rotate tibia to new position
K : /
K : o
K : p
K : h
K : 2
K : k
K : -97.8 -97.7 -858
K : 1
K : po
K : h
K : 2
K : 2
K : k
K : Knee(1) Knee(2) Knee(3)
C : translate head, torso to new positions
K : mt
K : h
K : 6
K : 1
K : po
K : h
K : 5
K : 4
K : k
K : Hip(1) Hip(2) Hip(3)
K : mt
K : h

```

```

K : 23
K : 1
K : po
K : h
K : 5
K : 4
K : k
K : Hip(1) Hip(2) Hip(3)
K : mt
K : h
K : 53
K : 1
K : po
K : h
K : 5
K : 4
K : k
K : Hip(1) Hip(2) Hip(3)
K : mt
K : h
K : 17
K : 1
K : po
K : h
K : 5
K : 4
K : k
K : Hip(1) Hip(2) Hip(3)
K : mt
K : h
K : 46
K : 1
K : po
K : h
K : 5
K : 4
K : k
K : Hip(1) Hip(2) Hip(3)
K : mt
K : h
K : 48
K : 1
K : po
K : h
K : 5
K : 4
K : k
K : Hip(1) Hip(2) Hip(3)
C : translate pelvis to new position
K : mt
K : h
K : 5
K : 1
K : po
K : h
K : 5

```

```

K : 4
K : k
K : Hip(1) Hip(2) Hip(3)
C : translate femur to new hip location
K : mt
K : h
K : 3
K : 1
K : po
K : h
K : 3
K : 2
K : k
K : Hip(1) Hip(2) Hip(3)
C : rotate femur to new position
K : p
K : h
K : 3
K : k
K : Hip(1) Hip(2) Hip(3)
K : 1
K : po
K : h
K : 3
K : 1
K : k
K : Knee(1) Knee(2) Knee(3)
C : #HERE:
C : measure final hamstring length
K : /
K : 1
K : me
K : po
K : 1
K : po
K : h
K : 5
K : 1
K : po
K : h
K : 2
K : 1
K : d
K : #Output"Final hamstring length is "Z_List(7)"mm."
K : /
C : Create hamstring muscles
K : #Output"Creating hamstring muscle bellies."
C : Establish dimensions of biceps femoris
K : #Declare Bicep(3)
K : #Bicep(1)=(Z_List(7)/2)
K : #Declare Hamz(1)
K : #Hamz(1)=(7200/Bicep(1))
K : #Bicep(2)=42
K : #Bicep(3)=Hamz(1)
K : /

```

```

K : nm
K : om
K : c
K : sp
K : 1.0
K : 16
K : 16
K : 11
K : sh
K : sc
K : k
K : 0 0 0
K : Bicep(1) Bicep(2) Bicep(3)
K : /
K : sto
K : hamstrings
K : nm
K : sa
K : cr
K : c
K : 1
K : hamstrings
K :
K : biceps
K : 1
K : d
K : /
K : TA
K : c
K : g
K : 69
K : aux
K : p
K : c
K : k
K : -Bicep(1) 0 0
K : d
K : /
K : Sto
K :
K : y
K : /
K : nm
K : sa
K : /
C : translate biceps
K : o
K : mt
K : h
K : 57
K : k
K : (Bicep(1)) 0 0
K : L
K : po
K : h
K : 2
K : 1

```

```

C : pivot biceps
K : p
K : h
K : 57
K : L
K : po
K : h
K : 2
K : 1
K : L
K : po
K : h
K : 57
K : 1
K : L
K : po
K : h
K : 5
K : 1
C : measure final quadriceps length
K : /
K : 1
K : me
K : po
K : L
K : po
K : h
K : 5
K : 5
K : po
K : h
K : 2
K : 3
K : d
K : #Output"Final quadriceps length is "Z_List(7)"mm."
K : #Output"Creating quadriceps bellies."
C : Establish dimensions of quadriceps
K : #Declare Quad(3)
K : #Quad(1)=(Z_List(7)/2)
K : #Declare Quadz(1)
K : #Quadz(1)-((8950*1.0)/Quad(1))
K : #Quad(2)=60
K : #Quad(3)=Quadz(1)
K : /
K : nm
K : om
K : c
K : sp
K : 1.0
K : 16
K : 16
K : 11
K : sh
K : sc
K : k
K : 0 0 0
K : Quad(1) Quad(2) Quad(3)

```

```

K : /
K : sto
K : quadriceps
K : nm
K : sa
K : cr
K : c
K : 1
K : quadriceps
K :
K : vastus
K : 1
K : d
K : /
K : TA
K : c
K : g
K : 70
K : aux
K : p
K : c
K : k
K : -Quad(1) 0 0
K : d
K : /
K : sto
K :
K : y
K : /
K : nm
K : sa
K : /
C : translate quads
K : o
K : mt
K : h
K : 58
K : k
K : (Quad(1)) 0 0
K : L
K : po
K : h
K : 2
K : 3
C : pivot quads
K : p
K : h
K : 58
K : L
K : po
K : h
K : 2
K : 3
K : L
K : po
K : h
K : 58

```

```

K : 1
K : L
K : po
K : h
K : 5
K : 5
C : measure final gastroc-Achille length
K : /
K : L
K : me
K : po
K : L
K : po
K : h
K : 3
K : 3
K : po
K : h
K : 4
K : 1
K : d
K : #Output"Calf length is  "Z_List(7)"mm."
K : #Output"Creating gastrocnemius muscle belly."
C : Establish dimensions of gastrocnemius muscle.
K : #Declare Gastroc(3)
K : #Gastroc(1)=(Z_List(7)/4)
K : #Gastroc(1)=(Gastroc(1)*1.1)
K : #Declare Gast(1)
K : #Gast(1)-((8740*0.65)/Gastroc(1))
K : #Gastroc(2)=57
K : #Gastroc(3)=Gast(1)
K : /
K : nm
K : om
K : c
K : sp
K : 1.0
K : 16
K : 16
K : 11
K : sh
K : sc
K : k
K : 0 0 0
K : Gastroc(1) Gastroc(2) Gastroc(3)
K : /
K : sto
K : calfmuscle
K : nm
K : sa
K : cr
K : c
K : 1
K : calfmuscle
K :
K : gastrocnemius

```

```

K : 1
K : d
K : /
K : TA
K : c
K : g
K : 71
K : aux
K : p
K : c
K : k
K : -Gastroc(1) 0 0
K : d
K : /
K : sto
K :
K : y
K : /
K : nm
K : sa
K : /
C : translate gastrocnemius
K : o
K : mt
K : h
K : 59
K : k
K : (Gastroc(1)) 0 0
K : L
K : po
K : h
K : 3
K : 3
C : Pivot gastrocnemius
K : p
K : h
K : 59
K : l
K : po
K : h
K : 3
K : 3
K : L
K : po
K : h
K : 59
K : 1
K : L
K : po
K : h
K : 4
K : 1
K : #Output "Creating Achille's Tendon."
K : /
K : nm
K : om
K : c

```

K : cy
 K : 13 260 16
 K : N
 K : 14
 K : /
 K : sto
 K : achilles
 K : nm
 K : sa
 K : cr
 K : c
 K : l
 K : achilles
 K :
 K : tendon
 K : l
 K : d
 K : /
 K : TA
 K : c
 K : g
 K : 72
 K : aux
 K : p
 K : c
 K : k
 K : 0 -130 0
 K : d
 K : /
 K : sto
 K :
 K : y
 K : /
 K : nm
 K : sa
 K : /
 C : Translate Achille's tendon
 K : o
 K : mt
 K : h
 K : 60
 K : k
 K : 0 130 0
 K : L
 K : po
 K : h
 K : 4
 K : l
 C : Pivot Achille's Tendon
 K : p
 K : h
 K : 60
 K : L
 K : po
 K : h
 K : 4

```

K : 1
K : L
K : po
K : h
K : 60
K : 1
K : L
K : po
K : h
K : 3
K : 3
C : #HERE:
C : Create gluteal musculature
K : #Output"Creating gluteal musculature."
K : /
K : nm
K : om
K : c
K : sp
K : 103.0
K : 16
K : 16
K : 11
K : sh
K : sc
K : k
K : 0 0 0
K : .73 .80 1.0
K : /
K : sto
K : butt
K : nm
K : sa
K : cr
K : c
K : 1
K : butt
K :
K : gluteals
K : 1
K : d
K : dr
K : #Output"Phew!!"
K : #echo all
K : /
E :

```

APPENDIX F

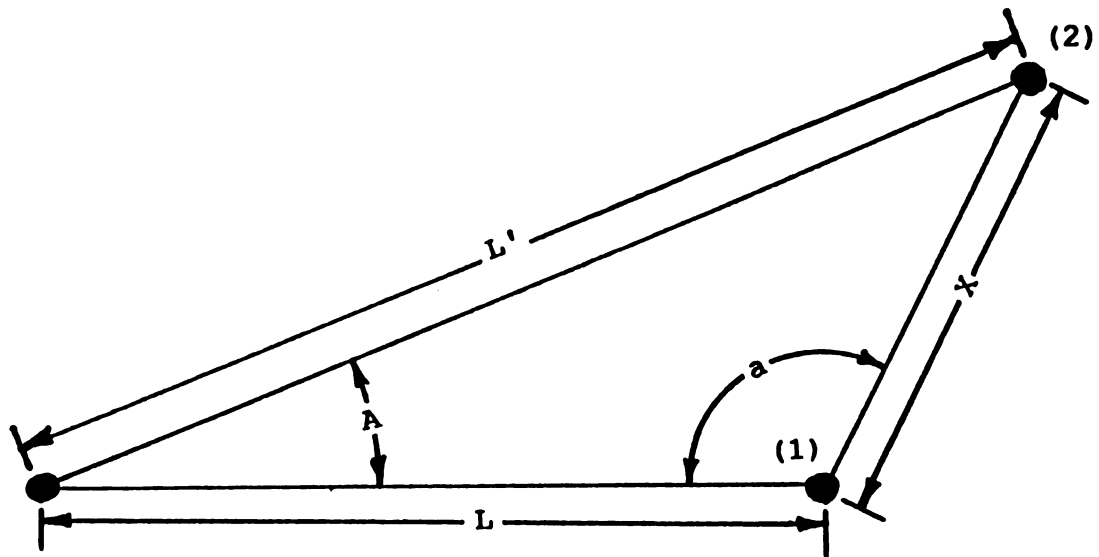
Sources of Error

Figure 69 illustrates that the angular error which may be introduced due to a target positioning error is:

1. proportional to the distance between the actual target location and its apparent location,
2. proportional to the sine of the angle between the actual link and the apparent link, and will therefore be greatest when angle "a" equals ninety degrees,
3. inversely proportional to the actual link length.

Using the assumption that random errors due to all causes in the determination of target positions during this experiment were likely to be of similar frequency and magnitudes in all directions, while noting that the largest link length error observed in the standing files was less than 3.0 mm. (the largest deviation from the mean link value was 2.8mm., occurring in the femoral link of Subject 3 at approximately 0.75 seconds), it may be concluded that the largest likely distance between the actual and apparent locations of any target is 3.0 mm.

Because the shortest nominal pelvic, femoral, and tibial link lengths for the test volunteers were 124mm, 351mm, and 88mm., respectively, the maximum probable angular error introduced by the tibial link = $\arctan (3/88) = 1.96$



- A = Angular Error
- L = Actual Link Length
- L' = Apparent Link Length
- X = Distance Between Actual and Apparent Target Locations
- 1 = Actual Target Location
- 2 = Apparent Target Location

FIGURE 69: ERROR ESTIMATION

degrees. The maximum probable angular error introduced by the femoral link = $\arctan (3/351) = 0.49$ degrees.

Similarly, the maximum angular error probably introduced by the pelvic link = $\arctan (3/124) = 1.38$ degrees. We now conclude that the maximum probable Hip Angle Error = $(1.38 + 0.49) = 1.87$ degrees. Likewise, the maximum probable Knee Angle Error = $(1.96 + 0.49) = 2.45$ degrees. The small magnitude of these probable errors suggests that the angular data gathered in the laboratory can be used with confidence to estimate the length of the subject's hamstrings.

The apparent change in bone lengths encountered during this experiment is the cumulative result of many unavoidable errors, namely:

1. Human error in the layout of the calibrated space resulting in errors in all position estimates made by the computer;

2. Human error in the positioning of the targets over the various anatomical landmarks resulting in a degradation in the ability to accurately determine the spatial locations of body parts;

3. The error inherent in using only reflected light to locate the exact center of targets also created errors in position reporting.

BIBLIOGRAPHY

BIBLIOGRAPHY

1. "Devices For Use in Defining and Measuring Vehicle Seating Accommodation", S.A.E. Handbook 1980- Part 2, Society of Automotive Engineers, Warrendale, Pennsylvania.
2. Beneck, G.J., "Influence of Motor Vehicle Seat Geometry on Pelvic Inclination", Master's Thesis, Michigan State University, 1990.
3. Haas, W.A., "Geometric Model and Spinal Motions of the Average Male in Seated Postures", Master's Thesis, Michigan State University, 1989.
4. SDRC IDEAS 3.8 and 4.0 GEOMOD Solid Modeling Package, Structural Dynamics Research Corporation, 1986.
5. Hubbard, R.P., McLeod, D.G., "A Basis for Crash Dummy Skull and Head Geometry", General Motors Corporation Research Laboratories, Research Publication No. GMR-1283, 1972.
6. Reynolds, H.M., Snow, C.C., Young, J.W., "Spatial Geometry of the Human Pelvis", Federal Aviation Administration, Memorandum Report No. AAC-119-81-5, 1981.
7. Robbins, D.H., "Anthropometric Specifications for the Mid-Sized Male Dummy", UMTRI-83-53-2, U.S. Department of Transportation, National Highway Traffic Safety Administration, Washington, D.C., 1983.
8. Koritka, J.C., and Sick, H. Atlas of Sectional Human Anatomy, Urban & Schwarzenberg, Baltimore, Md. 1983, Plates HT-1 through HT-15, also page XIV.
9. Panjabi, M.M., White III, A.A., Clinical Biomechanics of the Spine, J.B. Lippincott, Philadelphia, PA. 1978.
10. Clemente, C.D. Anatomy - a Regional Atlas of the Human Body, Urban & Schwarzenberg, 1981.
11. Hollinshead, W.H., Rosse, C. Textbook of Anatomy, 4th Edition, Harper and Row, 1985.

12. Peck, S.R. Atlas of Human Anatomy for the Artist, Oxford University Press, New York, NY. 1951.
13. Geiger, S.R., editor, Handbook of Physiology, Section 3: The Respiratory System, American Physiological Society, Bethesda, Maryland, 1986, pages 179, 431-453.
14. Carlson, Johnson, and Cavert, The Machinery of the Body, University of Chicago Press, 1961.
15. Halliburton, W.D. Handbook of Physiology, 16th Edition, P. Blakiston's Son & Co., 1923.
16. Greisheimer, E.M., Weideman, M.P. Physiology and Anatomy, 9th Edition, J.B. Lippincott Co., 1972.
17. Grollman, Sigmond, The Human Body - Its Structure and Physiology, 4th Edition, MacMillan Publishing Co., 1978.
18. Stokes, I.A.F., Aberly, J.M., "Influence of the Hamstring Muscles on Lumbar Spine Curvature in Sitting," Spine, Vol. 5, No. 6, Nov/Dec 1980.
19. Reed, M.P., Saito, M., KaKishima, Y., Lee, N.S., and Schneider, L.W., "An Investigation of Driver Discomfort and Related Seat Design Factors on Extended Duration Driving," presented at SAE Annual Meeting, Feb. 1991.
20. McMahan, T.A. Muscles, Reflexes, and Locomotion, Princeton University Press, 1984, page 4.
21. Brand, R.A., Crowninshield, R.D., Wittstock, C.E., Pedersen, D.R., and Clark, C.R., "A Model of Lower Extremity Muscular Anatomy," Journal of Biomechanical Engineering, Vol. 104, Nov. 1982, pages 304-310.
22. Jensen, R.H., and Davy, D.T., "An Investigation of Muscle Lines of Action About the Hip: A Centroid Line Approach Versus The Straight Line Approach," Journal of Biomechanics, Vol. 8, 1975, pp. 103-110.
23. Grabo, J.F., "Motion of the Pelvis During Passive Leg Lifting on Normal Subjects", Master's Thesis, Michigan State University, 1989.
24. Shigley, J.E., and Uicker, J.J., Theory of Machines and Mechanisms, McGraw-Hill, Inc., 1980.
25. Atha, J., and Wheatley, D.W., "The Mobilising Effects of Repeated Measurement of Hip Flexion," British Journal of Sports Medicine, 10:22-25, 1976.

MICHIGAN STATE UNIV. L



31293008964